

**Inverse Gas Chromatography Study of Small Molecules Transport in Hydroxypropyl
Xylan**

by

Fatemeh Bayati

A thesis submitted in partial fulfillment of the requirements for the degree of

Doctor of Philosophy

in

Chemical Engineering

Department of Chemical and Materials Engineering
University of Alberta

© Fatemeh Bayati, 2016

Abstract

Synthetic polymers are still widely used in today's life despite all environmental issues attributed to them. Replacing synthetic polymers with natural biodegradable polymers has been considered as a way of reducing these environmental impacts partially, if not completely. Hydroxypropyl xylan (HPX) a water soluble natural polymer from xylan has been considered a potential candidate for applications in food packaging. In order to achieve this goal, certain properties of HPX such as film forming and barrier properties should be studied.

HPX forms transparent but relatively rigid films. Sorbitol, a commonly used food grade plasticizer was added to improve the film forming properties of HPX. Cellulose nanocrystal (CNC) was added to improve barrier properties of the plasticized films. Inverse gas chromatography (IGC) was used to study the permeability of water through neat HPX film and HPX films containing sorbitol and CNC over the temperature range of 120 – 160 °C. Rotary evaporator was used to coat HPX with and/or without additives on inert support (glass beads). The IGC column was filled with the coated beads for the experiments (the details of the method are presented in Chapter 4).

Using IGC, diffusion and solubility coefficients at infinite dilution were measured and the corresponding permeability coefficients were calculated. It was found that almost 40 wt% of sorbitol would yield a HPX film with desirable flexibility, as quantified by its glass transition temperature (T_g). Also, addition of 1–5 wt% CNC to the plasticized films significantly decreased the diffusivity of water. In particular, the infinite dilution diffusion coefficient of water for the HPX film with 35 wt% of sorbitol and 5 wt% CNC was comparable to that of the bare HPX film. The diffusion data suggest that effects of sorbitol and CNC on the water diffusivity follow the

free volume theory. Based on the results, neat HPX films, films containing 40 wt% of sorbitol (as the best film forming concentration) and films with 35 wt% sorbitol and 5 wt% CNC (as the films least diffuse to water) were selected for the next steps of the experiments.

The selected films (from now on defined as HPX, HPX/Sorbitol and HPX/Sorbitol/CNC) were used for studying permeability of primary alcohols vapour (C_1 - C_4) representing aroma. It was observed that the alcohols exhibited lower solubility (three orders of magnitude) and diffusivity (two to three orders of magnitude) than that of water in the neat HPX film. Solubility coefficient showed a minimum over the range of the molecular weight of the selected alcohols. However, the diffusion coefficient decreased monotonically with increasing alcohol's molecular weight. Presence of sorbitol decreased solubility coefficients slightly but increased diffusion coefficients by about one order of magnitude. However, adding CNC to the plasticized film did not alter the solubility coefficients much but decreased diffusion coefficients by approximately half of the values of the HPX/Sorbitol film. Permeability was observed to decrease with increasing alcohols' molecular weight. This implies that diffusivity controls the permeability of the alcohols at high molecular weights. As expected, sorbitol increases while CNC decreases permeability. However, effects of additives are stronger for methanol and ethanol than for propanol and butanol. Temperature also exerts stronger effects for methanol and ethanol than for propanol and butanol. The above observation is likely due to the differences in the abilities of the low and high molecular weight alcohols to form hydrogen bonds with HPX, sorbitol and CNC.

Further, effect of relative humidity (RH) on transport properties of the alcohols was studied at (RH) values of 30%, 50% and 70% of the carrier gas (helium). Diffusion coefficients of the alcohols showed a maximum at about 50% RH in all films. And solubility coefficients of the

alcohols were more or less insensitive to the RH. Permeability coefficients of the alcohols exhibited a maximum at around 50% RH as well suggesting that diffusion, not dissolution, dominated the permeability behaviour. The RH dependence of diffusion, thereby permeability, was attributed to the combined effects of plasticizing, swelling, water clustering and alcohol-water clustering. The measured weight-fraction-based Henry's constants suggested that water contents in the films were relatively low; suggesting that water clustering might only take place in the neat HPX film at 70% RH.

Preface

Chapter 2 of this thesis is accepted for publication as: F. Bayati, Y. Boluk, and P. Choi, “**Using Wood Fibers in Food Packaging**”, *Journal of Science and Technology for Forest Products and Processes (J-FOR)*. I was responsible for manuscript composition.

Chapter 5 of this thesis was published as: F. Bayati, Y. Boluk, and P. Choi, “**Diffusion Behavior of Water at Infinite Dilution in Hydroxypropyl Xylan Films with Sorbitol and Cellulose Nanocrystals**”, *ACS Sustainable Chemistry and Engineering*, 2014, 2 (5), 1305-1311. I was responsible for data collection and analysis as well as the manuscript composition.

Chapter 6 of this thesis was published as: F. Bayati, Y. Boluk, and P. Choi, “**Inverse Gas Chromatography Study of the Permeability of Aroma through Hydroxypropyl Xylan Films**”, *ACS Sustainable Chemistry and Engineering*. 2015, 3 (12), 3114-3122. I was responsible for data collection and analysis as well as the manuscript composition.

Chapter 7 of this thesis was published as: F. Bayati, Y. Boluk, and P. Choi, “**Effect of Humidity on the Permeability of Alcohols in Hydroxypropyl Xylan Films**”, *ACS Sustainable Chemistry and Engineering*. 2016, 4 (5), 2578-2583. I was responsible for data collection and analysis as well as the manuscript composition.

Dedication

To my dear husband, Abolfazl, for his constant support and encouragement along the way

To my parents for their unconditional love and sacrifices for me to achieve my goals

Acknowledgements

I would like to express my gratitude to Dr. Phillip Choi for motivations, kindness, patience, knowledge, and all the valuable advice he provided me with through the time of research and writing the thesis. I would also like to thank Dr. Yaman Boluk and his research group for the valuable discussions we had and technical supports I received from their research laboratory. I must also acknowledge NSERC Innovative Green Wood Fibre Product Network for the financial support and Alberta Innovates – Technology Future for providing the cellulose nanocrystal samples.

Table of Contents

Chapter 1	1
1. Motivation	1
1.1. Problem statement	1
1.2. Approach	2
1.3. Objectives	6
Chapter 2	8
2. A Short Review of Using Wood Fibres in Food Packaging	8
2.1. Introduction	8
2.2. Petroleum-Based Polymers	11
2.3. Natural polymers	14
2.3.1. Cellulose	16
2.3.2. Cellulose Nanocrystals (CNC)	18
2.3.3. Hemicellulose	19
2.4. Conclusion	24
Chapter 3	26
3. Theory	26
3.1. Transport in polymers	26
3.2. Theory of Permeability in Polymers	30
3.2.1. Solubility of small molecules in polymers	32
3.2.2. Diffusivity of small molecules in polymers	33
3.3. Free Volume Theory	34
Chapter 4	39
4. Method	39
4.1. Brief History of Inverse Gas Chromatography	39

4.2.	Inverse Gas Chromatography.....	40
4.2.1.	Finite Concentration and Infinite Dilution.....	43
4.3.	IGC Components.....	43
4.3.1.	Carrier gas.....	44
4.3.2.	Columns Types.....	45
4.3.3.	Detector.....	46
4.4.	Theory of Chromatography.....	47
4.4.1.	Rate Theory and Plate Theory [113].....	49
4.4.1.1.	Plate theory.....	50
4.4.1.2.	The Rate Theory According to Van Deemter.....	51
4.5.	Solubility Coefficient.....	58
Chapter 5.....		64
5.	Diffusion Behavior of Water at Infinite Dilution in Hydroxypropyl Xylan Films with Sorbitol and Cellulose Nano Crystals.....	64
5.1.	Introduction.....	64
5.2.	Inverse Gas Chromatography Theory.....	67
5.3.	Materials and Method.....	70
5.3.1.	Materials.....	70
5.3.2.	Preparation of Hydroxylpropyl Xylan.....	70
5.3.3.	Differential Scanning Calorimetry.....	70
5.3.4.	Inverse Gas Chromatography Procedure.....	71
5.4.	Results and Discussion.....	74
5.5.	Conclusion.....	85
Chapter 6.....		86
6.	Inverse Gas Chromatography Study of the Permeability of Aroma through Hydroxypropyl Xylan Films.....	86

6.1.	Introduction	86
6.2.	Theory	88
6.3.	Materials and Method.....	92
6.3.1.	Materials.....	92
6.3.2.	Column preparation.....	92
6.3.3.	Inverse gas chromatography procedure.....	94
6.4.	Results and Discussion.....	95
6.4.1.	Infinite dilution solubility coefficient	95
6.4.2.	Infinite dilution diffusion coefficient	101
6.4.3.	Permeability coefficient	105
6.5.	Conclusion.....	112
Chapter 7.....		113
7.	Effect of Humidity on the Permeability of Alcohols in Hydroxypropyl Xylan Films	113
7.1.	Introduction	113
7.2.	Materials and Method.....	116
7.2.1.	Materials and Alcohols.....	116
7.2.2.	Column Preparation.....	117
7.2.3.	Inverse Gas Chromatography (IGC).....	118
7.3.	Results and Discussion.....	121
7.3.1.	Diffusion Coefficient.....	121
7.3.2.	Solubility Coefficient	125
7.3.3.	Permeability Coefficient	127
7.4.	Conclusion.....	128
Chapter 8.....		130
8.	Conclusions and Future Works.....	130

8.1. Conclusions	130
8.2. Future Work	132
Bibliography	135
Appendix A: Study of thermodynamic parameters of adsorption of small molecules on HPX films	160
A.1. Abstract	160
A.2. Theory	161
A.3. Experimental conditions.....	162
A.4. Results and Discussion.....	162
A.4.1. Enthalpy of adsorption.....	163
A.4.2. Gibbs free energy of adsorption	166
A.4.3. Adsorption constant.....	166
A.4.4. Weight fraction activity coefficient.....	167
Appendix B: Acetylation of HPX.....	172
B.1. Acetylation of HPX.....	172
B.2. FTIR analysis of HPX and APX	173

List of Figures:

Figure 1.1. Flexible packaging material market share 2008	2
Figure 2.1. Importance of packaging in protecting packaged food quality	9
Figure 2.2. Plastics end-use market (Industry Canada Estimates)	12
Figure 2.3. Percentage of plastics and other materials in landfills	14
Figure 4.1. GC column.....	41
Figure 4.2. Schematic of gas chromatography system	44
Figure 4.3. Gaussian profile of a peak. Peak widths are given in the dimension of retention	49
Figure 4.4. Graphical presentation of the A, B, and c terms in van Deemter equation	52
Figure 4.5. Relationship between gas flow rate and peak efficiency	55
Figure 4.6. Retention diagram for semicrystalline polymer].....	59
Figure 5.1. Molecular structures of a) the repeating unit of HPX b) Sorbitol ($C_6H_{14}O_6$).	67
Figure 5.2. DSC curves for HPX films with sorbitol.....	75
Figure 5.3. T_g of plasticized films as a function of weight fraction of sorbitol compared with two mathematical models	76
Figure 5.4. Effect of adding 1-5% CNC to plasticized HPX films on T_g (Data is presented as mean+ standard error for n=3).....	77
Figure 5.5. Van Deemter Plots for the neat HPX film at various temperatures from 120 °C to 170 °C	78
Figure 5.6. Effect of sorbitol concentration on the diffusion coefficient of water at various temperatures.....	81
Figure 5.7. Effect of adding CNC to HPX films with 60%w/w HPX (40%w/w Sorbitol) on diffusion coefficient of water at various temperatures	81
Figure 5.8. Inverse temperature dependence of the diffusion coefficient of water in HPX films with various concentrations of sorbitol.....	83
Figure 5.9. Inverse temperature dependence of the diffusion coefficient of water in HPX films with 60 wt % of HPX and various concentrations of sorbitol and CNC.	84
Figure 6.1. SEM of glass bead supports coated with HPX films.....	93
Figure 6.2. Dependence of infinite dilution solubility coefficient of alcohols in HPX films with and without additives on molecular weight of alcohols at 120 °C □, 130 °C Δ, 140 °C ○, 150 °C ◇ and 160 °C *	96

Figure 6.3. Temperature dependence of solubility and diffusion coefficients of water in HPX films. (symbols representing data for HPX: solid, HPX/Sorbitol: patterned and HPX/Sorbitol/CNC: open).....	98
Figure 6.4. Temperature dependence of the solubility coefficient of selected alcohols (Methanol □, Ethanol Δ, Propanol ○, Butanol ◇) in HPX films.	99
Figure 6.5. Dependence of infinite dilution diffusion coefficient of alcohols in HPX films with and without additives on molecular weight of alcohols at 120 °C □, 130 °C Δ, 140 °C ○, 150 °C ◇ and 160 °C *.....	102
Figure 6.6. Temperature dependence of infinite dilution diffusion coefficient of alcohols (Methanol □, Ethanol Δ, Propanol ○, Butanol ◇) in HPX films. (Data regarding HPX reads from left axis, HPX/Sorbitol and HPX/Sorbitol/CNC read from right axis).....	104
Figure 6.7. Dependence of infinite dilution permeability coefficient of alcohols in HPX films on molecular weight of alcohols at 120 °C □, 130 °C Δ, 140 °C ○, 150 °C ◇ and 160 °C . (Data regarding HPX reads from left axis, HPX/Sorbitol and HPX/Sorbitol/CNC read from right axis).....	106
Figure 6.8. Effect of temperature on permeability coefficients of alcohols (Methanol □, Ethanol Δ, Propanol ○, Butanol ◇) in HPX films.	111
Figure 6.9. Effect of temperature on the permeability coefficient of water in HPX, HPX/Sorbitol and HPX/Sorbitol/CNC films.	111
Figure 7.1. A Schematic diagram of the humidifier setup used for humidifying the carrier gas	119
Figure 7.2. Infinite dilution diffusion coefficients of alcohols in HPX, HPX/Sorbitol and HPX/Sorbitol/CNC at 120 °C and under different levels of relative humidity.....	125
Figure 7.3. Infinite dilution solubility coefficients of alcohols in HPX, HPX/Sorbitol and HPX/Sorbitol/CNC at 120 °C and under different levels of relative humidity.....	126
Figure 7.4. Infinite dilution permeability coefficients of alcohols in HPX, HPX/Sorbitol and HPX/Sorbitol/CNC films at 120 °C and under different levels of relative humidity.	128

List of Tables:

Table 2.1. Schematic illustration of various sugar units of hemicelluloses.....	21
Table 5.1. Concentrations of HPX solutions used for the preparation of the films and coating of the glass beads.....	73
Table 5.2. Specifications of the packed columns.....	73
Table 5.3. Infinite dilution diffusion coefficients of water in HPX films with different amounts of sorbitol and CNC at various temperatures	79
Table 5.4. Dependence of the activation energy of water diffusion in HPX films on the sorbitol and CNC concentrations (films contained 60 wt % HPX).	84
Table 6.1. Specifications of the IGC columns	94
Table 6.2. Measured infinite dilution solubility coefficients (cm^3 [STP]/ cm^3 .atm), infinite dilution diffusion coefficients ($\times 10^{-11}$ cm^2/s) and calculated infinite dilution permeability coefficients ($\times 10^{-11}$ cm^3 [STP]/ cm .atm.s) of alcohols and water in HPX films with and without additives at 120-160 °C.....	100
Table 6.3. Activation energies of diffusion for solvents in HPX films	104
Table 6.4. Permeability coefficients of methanol, ethanol and water in the studied polymers at 120 °C compared to polymers that are commonly used in food packaging.....	108
Table 7-2. Measured infinite dilution solubility coefficients (cm^3 [STP]/ cm^3 .atm), infinite dilution diffusion coefficients ($\times 10^{-11}$ cm^2/s) and calculated infinite dilution permeability coefficients ($\times 10^{-11}$ cm^3 [STP]/ cm .atm.s) of alcohols in HPX films with and without additives at 120 °C and under different levels of relative humidity.	122
Table 7-2. Estimated water contents in HPX films at 120 °C based on Henry's law.....	123

List of Symbols:

A, Eddy Diffusion	EVOH, Ethylene Vinyl Alcohol
AcGGM, Acetylgalactocomannan	Fc, Corrected Volume Flow Rate
B, Longitudinal Diffusion	FID, Flame Ionization Detector
B ₂ , Second Virial Coefficient	GC, Gas Chromatography
C, Resistance to Mass Transfer in Stationary Phase	H ₁₂ ⁰ , Weight-Fraction-Based Henry's Constant
C _D , Concentration of sorbed/ penetrant molecule	h (hr), Hour
CMA, Cellulose Monoacetate	H, Height Equivalent to one Theoretical Plate (Plate Height)
CNC, Cellulose Nanocrystals	HDPE, High Density Polyethylene
CTA, Cellulose Triacetate	HETP, Height Equivalent to one Theoretical Plate (Plate Height)
C-K, Couchman and Karasz Equation	HPC, Hydroxypropyl Cellulose
D, Diffusion Coefficient	HPX, Hydroxypropyl Xylan
D ₀ , Diffusion Pre-Exponential Factor	IGC, Inverse, Gas Chromatography
d _f , Thickness of Stationary Phase	j, James Martin Correction Factor (Compressibility Factor)
DSC, Differential Scanning Calorimetry	J, Permeation Flux
D _p , Diffusion Coefficient in Polymer	k, Partition Ratio
E _a , Activation Energy	K, Partition Constant
EC, Ethyl Cellulose	k _D , Henry's Coefficient (Solubility)
E _D , Activation Energy of Diffusion	
E _p , Activation Energy of Permeation	

kDa, Kilo Daltons	t_f , Retention Time of Non-Reacting Indicator
L, Column Length	t_m , Helium or Air Retention time
LDPE, Low Density Polyethylene	t_r , Retention Time of Solvent
m, meter	T, Temperature
M, Molecular Weight	TCD, Thermal Conductivity Detector
N, Number of Theoretical Plates	T_{col} , Column Temperature
PET, Polyethylene	T_{flow} , Temperature of Flow Meter
p, Partial Pressure of the Solvent Molecule	T_g , Glass Transition Temperature
P, Permeability Coefficient	TGA, Thermal Gravimetric Analysis
P_0 , Permeability Pre-Exponential Factor	u, Carrier Gas Linear Velocity
PET, Poly(Ethylene Terephthalate)	v_1 , Solvent Partial Molar Volume
PHB, Poly (3-Hydroxybutyrate)	V_g^0 , Specific Retention Volume
P_i , Inlet Pressure	V_f , Fractional Free Volume
P_o , Outlet Pressure	V_N , Net Retention Volume
PS, Polystyrene	w_p , mass of polymer
R, Universal Gas Constant	W, fractional Loading of the Polymer
r_s , Average Radius of Inert Support	$W_{1/2}$, Peak Width at Half Height
RH, Relative Humidity	Wt%, Weight Percent
S, Solubility Coefficient	WVP, Water Vapor Permeability
S_0 , Solubility Pre-Exponential Factor	WVTR, Water Vapour Transmission Rate
SEM, Scanning Electron Microscopy	

Chapter 1

1. Motivation

1.1. Problem statement

“Where You Find BioProducts You Find the Future”[1]

Due to wide range of properties, synthetic polymers are widely used in numerous applications nowadays (Figure 1.1). The very first drawback of using this class of materials is their limited bio-degradability which makes them a great danger to environmental sustainability. 40% of synthetic polymers are used for packaging industry which is more than 13 and 14 million tonnes per year in Western Europe and USA, respectively. Almost 40% of the polymers used for packaging applications are disposed in landfills, or incinerated which cause air pollution. A small portion of the synthetic polymers are recyclable, like PET [2]. Replacing synthetic polymers with their biopolymer counterparts is considered one of the major ways of reducing this environmental impact. Much research has been done on producing commercial biopolymers to replace synthetic polymers. Using natural polymers instead of traditional synthetic polymers would be advantageous due to their availability, lower cost and biodegradability, when they can show competitive properties [3]. In addition, excess of waste material from agriculture, forestry and pulp and paper industry can be converted to a valuable source for production of natural polymers [4]. Bio-chemicals have a potential market worth of \$1.7 billion in Canada, with a potential of 280 million tonnes of forest-derived biomass available for production and industrial use without interfering with current forestry operations which are currently around 500 types of bio-products[1]. Polysaccharides -cellulose, lignin, and hemicelluloses- the main components of

plants and woods, belong to this class of natural polymers. Owing to their competitive properties, this class of polymers and their derivatives found many applications in food, textile, pharmaceutical and other industrial applications [5]. In this study, with the consideration that polysaccharides generally show good barrier properties, we have selected a modified hemicellulose to investigate its potential to be used as a barrier film in food packaging. More specifically, this study investigates the potential of hydroxypropyl xylan (HPX), a water soluble chemically modified xylan, as a water and aroma barrier material for food packaging.

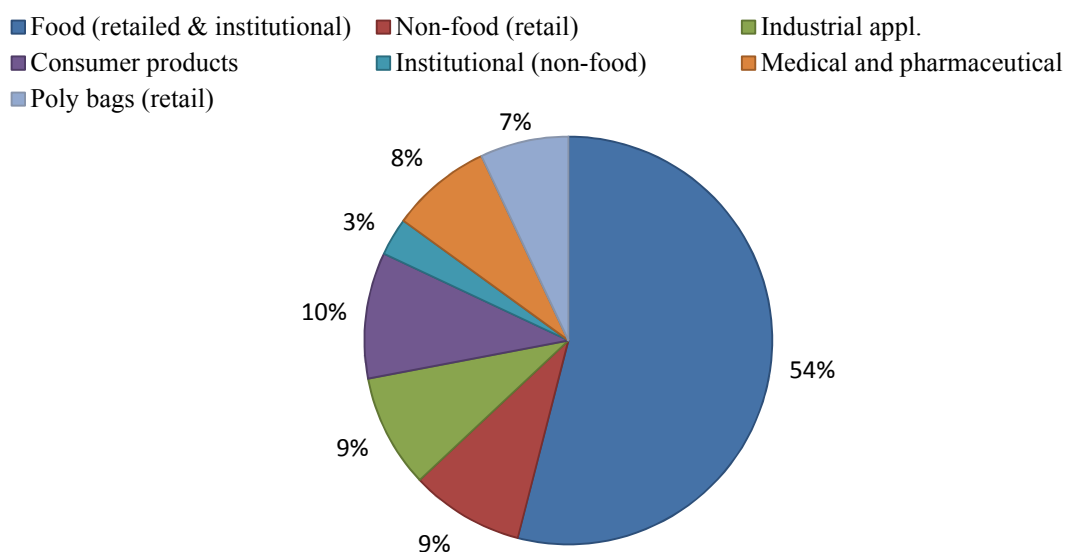


Figure 1.1. Flexible packaging material market share 2008 (Adopted from Flexible Packaging Association)

1.2. Approach

Polymers with barrier properties can be defined as macromolecules with the ability to limit transport of gases, vapors and liquids. Depending on the end-use application, a particular

macromolecule should be able to provide sufficient barrier to particular molecules of interest. Unfortunately, it is difficult to find a polymeric material which has high barrier properties to every gas and vapor while having good mechanical, thermal and optical properties let alone being inexpensive, recyclable and easy to process. Therefore, selecting a polymer for specific application involves a compromise between good barrier and mechanical properties on one hand and economic and environmental considerations on the other hand. In order for a new candidate polymer (in this case with natural source) to be considered as a potential for food packaging application, a comprehensive study of the aforementioned properties is required. Results of such study will determine the applicability of the new candidate comparing to common materials in use.

Being biodegradable, with renewable resources available, natural polymers logically reduce environmental concerns. Also, when the oil price rises, natural polymers are more economic as they are obtainable from cheap and readily available resources. With over 401 million hectares of forests, which is 10% of the earth's forests, Canada is a global leader in forest products export. It has much resources available to replace synthetic polymers with natural polymers with commitment to research in this area [1]. However, yet there is much research required for natural polymers to be able to gain a major role in the packaging market, because of lower mechanical and barrier properties compared to especially crafted synthetic polymers. The main concern which is the barrier properties of selected polymer for packaging applications remains as the main purpose of the current study.

The main component of plants, cellulose (which is 40-50% of biomass) and its derivatives have found their way in packaging industry, while hemicelluloses which are the main constituents of wood and other plants (25-35% of plants structure) and exist in major quantities in agricultural

waste, are remained obscure in this industry [1], [2]. Among the hemicelluloses, xylans which are the main hemicelluloses found in hardwood have been used in many applications, such as adhesives, thickeners, stabilizers, decorative paints and hydrogen. Now the question is: Can xylan and its derivatives which have shown some film forming abilities, be used as a film or coating in food packaging material? In order to meet this purpose, films produced from xylan should be able to provide promising barrier properties to various molecules (e.g. water, aroma compounds, oxygen, CO₂, etc.) depending on the end-use application.

Chemical modification of xylan with propylene oxide results in preparation of hydroxypropyl xylan (HPX) which is water soluble, with the ability to form uniform films from its aqueous solution which has the potential to be used in food packaging. Although, mechanical properties are not the main focus of this study, we tried to improve the flexibility of the films as it is a key factor in the entire process. Low molecular weight plasticizers such as glycerol, xylitol and sorbitol are frequently used for further improvement of flexibility and mechanical properties of food packaging material [2]. We chose sorbitol for improving film formation as the prepared films from sorbitol were visually more uniform and had better transparency compared to the two other plasticizers. However, adding plasticizer reduced barrier properties of the films. Several studies have shown improvement of barrier properties of biopolymers by the addition of a recyclable and natural polymer: cellulose nanocrystals (CNC) [6],[7],[8],[9]. Crystalline structure and rigid hydrogen bonded network of CNC can be utilized to improve barrier properties [6]. Also, due to the high surface area and aspect ratio, a small concentration of CNC can improve the barrier properties significantly [10]. So, sorbitol and cellulose nanocrystals (CNC) were the two additives added to HPX to improve film formation and barrier properties of the HPX films.

In addition to effect of plasticizers and fillers (as mentioned above) other factors affect barrier properties: nature of the polymer, nature of the penetrants (molecular weight, polarity and etc.) and environmental factors (temperature and humidity) that we tried to address in this study.

Water vapour and low molecular weight alcohols (representing aroma in foods) were selected as the solvents/penetrants for the purpose of this study. Infinite dilution of the solvents was the region of concentration used in this work, to determine barrier properties of the films when low concentration of solvents is available in the environment. This can be the case for very small concentration of aroma molecules in food or when the HPX films may be used as an inner layer accompanying a water barrier polymer in multi-layer films. In addition, infinite dilution data give valuable information in terms of molecule-molecule interaction compared to the finite concentration region of the solvents. Effect of molecular weight of the solvents/penetrants was also studied on the barrier properties.

Barrier properties were studied in form of permeability coefficients using the technique of inverse gas chromatography (IGC). IGC is proved to be a fast, reliable technique which has shown to be able to measure various thermodynamic properties of polymers within short time compared to conventional gravimetric methods. IGC can measure diffusion coefficient in polymers within minutes and hours while the gravimetric methods require days and weeks when the diffusion is too slow. Also, due to high sensitivity of the method, the method is applicable at very low amount of the solvent ($\sim 10^{-9}$ moles) while applicability of conventional methods is difficult when the amount of solvent is vanishingly small or at temperatures close or below the glass transition temperature of the polymer [11]. Meanwhile, in order to get the sorption data at infinite dilution with gravimetric methods, data from finite concentration region should be extrapolated to infinite dilution while with IGC, the data at infinite dilution can be directly

determined. Solubility coefficient and diffusion coefficient were the two parameters measured for determining permeability coefficient of the aforementioned solvents in HPX films. To study environmental effects on the barrier properties of HPX films, experiments were carried over wide range of temperature and humidity. In order to reduce effect of adsorption on diffusion coefficient measurements, the experiments were carried over temperatures close and above the glass transition temperature (T_g) of the HPX polymer. So, in the first step, T_g of the films was determined using differential scanning calorimetry (DSC) and then the experiments were designed accordingly.

Changes to the sorption characteristics of polymers upon introduction of humidity is one of the main concerns in food packaging. Humidity has a considerable effect on permeability properties of most of the polymers, particularly the hydrophilic polymers. Most of the researches have been conducted on effect of humidity on permeability of gases. However, the few studies on the subject, for permeability of organic vapors (e.g. alcohols) have shown contradictory results [12], [13], [14]. We conducted a series of experiments on the permeability behaviour of the alcohols on the HPX films to see how water change permeability in the films when the films contain sorbitol and CNC.

1.3. Objectives

Based on the above discussion, the objectives of this study can be achieved in the following chapters as described below:

In Chapter 5, the following objectives will be discussed:

- Preparation of hydroxypropyl xylan from xylan.
- Preparation of HPX films with different concentrations of sorbitol and CNC.

- Effect of addition of CNC and sorbitol on glass transition temperature of the films.
- Effect of addition of CNC and sorbitol on diffusion coefficient of water.
- Temperature dependency of diffusion coefficient of water in HPX films.

Chapter 6 will achieve:

- Permeability of low molecular weight alcohols and water in selected HPX films by investigating the effects of:
 - Solvent molecular weight on solubility, diffusivity and permeability coefficients of alcohols in HPX films,
 - Addition of CNC and sorbitol on permeability of water and alcohols in HPX films

And in Chapter 7, we will investigate the effect of humidity on the mass transport of alcohols in HPX film.

Chapter 2

2. A Short Review of Using Wood Fibres in Food Packaging

2.1. Introduction

Over the past several decades, the food packaging technology has improved dramatically. Such improvement is somewhat driven by the fact that packaged food needs to travel longer journeys from farms or factories to reach their consumers as well as to have longer shelf life. Good packaging helps the merchandising, marketing and distribution of various food products to farther locations that were not possible before. Another important function of packaging is to make food products more appealing to the consumers. It is a common belief in the food industry that food products and their packaging are considered to be inseparable and properties of one effect and determine those of the other, thereby the ultimate profit of the industry. Therefore, selection of the right packaging material for the food item in hand is an important decision [15], [16]. A suitable packaging material must be able to protect food from oxygen (which causes oxidation and deterioration of the food), loss of carbonation, transport of moisture (loss or gain on moisture), contamination and infection, permeation of solvents and odours and flavours of the food, and absorption of flavour components by the packaging material (Figure 2.1) [9], [13], [17].

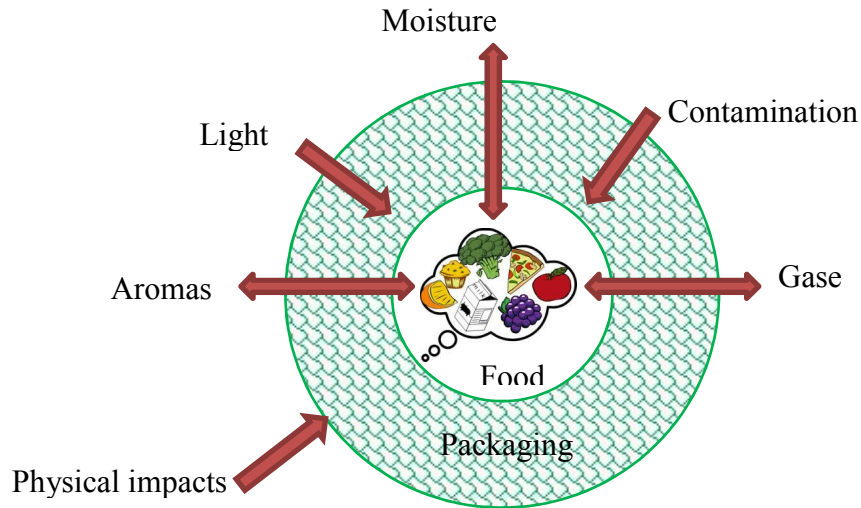


Figure 2.1. Importance of packaging in protecting packaged food quality

Among all properties, barrier properties such as water vapour transmission rate (WVTR), aroma permeability and oxygen permeability are the most important criteria when it comes to the selection of a polymer for food packaging. Based on the food for which the packaging is used, the packaging should meet certain properties. For example, according to Oswin [18], for relatively dry foods such as biscuits, water vapour permeability (WVP) of the packaging film should be lower than $2.1 \text{ nanomoles.N}^{-1}.\text{s}^{-1}$ ($378 \times 10^{-10} \text{ gr.m}^{-2}.\text{s}^{-1}.\text{Pa}^{-1}$) to prevent absorption of water onto the biscuit whereas for bread, water permeability of $20\text{-}50 \text{ nanomoles.N}^{-1}.\text{s}^{-1}$ is sufficient to prevent formation of mold while keeping the bread dry. For fresh cuts of vegetables that still breathe oxygen and exhale carbon dioxide, using a film with low permeability develops anaerobic conditions and in the moist atmosphere causes the vegetables to deteriorate. So, water vapour permeability of about $15 \text{ nanomoles.N}^{-1}.\text{s}^{-1}$ ($2700 \times 10^{-10} \text{ gr.m}^{-2}.\text{s}^{-1}.\text{Pa}^{-1}$) and oxygen permeability of over $10 \text{ picomoles.N}^{-1}.\text{s}^{-1}$ ($1.6 \times 10^{-10} \text{ gr.m}^{-2}.\text{s}^{-1}.\text{Pa}^{-1}$) is needed for most of the vegetables. Then again, another important group of food, red meat, needs water vapour permeability of $5\text{-}25 \text{ nanomoles.N}^{-1}.\text{s}^{-1}$ ($900\text{-}4500 \times 10^{-10} \text{ gr.m}^{-2}.\text{s}^{-1}.\text{Pa}^{-1}$) and oxygen permeability

of about 20 picomoles. $\text{N}^{-1}.\text{s}^{-1}$ ($3.2 \times 10^{-10} \text{ gr.m}^{-2}.\text{s}^{-1}.\text{Pa}^{-1}$) to prevent meat from getting rotten and drying out to keep the colour. For frozen meat, keeping the colour is not important. Instead, preventing dehydration in a freezer environment is more important, water vapour permeability lowers than 500 nanomoles. $\text{N}^{-1}.\text{s}^{-1}$ ($9.0 \times 10^{-6} \text{ gr.m}^{-2}.\text{s}^{-1}.\text{Pa}^{-1}$) is desired.

In addition to water, oxygen, and CO_2 , aromas and flavours are the other molecules that can transport through the packaging and change the quality of packaged food. If transport of oxygen, water and CO_2 are controlled, concerns for deterioration of the food will be reduced while if natural flavours of food can be preserved longer, there will be no need to add artificial flavours to keep the quality of the food. Unlike glass and metal, polymers have different barrier properties to small organic molecules, aromas, flavours, and additives in the food. The barrier properties of the packaging polymers are strictly related to the nature of the polymer: e.g., its chemical structure and chemical functional groups (polar or nonpolar groups), its glass transition temperature (T_g), its thermal and mechanical history and its crystalline to amorphous phase ratio, of the polymer [19]. Composition of the packaged food (e.g., flavour and aroma content, water content, pH, fat and grease content, etc.) and other environmental factors, mainly temperature and relative humidity [13] affect the sorption characteristics of the packaging materials and thus their barrier properties.

Although materials with low permeability are most desirable for the food packaging industry, the other important factor for a good packaging material is its cost since the cost of a packaging material represents about 17% of the total cost of the final product (Nestlé average). So, reducing the cost of packaging will be highly beneficial.

2.2. Petroleum-Based Polymers

Packaging materials are mostly made from glass, metals such as aluminum and steel, wood or wood derivatives like paperboard and folding cartons [16]. Glass and metals provide a nearly absolute barrier to chemical or other environmental factors but not all the packages can be made from glass and metal due to difficulty of handling these materials. Concerns such as brittleness, thermal shock and heavy weight (high transportation costs) are some of the disadvantages of using glass in packaging. The main disadvantage of metals such as aluminum and steel is their high cost even though they can be used in specific applications. In order to meet the optimum properties and costs, use of combination of two or more of these basic materials was developed [20]. Improving barrier properties by using multiple layered structures and improving transparency of a packaging film with good barrier properties are also some of the desired options in improving the packaging. Many changes in packaging of different food products have been proposed.

Introduction of plastics that are now widely used in food packaging was a breakthrough in the industry. The main reasons for the plastics to take over the market can be attributed to having wide range of barrier and mechanical properties, ease of design and manufacturing proper shapes and structures compared to other packaging materials. Also, lower costs and weight, as well as the possibility of being used in a wider range of temperatures and microwaves are some of the other reasons for the extensive use of plastics in food packaging [16].

Plastics are used in three main applications – packaging, construction and automotive. Nonetheless, packaging applications (covering 39% of end-use market) remains the major use of plastics (Figure 2.2) [21].

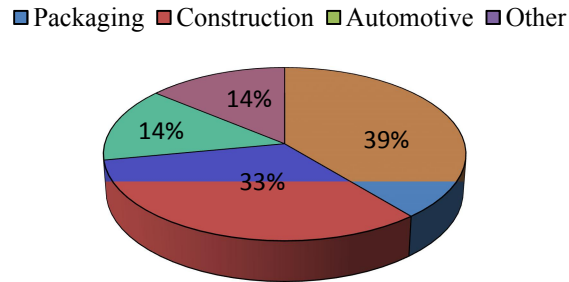


Figure 2.2. Plastics end-use market (Industry Canada Estimates) [21]

According to Schaper [15], until early 1970, glass, metal and poly(vinylidene chloride) (PVDC) were the only packaging materials. In 1973, ethylene vinyl alcohol (EVOH) resins with high barrier properties were introduced and used as flexible films for food packaging. In late 70s, combinations of various packaging materials started to be used for different applications. One of the greatest combinations was a structure of LDPE-Paperboard-Tie-Foil-Tie-LDPE for citrus juice packaging. However, due to selective absorption of flavours from the juice and shortening the shelf life of the package, a new structure of LDPE-Paperboard-Tie-EVOH-Tie-EVOH was used which would prevent flavour scalping due to the presence of EVOH layers in contact with the food as well as being a better oxygen barrier. Generally, for a polymer to be an excellent barrier, it is important to have some degree of polarity, chains with high rigidity, close chain to chain packing (crystallinity), some bonding and attraction between chains, and high glass transition temperature [22], [23]. Nowadays, there are a lot of polymers used in food packaging

industry with great thermal and mechanical properties, various gases, aroma, flavour, solvent permeability and water transmission rate, great chemical and heat resistance [19]. Most of the nonpolar hydrocarbon polymers are good water barriers but have poor gas barrier properties. On the other hand, polar polymers such as nylon or ethylene vinyl acetate that contain hydroxyl groups are good gas barriers but poor water barriers.

Despite all the great properties (great barrier properties, temperature resistance, lower cost, ease of processing) that make synthetic plastics attractive to the industry, ecological and environmental concerns regarding their solid waste management are growing fast. Two methods are generally used for disposing plastics: landfills and incineration. With 30% of municipal solid waste in North America being derived from packaging [24] and with the large share of plastics in landfill (Figure 2.3), use of lands for landfills is becoming scarce and expensive and disposing the plastics in landfills is not efficient. Incineration has become the common practice in many parts of the world: 40% in Germany, 50 to 75% in Sweden and Switzerland, 55% in Japan [16]. However, this method also, has its own problems including energy costs and air pollution. In order to reduce environmental concerns regarding the solid wastes from plastics, some solutions are applied. The first solution to reduce some of the environmental concerns is to redesign and to use less packaging materials. But this cannot solve the issue since the concerns about disposing the materials still exist. The other option will be recycling of the packaging materials. Currently, only a small portion of such plastics are recycled, only 1%, while 45% of aluminum, 30% of papers and 25% of glasses are recycled. [16] PET and HDPE are the two major plastics that are widely used in food packaging and thus there has been more focus on recycling these materials. In addition to environmental issues, dependency of plastic industry on the price of crude oil has a great economic impact on the plastic market [25]. Also, with the fossil resources

being scarce and non-renewable, replacing synthetic polymers with polymers from alternative renewable resources is another way to help alleviate these concerns.

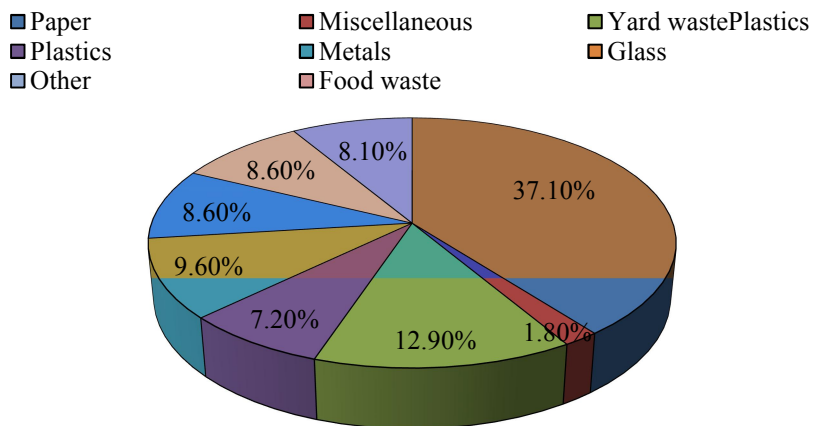


Figure 2.3. Percentage of plastics and other materials in landfills [16]

2.3.Natural polymers

Replacement of synthetic polymers with natural polymers has been considered to be a viable option of reducing the negative impact on the environment of using synthetic polymers. In fact, using natural polymers is advantageous due to their availability, lower costs and biodegradability, when they can show competitive properties [3]. The biodegradability is an important factor. Since recycling at the end of life cycle requires a lot of energy (environmentally and economically inefficient), the ability to biodegrade and compostability allows disposal of the material in the soil while the product of degradation is water, carbon dioxide and nontoxic inorganic compounds [19]. The aim of use of bioplastics is consistent with the life cycle of biomass, which includes conversion of natural resources to water and CO₂.

Natural polymers can be used as coatings on paper and paperboard or as bioplastics in the form of thin films for packaging. Usually, they show good barrier properties to fat but are moderate water vapour barriers. Also, weak mechanical properties and sensitivity to moisture is another disadvantage of bio-based polymers compared to petroleum-derived polymers. Much work has been conducted on biopolymers to improve their film-forming properties, transparency, and barrier and mechanical properties to make them an acceptable substitute for synthetic polymers used in packaging. Although commercial applications of these materials are still limited, the vast ongoing research will certainly bring up more applications in the future.

With respect to the source of biopolymers used in packaging, they can be categorized in three main groups [17], [26], [27]:

1) Polymers such as polysaccharides (cellulose, starch, chitin, etc.), lignin, proteins and lipids, which are directly extracted from natural sources. For example, regenerated cellulose, such as cellulose esters, cellophane, cellulose acetate, nitrocellulose, carboxymethyl cellulose (CMC), and ethyl cellulose are some of the derivatives of polysaccharides widely used in food packaging e.g. baked goods and fresh produce.

2) Polymers such as polylactide (PLA) or bio-PE which are produced from chemical synthesis from renewable bio-derived monomers. Polylactic Acid (PLA) derived from cornstarch, sugarcane, or other starchy sources has good mechanical and thermal properties and good barrier to flavor and aroma such as limonene.

3) Polymers such as polyhydroxyalkanoates (PHAs), polyhydroxybutyrate (PHB), Poly-3-hydroxybutyrate (PH3B), Polyhydroxyhexanoate (PHH), Polyhydroxyvalerate (PHV), and copolymers of hydroxybutyrate and hydroxyvalerate (PHBV) which are produced by

microorganisms or bacterial fermentation. PHAs, basically produced by bacterial fermentation from sugar, lipids, starch and cellulose, depending on the composition of monomer units, exhibit variety of mechanical properties from hard crystalline to elastic. They show intermediate to high oxygen barrier properties as well as being a good barrier to light frequency when pigmented which makes them suitable candidates for food packaging.

Natural polymers in the first group can be divided in two sub-groups with sources from animals, or wood and plants. However, our discussion will focus on the biopolymers from polysaccharides obtained from wood and plants that have been or the potential to be used for food packaging. This limits our discussions to cellulose and hemicelluloses, the two main components of plants.

2.3.1. Cellulose

Cellulose, lignin and hemicelluloses are the main components of plants and woods. In fact, their derivatives found many applications in food packaging, textiles, pharmaceutical and other industrial branches already [5]. Cellulose is the most abundant renewable organic material with annual production of more than 25 billion tons [28]. Cellulose-based materials have widely been used in packaging in forms of papers or cardboard for wrapping food, or as coatings, or flexible or rigid films. Cellulose with a crystalline and fibrillary structure is the main part of the structure of wood which includes 40-45% of the dry basis of wood. It is the most abundant natural linear polymer [29] which is made up of anhydroglucose ($C_6H_{10}O_5$) units which are joined together by 1,4 glycosidic bonds where the degree of polymerization is typically around 3,000-15,000 leading to molecular weight of 540-27,000 kDa [28], [30]. The hydroxyl groups of the repeating units form hydrogen bonds between the polymer molecules and cause crystalline packing of cellulose. Because of strong hydrogen bonds and fibrous structure of cellulose, it is

insoluble in most of the solvents. In order to make cellulose soluble in organic or inorganic solvents, chemical modification of cellulose is required.

The esterification is one way to improve solubility of cellulose in solvents. As a result, some of the cellulose esters such as cellulose acetate are useful in food packaging. Due to low gas and moisture barrier properties, cellulose acetates are used for baked goods and fresh products [27]. Cellulose acetate (CA), along with cellulose diacetate and cellulose triacetate have been widely used for packaging as a rigid film [31]. CA films coated with vinyl used for packaging have WVP of 1.1×10^{-12} to 1.7×10^{-12} $\text{g.m.m}^{-2}.\text{s}^{-1}.\text{Pa}^{-1}$ (WVTR 25.8 to 39.8 $\text{g.m}^{-2}.\text{day}^{-1}$) at 38 °C and 90% RH with film thickness of 22 μm [32]. Composite films of CA and keratin from wool waste have been used as compostable packaging [33]. Cellophane is the other widely used cellulose-based polymer that forms thin, clear, strong flexible films. Various organic solvents have been proposed for cellophane and cellulose fibres production to reduce environmental concerns due to the chemicals used [28], [34], [35]. Cellophane coated with nitrocellulose wax or poly(vinylidene chloride) (PVDC) is used for packaging of baked goods, processed meat, cheese and candies [36]. The esterified cellophane films with fatty acids decrease permeability of oxygen by 8% to the value of 3.7×10^{-14} $\text{cm}^3.\text{m.m}^{-2}.\text{s}^{-1}.\text{Pa}^{-1}$ at 25 °C and water vapour transmission rate (WVTR) of 8.3×10^{-3} $\text{g.m}^{-2}.\text{s}^{-1}$ (717.12 $\text{g/m}^2.\text{day}$) by 50% at 26 °C and 72% RH [37]. Methyl cellulose (MC), ethyl cellulose, hydroxymethyl cellulose, and hydroxypropyl cellulose are some of other commercial cellulose derivatives used in food packaging where one or more of the hydroxyl groups (-OH) on the anhydroglucose unit are replaced by methoxy (-OCH₃), ethoxy (-OC₂H₅) or hydroxypropyl (-OCH₂CH(OH)CH₃) [33], [36]. MC, for example, produces transparent, flexible films with promising oxygen barrier properties but poor water barrier properties [38]. Carboxymethyl cellulose (CMC) films used in packaging are generally

permeable to water vapor. Cross linking CMC with other copolymers such as starch or gelatin improves water vapor barrier properties [39]–[41]. Using lipids, inorganic or organic fillers, changing preparation methods and an optimum degree of substitution of CMC are some other ways to reduce WVP in CMC films [39], [40], [42].

2.3.2. Cellulose Nanocrystals (CNC)

Cellulose nanocrystals (CNC) is generally referred to cellulose particles with at least one dimension in nanoscale (diameter of 3-50 nm while the other dimensions can range from nanometers up to tens of micrometers).[28], [32] Similar to cellulose, CNCs are obtained from wood or non-wood biomass by removing amorphous cellulose, lignin, and hemicellulose.[43] CNC can be used as coating, film, filler, or in a composite structure used for food packaging. Because of crystalline structure, CNC improves mechanical and barrier properties (reduce oxygen and water vapor permeability) of the base polymer when used in biocomposites.[44] Being more than 60% crystalline together with the rigid hydrogen bonded network of cellulose nanocrystals can increase tortuosity and reduce the pore size for creating high barrier nanocomposites [45], [46].

Many studies have been conducted on studying effect of crystalline nanocellulose (CNC) on barrier properties of polymers used for food packaging. Sanchez-Garcia [47] showed that addition of 3 wt% CNC to water soluble carrageenan extracted from red algae reduced water vapor permeability up to 70% in the carrageenan matrix. They suggested application of this biocomposite for food packaging application. In another study by da Silva et al. [48] mechanical and water resistance properties of nanocomposite films from cassava starch plasticized with sucrose and inverted sugar were improved by adding CNC to the polymer matrix. The high crystallinity of the CNC resulted in reduction of water permeation.

CNC can also be used with water-soluble cellulose derivatives such as methyl cellulose (MC) and carboxymethyl cellulose (CMC) where the polymer matrix and nanocellulose are compatible and polar, or with cellulose derivatives such as cellulose acetate or cellulose acetate butyrate which are soluble in organic solvents. Saxenta et al. [6] produced xylan based films with low oxygen permeability from aqueous solution of xylan, sorbitol and CNC. Films containing CNC showed promising barrier properties compared to the films prepared solely from xylan and sorbitol. Using higher concentrations of CNC decreased oxygen permeability. In another study by Saxena and Raqauska [7] addition of 10% sulphonated CNC reduced water transmission rate of xylan films and films reinforced with 10% softwood kraft fibers 74% and 362%, respectively. Lagaron et al. [49] emphasized that crystalline structure of polymers improves barrier properties.

2.3.3. Hemicellulose

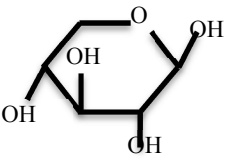
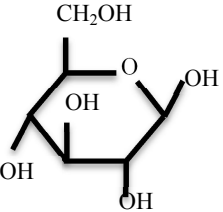
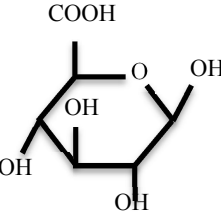
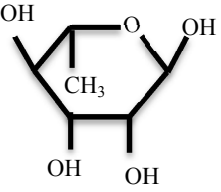
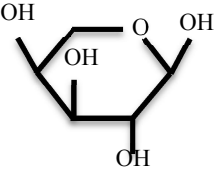
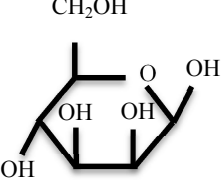
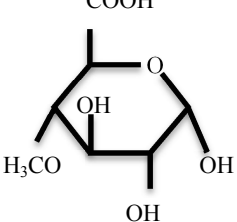
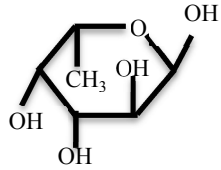
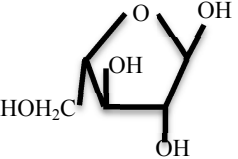
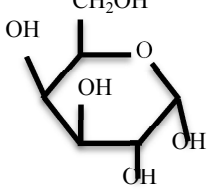
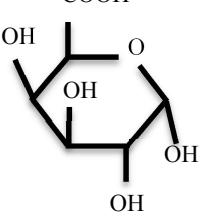
Hemicelluloses are the second abundant component in wood and plants after cellulose [50]. Hemicelluloses are heteropolysaccharides that are composed of several types of sugar units (combination of 5- and 6- carbo rings) arranged in different proportions and with different substituents. They are short-branched polymers with degrees of polymerization in the range of 50-300 and are amorphous in nature. Hemicelluloses are hydrophilic and are partially soluble in water. The main sugar components of hemicelluloses are shown in Table 2.1 [30], [50], [51]. Although cellulose and cellulose derivatives have found their way in the packaging industry, hemicelluloses with similar properties have not. Low molecular weight and heterogeneous structure are the reasons why hemicelluloses have less usage as a macromolecular substance, compared to starch and cellulose [52].

Native or modified forms of hemicelluloses are a potential renewable source of biopolymers that can be used in different areas like food and non-food applications. This is because they show

good properties for making adhesives, thickeners, stabilizers, decorative paints, film formers, gels, coatings and emulsifiers [30], [51]. Recently, they have received increasing attention as potential films or coatings for being used in the food packaging industry because of their film-forming properties. In order to meet this purpose, barrier properties of the hemicellulose-based films have been investigated by many researchers. Hartman et al. [53] studied oxygen barrier properties of O-acetylgalactocomannan (AcGGM). They found that AcGGM films containing 17.5 wt% of alginate exhibited the highest oxygen permeability compared to films plasticized with sorbitol and xylitol. In another study by Hartman et al. [54], it was found that benzylation of AcGGM formed strong, flexible films which showed lower oxygen permeability than alginate-AcGGM films while a multilayer film made up of lamination of benzylated AcGGM on the alginate-AcGGM exhibited significantly lower oxygen transmission rates. Water vapor permeability of plasticized β -glucan extracts from hulled barely, hull-less barely, and oats was studied by Tejinder [55]. Smooth, translucent, and homogeneous films showed water vapour transmission rates in the range of 0.47-0.60 g.m⁻².h⁻¹ (11.28-14.4 g.m⁻².day⁻¹) at 30 °C and 100% RH. In an attempt by Kayserilioglu et al. [56], wheat gluten was mixed with 0-40 % birchwood xylan and cast under acidic and alkaline conditions at different temperatures. Films cast at higher temperatures showed slightly lower water vapour transfer ranging from 6 g.m⁻².day⁻¹ at room conditions (approximately 20 °C and 35% RH) to 8 g.m⁻².day⁻¹ at 80 °C and 35% RH.

Although there has been a considerable amount of work on improving barrier properties of hemicelluloses but not much success has been obtained. Additional work is still required to enable them to compete with commercial polymers from non-renewable resources such as PET, LDPE, and PS (especially in terms of water vapour barrier properties) or with commercial polymers from natural resources such as water-soluble hydroxypropyl cellulose and starch

derivatives which have found many applications in the food industry (even as food additives in salad dressings) [57], [58].

PENTOSES	HEXOSEs	HEXURONIC ACIDS	DEOXY- HEXOSEs
<p>β-D-Xylose</p> 	<p>β-D-Glucose</p> 	<p>β-D-Glucuronic acid</p> 	<p>α-L-Rhamnose</p> 
<p>α-L-Arabinopyranose</p> 	<p>β-D-Mannose</p> 	<p>α-D-4-O-Methylglucuronic acid</p> 	<p>α-L-Fucose</p> 
<p>α-L-Arabinofuranose</p> 	<p>α-D-Galactose</p> 	<p>α-D-Galacturonic acid</p> 	

2.3.3.1. Xylan and its derivatives

The xylose is one of the important sugar units of hemicelluloses components [51]. Xylans are the second abundant biopolymers (with cellulose being the first) and the most common hemicellulose present in wood and other plants such as cereals, grasses, and herbs. Being the main component of hemicelluloses in many plants, xylan constitutes 20-35% total dry basis of plants. Xylan, with xylose content of 60-70%, is one of the highly branched, low molecular weight, non-cellulosic, noncrystalline heteropolysaccharides. The main sources of xylans are not only from wood, but also from other plants such as grasses, cereals and herbs [59]. Having been known for a long time, xylan-type polysaccharides have attracted much more attention recently. Willingness to develop new biopolymer-based materials and the availability of xylan type polymers from agricultural, wood and pulp and paper industries increases activities in research on xylan and its derivatives. Each year, large amount of xylans are produced in many countries such as Japan, Finland, Denmark, Germany, USA, and Canada [60]. Xylan is now mostly used for conversion to xylose, xylitol and furfural. It is widely used in animal feed, manufacture of bread, food and drinks, pharmaceutical and chemical applications, textiles, and bleaching of cellulose pulp and paper [59], [61], [62].

Although numerous xylan derivatives have been reported in literature, none of them have achieved commercial applications in food packaging. Owing to having high density of hydrogen bonds in xylans, it is difficult to dissolve xylans in most of the organic solvents. Besides, it is not always a great film former in its natural form. Therefore, substituting the hydroxyl groups of xylan with other chemical groups can result in production of film-forming material which can be used as edible or non-edible film and coating. Esterification can be used to improve solubility and film forming ability of xylans. Fundador et al. [63] synthesized hydrophobic xylan esters

with different alkyl chains with improved thermal and mechanical properties which could form films by solvent casting from chloroform solution. According to Šimkovic et al. [64], sulphation of xylan with low degrees of substitution forms partially water soluble films with good mechanical properties. Presence of more sulphate groups results in lower mechanical stability due to less intermolecular hydrogen bonds interaction. In another study by Goksu et al. [65], cotton stalk and birchwood xylan with different concentrations of lignin were used to form films. They found that 1 % (w/w lignin/xylan) was necessary to form films and addition of glycerol as a plasticizer resulted in more stretchable films. Fat addition improved water barrier property and hydrophobicity of arabinoxylan films similar to those of LDPE [66]. Escalante et al. [67] developed clear, flexible films from arabinoglucuronoxylan which showed great oxygen barrier properties. Addition of sorbitol increase oxygen permeability in arabinoxylan films. Some of the chemical modifications of xylan have been done with the purpose of making xylan soluble in organic or non-organic solvents; e.g., O-Benzyl xylan acetate in acetone, xylan butyrate in chloroform, xylan acetate in chloroform/ethanol, and tetrachloroethane [68]. In addition to xylan acetate, the derivative which has been well studied, other esters such as benzoate, caprate, lurate and etc. have been prepared [62]. Zhang and Whistler [69] produced films from corn hull arabinoxylan, plasticized with 0-22 wt % propylene glycol, glycol, glycerol, or sorbitol. They reported that films plasticized with 13% sorbitol were the best water vapour barrier films with water vapour permeability (WVP) of $0.23 \times 10^{-10} \text{ g.m}^{-1}.\text{s}^{-1}.\text{Pa}^{-1}$ (WVTR $101.38 \text{ g.m}^{-2}.\text{day}^{-1}$) at 22 °C and 54% RH with film thickness of 28 μm . High concentrations of glycerol increased permeability due to hygroscopic nature of plasticizer. Several other studies have conducted on producing water vapour barrier films [66], [70]–[73]. In all attempts, extracted arabinoxylan from maize bran was plasticized with 15 or 20 wt % glycerol and modified with palmitic acid

(C₁₆), oleic acid (C₁₈) triolein, or a hydrogenated palm kernel oil (HPKO). The lipid-based films reduced WVP from $1.38\text{-}1.77 \times 10^{-10} \text{ g.m}^{-1}.\text{s}^{-1}.\text{Pa}^{-1}$ (WVTR $143\text{-}338.6 \text{ g.m}^{-2}.\text{day}^{-1}$) for arabinoxylan films with 15 wt % glycerol to $0.93 \times 10^{-10}\text{-}1.24 \times 10^{-10} \text{ g.m}^{-1}.\text{s}^{-1}.\text{Pa}^{-1}$ (WVTR $80\text{-}234.1 \text{ g.m}^{-2}.\text{day}^{-1}$ at 25 °C and 22%-84% RH) in presence of 25 wt % HPKO $\text{g.m}^{-1}.\text{s}^{-1}.\text{Pa}^{-1}$. The values of WVP were yet 3-100 times larger than for synthetic films such as LDPE.

Chemical modification of xylan by substituting xylan's hydroxyl group by alkoxy or acetoxy substitutes helps induce its solubility in organic solvents or water. Jain et al. [62] have prepared hydroxypropyl xylan (HPX) form hydroxypropylation of xylan by reacting caustic solution of xylan with propylene oxide. The HPX product is a water soluble polymer that forms transparent uniform films from solvent casting of the aqueous solution. HPX barrier properties has been studied for food packaging applications [74], [75] and the results suggest that HPX modified with CNC has the potential to be used as aroma barrier along with a strong water barrier film.

2.4. Conclusion

Increasing demand in the performance of food packaging has driven the food industry to improve the packaging technology considerably over the past few decades. This has, in turn, increased the volume of petroleum-based polymers being used in the industry. Disposal of such non-biodegradable polymers has raised serious environmental concerns. As a result, replacement of these polymers with those obtained from natural resources has received significant attention in the past decade. Wood and plants, being the largely available renewable resources, are good candidates for the food packaging applications. Cellulose and hemicelluloses as the two main components of wood and plants have been the aim of many studies for their suitability for being used for food packaging. Although some of the biopolymers such as cellophane, cellulose acetate and hydroxymethyl cellulose have found commercial applications in food packaging, yet

much work is needed to produce biopolymers with competitive properties to petroleum-based polymers. Many researchers have used different chemical modifications such as esterification, hydroxypropylation and sulphation to improve solubility of biopolymers in solvents. Furthermore, using lipids, inorganic or organic fillers, cellulose nanocrystals and chemical modification are some of the methods investigated to improve barrier properties of biopolymers obtained from cellulose and hemicelluloses.

Chapter 3

3. Theory

3.1. Transport in polymers

As we mentioned in the previous chapters, the key factor determining the applicability of the HPX in packaging industry is its ability to promote or prohibit the transport of small molecules through the film. This type of problems is not attractive just to packaging industry and has been studied during last decades as it influences many different industrial processes. Drug delivery devices, membrane separation, fertilizers and pesticides gradual release and solvent stripping after polymerization are typical area where the transport of small molecules via a polymeric medium are subject of interest. A key step in designing the process is molecular diffusion process which directs efficacy and manufacture of commercial products. Several experimental techniques such as NMR spectroscopy, inverse gas chromatography (IGC) and neutron diffraction can be used to yield new insights into mechanism of transport of small molecules in polymers. Due to so many different options available and the complexities involved in the polymeric materials transport phenomenon, applying experimental studies on the materials of interest is not always practical nor conclusive. Accordingly, a common practice is to use theoretical analysis on the problem in hand along with experimental investigation to gain better understanding of the process, explaining abnormalities and correlating the trends observed with underlying process variables. So, in this chapter we try to summarize some of the variables which play a role in transport of small molecules through the HPX film. Finally, we present a brief review of the theoretical frame works which is currently used in study of such problems.

The main factors contributing to transport process in the current study are[76]:

- Nature of the polymer
- Chemical treatments and cross linking
- Addition of plasticizers
- Nature of the penetrant (polarity and size)
- Addition of fillers
- Process variables (temperature and relative humidity)

The most important ones will be discussed briefly in the following section.

Nature of the polymer: The very first and the most important parameters governing the transport properties of a polymer are its chemistry and morphological properties. While the former is mostly affecting the polymer/solvent interaction (which can be either attraction or repulsion), the latter affects the ability of the polymer to accommodate and transport small molecules. Here we list some of the key factors:

- Polarity of the polymer/solvent pair (non-bonded interactions) affects the direction of the transport. While the favorable interaction (polymer and solvent are miscible) results in mixing of the polymer and solvent, an unfavorable interaction will force the transport toward the demixing according to basic law of thermodynamic (phase separation). Also, the mobility of the small molecules in the polymeric matrix is governed by so many other parameters (e.g. as free volume and nature of the penetrant which will be discussed later), this thermodynamic force can cause a unidirectional acceleration/deceleration depending on the polymer/penetrant pair under study.

- Available free volume within the polymeric medium is another important factor. The more the available free volume, the higher is the rate of transport within the medium. Free volume itself is affected by so many different parameters like the degree of crystallinity of the polymer (crystalline polymers are more compactly packed and the free volume is less), the rigidity of the polymer chain (rigid polymers have higher free volume due to less degree of freedom and inability to pack properly) and the degree of polymerization (longer polymer chain cannot pack as efficient as the shorter chain does).
- The segmental mobility of the polymer also plays a major role in the transport of small molecules. Assuming same average free volume for two different polymers, the mobility of the chain affect how fast the free volume holes can be redistributed and create opportunity for small molecules to diffuse. Segmental mobility of polymers is mostly governed by the non-bonded interaction (hydrogen bonding of the monomers), the monomer size (steric effects are larger for larger monomers) and the polymer chain length (larger chains have smaller mobility). But the segmental mobility can be externally stimulated using plasticizers (which makes it easier for the polymer chains to slide pass each other) or by changing the temperature (going from glassy region to rubbery region).The segmental mobility of the chains also depends on degree of crosslinking, extent of unsaturation and nature of substituents.

Effect of plasticizer: addition of plasticizer to a polymer increases segmental mobility as mentioned before, resulting in increase of penetrant transport. Plasticizer increases diffusion coefficient while it may decrease or increase solubility coefficient.

Nature of the Penetrant: The size and shape of penetrant molecule will affect rate of transport in the polymer matrix as the available free volume is limited. Increase in size of the penetrant

decreases diffusivity as has been reported by many researchers. In addition to size, shape of the penetrant also influences permeability. For example, diffusion coefficient of spherical molecules is lower than flattened or elongated molecules with equal molecular volume. Effect of permeant size and shape is more marked in glassy polymers than rubbery polymers due to the differences in polymer-permeant mixing processes. Since increasing permeant size increases heat of sorption, large permeants tend to sorb easily enhancing plasticization of polymer chains, even though diffusion coefficient is smaller. On the other hand, smaller molecules have larger diffusion coefficient and due to lower sorption the polymer will be less plasticized. Consequently, the overall effect of diffusion and sorption minimises the difference in permeation coefficient of small and large permeants.

Fillers: Nature of fillers, the degree of adhesion and compatibility with the polymer matrix are the factors affecting diffusion and transport in filled polymers. If the filler and the polymer matrix are compatible, the filler will take up the free volume within the polymer matrix and creates a tortuous path decreasing the permeation. Shape, orientation and volume fraction of the filler affect degree of tortuosity. On the other hand, incompatible filler creates voids at the interface, increasing free volume and consequently permeability.

Temperature: Temperature has a twofold effect on the transport. While it increases the kinetic energy of the penetrant on average (which obviously increase the transport rate), it also increase the chain segment mobility. In this perspective, in most of the common practices the Arrhenius relationship is used to predict the effect of temperature on diffusivity (D), sorption (S) and permeability (P) coefficients.

$$D = D_0(e^{\frac{-E_D}{RT}}) \quad (3. 1)$$

$$S = S_0(e^{\frac{-\Delta H_s}{RT}}) \quad (3.2)$$

$$P = P_0(e^{\frac{-E_p}{RT}}) \quad (3.3)$$

Where E_D and E_p are the activation energies of diffusion and permeation, respectively, and ΔH_s is the heat of solution of the penetrant. D_0 , S_0 and P_0 are the pre-exponential factors. R is the universal gas constant and T is temperature

3.2. Theory of Permeability in Polymers

Permeability or permeability coefficient, characterizes the steady state rate of mass transport of penetrant or solvent molecules through the polymer which has dimensions of mass, concentration or mole of penetrant times thickness per area, time and pressure. Several units can be used for permeability of gases and water vapor, a common unit which is used for permeability coefficient of gases in barrier polymers is $(cm^3(STP).ml/100in^2.day.atm)$. However other combinations of this unit are also used. Permeation of penetrant molecules is basically described by solution-diffusion model which defines permeability in three steps:

- 1) Adsorption of the penetrant due to high partial pressure or high thermodynamic activity on the surface of the polymer.
- 2) Dissolution and diffusion of the penetrant molecules through the polymer thickness.
- 3) Desorption from the other surface due to low partial pressure of low thermodynamic activity.

Since in most cases, the bulk and surface properties of the polymer are indifferent and at equilibrium state, rate of adsorption and desorption can be the same. With this assumption

the adsorption and desorption steps can be negligible and the rate-limiting step will be diffusion through the polymer film [77].

The sorption or dissolution behaviour is described by Henry's law of solubility, as [22]:

$$C_D = k_D \cdot p \quad (3.4)$$

where C_D is the concentration of the sorbed/penerant molecule, k_D is Henry's coefficient (solubility) and p is the partial pressure of the solvent molecule. Under steady state conditions, Wroblewski, showed that the permeation flux, assuming independency of diffusion and solubility coefficient from concentration, can be described as:[78]

$$J = D \cdot S \cdot \left(\frac{p_f - p_p}{l} \right) = P \left(\frac{\Delta p}{l} \right) \quad (3.5)$$

where $\left(\frac{\Delta p}{l} \right)$ is the applied pressure gradient across the polymer thickness. P is the permeability often expressed as $mol Pa^{-1} m^{-1} s^{-1}$ or $Barrer = 10^{-10} (cm^3(STP)/cm \cdot sec \cdot cmHg)$.

In the late 1870, gas permeation was described by Stefan and Exner as the product of Fick's diffusion coefficient, D (cm^2/s), and the sorption coefficient or solubility coefficient, S ($mol m^{-3} Pa^{-1}$). If the ideal solution-diffusion model is followed [79],[80] and diffusion coefficient is assumed to be constant, the relationship between diffusion coefficient, solubility coefficient and permeation coefficient simplifies to:

$$P = D * S \quad (3.6)$$

Thus, diffusion coefficient is determined and the solubility coefficient is known, the permeation coefficient can be easily calculated.

Permeability coefficient is used to characterize transport of gases or liquids through amorphous polymeric barriers, which typically occurs in the amorphous phase of polymer while the crystalline phase is the impermeable phase of the polymer. Solubility coefficient, S , which is the thermodynamic component of permeability coefficient, is the reciprocal of the Henry's law constant which describes the amount of solvent molecules which are soluble in a rubbery polymer. If swelling of the polymer matrix occurs during the penetration of the penetrant molecules the model will not be reliable.

3.2.1. Solubility of small molecules in polymers

Sorption which is quantified by sorption or solubility coefficient is a thermodynamic parameter which indicates the quantity of sorbed molecules in the polymer at the equilibrium. Solubility of a penetrant in the polymer mainly depends on the affinity between the polymer and the penetrant, temperature and the total pressure, while the relationships between solubility and free volume are not always obvious [22][77]. During sorption free volume holes are created by Brownian motions of the polymer chain or by thermal deviations. The penetrant molecules locate in these free volume holes. In rubbery polymers, facility of movement of the penetrant molecules between the polymer chains determines Henry's constant since the penetrant molecules dissolve in the matrix like what happens in liquids. Therefore Henry's sorption cannot be directly related to the existing free volume hole structure. In other words, size of the free volume holes does not affect the solubility coefficient while the number of free volume holes does. This happens when the holes are large enough to accommodate the penetrant molecules between the polymer chains. But if the size of the holes are not big enough, increasing the hole size increases solubility. Choudalakis et al. [81] have verified the relation between the fractional of free volume in an amorphous polymer above T_g and the solubility coefficient, S ($\text{mol/m}^3 \cdot \text{Pa}$):

$$V_f \sim S/\rho_g \quad (3.7)$$

Where V_f (%) is the fractional free volume, and ρ_g (kg/m^3) is the density of the sorbed molecule.

3.2.2. Diffusivity of small molecules in polymers

According to Fick's law, "the mathematical theory of diffusion in isotropic substances is based on the hypothesis that the rate of transfer of diffusing substances through unit area of a section is proportional to the concentration gradient measured normal to the section[82]" which is defined as:

$$J = -D \frac{\partial C}{\partial x} \quad (3.8)$$

Where J ($\text{mol/m}^2.\text{s}$) is the rate of transfer per unit area (flux), D (m^2/s) is the diffusion coefficient, C (mol/m^3) is the concentration of the diffusing molecules, and x (m) is the Cartesian coordinate in the direction of diffusion.

Considering the mass balance of the diffusing molecules, equation (3.8) can be used to derive the fundamental differential equation of diffusion:

$$\frac{\partial C}{\partial t} = D \left(\frac{\partial^2 C}{\partial x^2} \right) \quad (3.9)$$

In polymeric and non-homogeneous systems where diffusion coefficient depends on the concentration and varies from point to point, D is a function of x , and C and equation (3.10) can be expressed as:

$$\frac{\partial C}{\partial t} = \frac{\partial}{\partial x} \left(D \frac{\partial C}{\partial x} \right) \quad (3.10)$$

Diffusion is a kinetic process which depends on the mobility of penetrant molecule in the polymer matrix. In dense polymers, successful jump for penetrant during diffusion in polymers matrix is mostly governed by polymer segment dynamics which occasionally result in creation of big enough holes for penetrant molecules to fit in. At temperatures below T_g , where the polymer is at glassy state, the segmental chain motions are significantly reduced. Since the polymer backbone is considered to be in frozen state, hole redistribution is less probable to happen. Also, since the number of the free holes is constant, transport of the penetrant molecule is assumed to be through fixed (existing) holes which have an appropriate size (jump/hopping). So, the number of the holes which are large enough to accommodate a penetrant molecule is an important factor determining the magnitude of diffusivity as the segmental rearrangements are very small. A penetrant molecule existing in a hole with sufficient size, can jump into the neighbouring hole acquiring sufficient amount of energy. This energy is justified by Arrhenius behaviour of diffusion coefficient, D (m^2/s) as:

$$D = D_0 \exp\left(\frac{-E_a}{RT}\right) \quad (3.11)$$

Where E_a (J/mol) is the activation energy of diffusion, D_0 (m^2/s) is pre-exponential constant, R (J/K.mol) is the gas constant and T (K) is the absolute temperature.

3.3. Free Volume Theory

The free volume theory is the most successful theory for interpreting diffusivity data of low molecular weight solutes at infinite dilution in amorphous polymers at temperatures below and above their glass transition temperatures. The theory describes the diffusion process as migration of the solute by jumping into free volume holes. According to free volume theory transport of small molecules through the polymer matrix is dependent on the available free volume in the

matrix formed by natural thermal fluctuations of the polymer molecules as well as sufficient energy of the diffusing molecules to overcome the active forces between the chains [83], [84]. To describe free volume total volume of any polymer can be defined as: The occupied volume by the polymer molecules, and the free volume which can be defined by various definitions such as, hole, configurational, fluctuational and excess free volume. Hole free volume: is defined as the free space between the polymer chains, even if the chains were perfectly aligned. Configurational free volume: is the additional free space created due to insufficient chain packing. Fluctuational free volume: is described as the extra free volume created by the transient gap which is generated by random movement of the polymer chains (rotation, vibration, etc.) due to thermal activation. Excess free volume: the larger specific volume which is created due to cooling of the polymer below its glass transition temperature [85]. If the polymer is allowed to cool down slowly under equilibrium condition the specific volume would be smaller. The difference between the actual volume and the equilibrium free volume is the excess free volume [22]. If the diffusing molecule has sufficient energy, it can break away from its neighboring molecules and jump into the hole which is opened due to the natural fluctuation of sphere molecules in their place before the next molecule returns to its initial position and so the diffusional transport will be completed [86].

The theory has been developed based on the original free volume theory for self-diffusion of simple glass forming liquids proposed by Cohen and Turnbull. According to Cohen and Turnbull the self-diffusion¹ of molecules in liquid of hard sphere is facilitated by redistribution of free volume in the system. Although this theory was initially believed to be suitable only for simple liquids, the greatest impact of the theory has been on describing mass transfer in concentrated

¹ Self diffusion: related to thermal motion of molecules in system
Mutual diffusion: diffusion of solute under the chemical potential

polymeric solutions. However, the application of free volume theory on polymeric systems and some modifications has been introduced to original theory mostly by Vrentas and Duda. Fujita modified the theory for amorphous, rubbery polymers and derived a free volume theory for self-diffusion in solvent- polymer systems. Vrentas and Duda re-examined the theory and proposed a more general version of the theory [87].

In the original Cohen-Turnbull framework, a molecular jump does not involve any activation energy but is solely related to the probability of locating a sufficiently large free volume void. Some researchers challenged this conceptual notion and suggested that a jumping unit must overcome the attractive forces with adjoining molecules prior to a diffusive step. According to their viewpoint, therefore, the appropriate expression is [22]:

$$D_1 = D_0 \exp\left(-\frac{E}{RT}\right) \quad (3. 12)$$

When proposed modifications to the original Cohen and Turnbull theory are incorporated, the self-diffusion coefficient of a solute in a polymeric solution can be calculated by:

$$D_1 = D_0 \exp\left(\frac{-E}{RT}\right) \exp\left(\frac{-\gamma(\omega_1 \hat{V}_1^* + \omega_2 \xi \hat{V}_2^*)}{\hat{V}_{FH}}\right) \quad (3. 13)$$

Where \hat{V}_{FH} is the specific hole free volume of a liquid with a weight fraction ω_i of species i , and with jumping unit molecular weights of M_{ij} . Note that M_{ij} for simple molecule is the entire molecular weight of the component but in the case of polymer chain is a small fraction of the total chain molecular weight. \hat{V}_1^* is the specific hole free volume of component 1 required for a diffusive step and $\xi = \frac{\bar{V}_{1j}^*}{\bar{V}_{2j}^*}$. \bar{V}_1^* is the critical molar free volume required for a jumping unit of species of 1 to migrate. E is the activation energy required for the molecules to escape from the

surrounding environment and jump to the next available hole. D_0 is the proportionality coefficient and is related to the size and shape of the penetrant molecule:

$$D_0 = \frac{RT\sigma^2}{M^{1/2}} \quad (3.14)$$

Where σ is the Lennard-Jones size parameter and M is the molecular weight of the penetrant.

If one is able to obtain or estimate all of the required parameters, free volume theory is able to provide excellent predictions of diffusion coefficients as a function of both polymer weight fraction and temperature in the rubbery regime.

Now having the self-diffusion of solute in polymer film from an experimental method such as inverse gas chromatography (IGC) (the method will be described in Chapter 4) and noting that concentration of solvent is low, the mutual diffusion coefficient for low solvent concentration will be:

$$D = D_1(1 - \phi_1)^2(1 - 2\chi\phi_1) \quad (3.15)$$

where χ is the Flory-Huggins interaction parameter and ϕ_1 is the penetrant volume fraction which reaches zero in infinite dilution regime. Note that in this situation (not always) both diffusion coefficients are the same. The Flory-Huggins interaction parameter can be calculated from the equilibrium pressure, the vapor pressure, the second virial coefficient, and the volume fractions in the polymer phase.

One of the greatest advantages of free volume theory over others is the ability to incorporate the glass transition phenomenon in its predictions. Glass transition temperature, T_g , is the temperature where an amorphous polymer changes from rubbery to glassy. Around the glass transition temperature the mobility of polymer chains change significantly and abruptly, as the

freedom of the molecular chains changes. Below glass transition temperature where the polymer is glassy and the segment motion is almost frozen, it is treated as a solid and thermal expansion of free volume is almost impossible and the size, shape and position of the free volume holes remain constant. On the other hand, above T_g where the polymer is in rubbery state it is treated like a viscous liquid since the polymer chains have high mobility and short relaxation time. This liquid-like motion is related to the increase in free volume caused by thermal expansion. Opposing to glassy polymers, the shape, size and position of the free volume holes change with time in rubbery polymers and the holes can move freely in the polymer since no energy change is required for their redistribution. However, at a constant temperature the number of holes remains constant. Therefore the main difference between the rubbery and glassy state of an amorphous polymer is the interstitial volume which is dependent on temperature [22][77].

Chapter 4

4. Method

4.1. Brief History of Inverse Gas Chromatography

Martin and Synge were the first people who used chromatography to measure partition coefficient between two liquids in 1941 and introduced inverse gas chromatography (IGC). However, application of IGC to measure physicochemical properties was presented by Wicke (1947), Glueckauf (1947), Cremer and Prior (1951) and James and Phillips (1954) who determined adsorption isotherms from IGC [88]. In 1960s, Kiselev published a book in capabilities of GC in determining surface properties such as activity coefficients, entropies, heats of solution, heat and entropies of adsorption, vapor pressure, molecular weight, diffusion coefficients, activation energies for diffusion, adsorption isotherms, surface free energies, as well as molecular interactions and gas-liquid interface resistance investigations [89]. Smidsrød and Guillet[90] introduced study of polymer properties and interactions by IGC. In 1970s IGC became more popular as a powerful technique for determining surface and bulk characteristics of polymers and polymer blends. It can provide lots of useful information about physicochemical properties such as solubility and thermodynamic interaction parameters, surface energy heterogeneity, acid-base properties, BET surface area, diffusion kinetics, glass transition temperatures, work of cohesion, polarity on the surface of materials, adsorption isotherms and much more [88], [91]–[93]. Inverse gas chromatography has also shown to be a reliable and efficient method for obtaining solubility and diffusion coefficient of solvents in polymers when the solvents are in finite concentration or infinitely dilute [92].

4.2. Inverse Gas Chromatography

Versus gas chromatography in which study of the solute (solvent/sorbate/probe) is important, inverse gas chromatography (IGC) studies the material in the column (Figure 4.1). The particular properties of the stationary phase can be investigated by analysing retention data of interaction of the probe with the stationary phase[88]. In case of polymers, inverse gas chromatographic methods have shown to be suitable for providing useful information on thermodynamics of polymer- solute interactions [7], transition temperatures, crystallinity and surface characteristics of polymers [8]. In recent years, inverse gas chromatography has shown to be a fast and reliable technique for measuring sorption tendency, activity coefficients and diffusion coefficients of various solutes in polymers. It has shown good results in highly polymer concentrated region which is an interesting region in polymer studies, especially in production of polymer films and coating/ drying operations [8], [9]. Other great advantages of IGC compared to other surface energy analysing techniques is that minimum sample preparation is required [88], the ease of running experiments in a wide range of temperature and under infinite dilution of the solvent/sorbate [25]. In order to reduce the possible errors regarding the IGC measurements, following components should be taken care to make sure the results are not vague [4]: Equipment, sample preparation, data correction, physicochemical data linking retention data with established physicochemical parameters and calculation of the parameters describing the interesting property of the examined material.

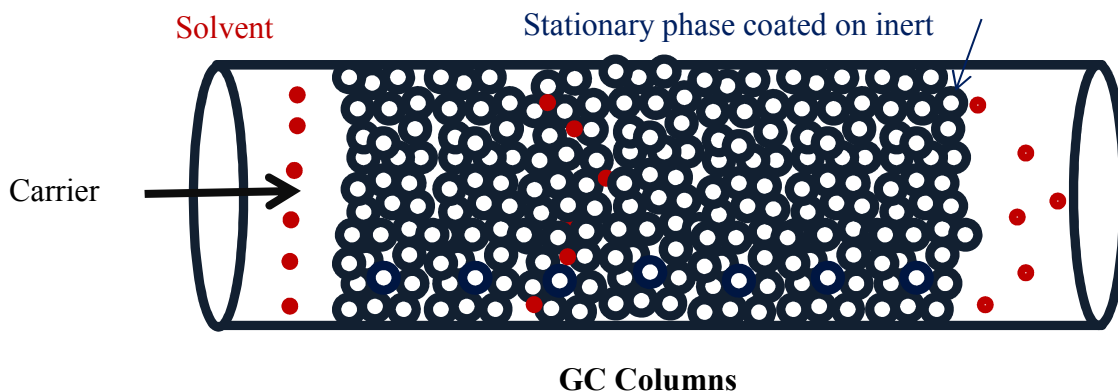


Figure 4.1.GC column

Inverse gas chromatography is based on the characteristic equilibrium partitioning of the solute between the mobile phase and the stationary phase. In fact, like any sorption method, the main purpose of IGC is to determine the partition coefficient of the solvent between the stationary phase and gas phase. Two important resistances occur as a solute passes through the column via an inert gas: the longitudinal diffusion in the gas phase and the mass transfer in the stationary phase. The tendency of solute molecules to move from the center of the peak to the edges results in longitudinal diffusion. The mass transfer resistance in stationary phase results in the equilibrium of the solute between the mobile and stationary phase not to be reached instantaneously. The elution profile of the peak from the gas chromatography gives the solubility or partition coefficient and diffusion coefficient of the polymer/solute system. The simplest theory of gas chromatography assumes that the partitioning of the solute between the stationary phase and the gas phase reaches an equilibrium state immediately. This simplification of mass transport in phases does not consider the axial dispersion of the solute which means that the elution peak is the same as the inlet peak. In the simplified theory, partitioning serves only to reduce the mean axial velocity of the solute, however, in reality, it is not possible to neglect one of the mass transfer processes as the solute is always partitioning between the two phases with a

finite rate. Transport resistance, delays the transport of solute between phases. As a result, axial spreading and deformation of the solute peak through the column is inevitable. Diffusion coefficient in the stationary phase can be obtained by measurements of peak broadening and distortion. The only problem is that other factors in addition to the stationary phase transport affect the peak shape. [21]

The reasons for broadening the peaks can be divided in three main classes: The first reason is instrumental factors such as sample injection time, nonuniform injection of sample, detector dead volume, detector lag time and recorder response which should be minimized by careful choosing of the experimental conditions. The second as mentioned before is the thermodynamic interaction of solute and the polymer. By using very small concentration of the solute vapour, it can be assumed that the concentration of vapour in carrier gas is linearly related to concentration in stationary phase so, equilibrium is reached very fast and as a result the peak shape will not change. The other factor affecting peak shape comes from the finite time required for reaching equilibrium during the time the peak passes through the column at each point [19]. These factors and other factors like: channeling of the carrier gas, back mixing in the injector and detector, gas phase mass transfer resistance, surface adsorption effects and nonlinearity of absorption isotherms must be considered in experiments and the model for analysis of data [21].

IGC can also determine sorption of solvents in polymers at different temperatures or concentrations of the solvents within a good agreement with data from gravimetric sorption [88]. It has shown to be a reliable method in determining solubility and diffusion coefficient of probes in infinite dilution. Diffusion coefficients can be obtained by analyzing the elution peak from the column using the approach of van Deemter et al. [8] and Gray and Guillet [21] or a moment analysis [22], [92].

4.2.1. Finite Concentration and Infinite Dilution

IGC experiments can be directed through two chromatographic conditions: finite concentration and infinite dilution. At finite concentration a high quantity of the probe molecule is introduced to the system. Interaction with all the sites of the surface of the stationary phase gives information on adsorption isotherms and has more accuracy compared to volumetric measurements. At infinite dilution a very small concentration of the probe molecule is injected and the partial pressure of the probe/solvent tends toward zero. At this concentration/pressure range the interaction of the probe-probe molecules is negligible and the sorption isotherms follow Henry's law. Thus, linear adsorption isotherms and symmetrical chromatographic peaks are expected. There is no correlation between the corrected retention volume and the amount of the sample injected and retention volume should not change with changing the sample amount injected. If this condition is not satisfied, the corrected retention volume must be extrapolated to zero peak height as suggested by Smidsrød and Guillet [90],[10]. In order to confirm that the data obtained correspond to equilibrium condition, the specific retention volume should not have any dependence on the carrier gas velocity. This behaviour is most expected when the polymer is in rubbery state. In the case of weak dependence, the retention parameters can be extrapolated to zero velocity of carrier gas [25]. Most of the IGC experiments to determine thermodynamic properties are conducted at infinite dilution. The high sensitivity of IGC detectors ($\sim 10^{-9}$ moles) makes the technique more applicable compared to other techniques [88].

4.3.IGC Components

Figure 4.2 is a schematic diagram of IGC unit. Similar to classical GC, an IGC instrument consists of a column, an oven, detector, mass flow controller and a computer which processes and controls the data.

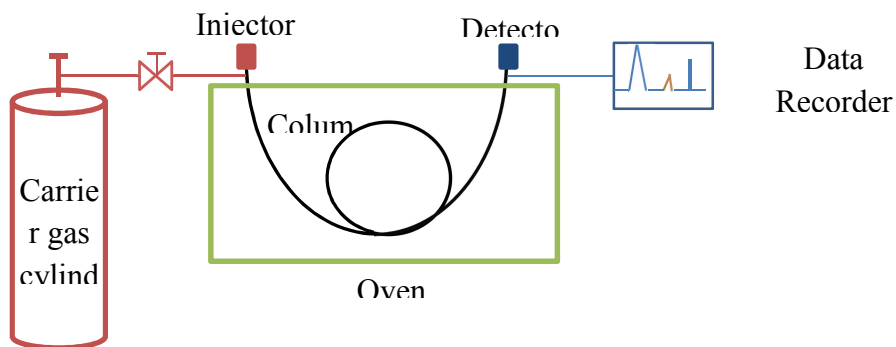


Figure 4.2. Schematic of gas chromatography system

4.3.1. Carrier gas

A low concentration pulse of gas or vapor of a volatile substance (solvent/sorbate/probe) is injected which is carried through the column by a constant flow of a high purity inert carrier gas. The carrier gas flows directly to the detector passing through the temperature controlled oven. The most common carrier gases are hydrogen, helium, nitrogen, and Argon. Selecting the appropriate carrier gas is an important factor in gas chromatography. Argon and nitrogen, the heavier gas with higher viscosity, slowdown diffusion rates and increases the contribution of mobile phase mass transport in peak broadening. Also, optimum velocity of the carrier gas is more favorable for the lighter gases, hydrogen and helium. Meaning that the velocity at which the highest efficiency of the column is obtainable is higher for lighter gases which results in shortening of the analysis time. Hydrogen is actually the best choice. However, due to safety considerations and explosion risk of hydrogen, helium is the most appropriate gas although it is more expensive.

4.3.2. Columns Types

There are two numbers of types of columns that can be used for IGC studies:

Packed Columns

Packed columns are made of glass or metal tubes with 2-4 mm I.D. and 0.5-6 m length. In packed columns, the stationary phase is coated on very small inert spheres, which are then packed in the column. The common supports are made from diatomaceous earth (Chromosorb), glass beads or polymeric supports. In order to coat the supports, the stationary phase (here, the polymer under study, e.g. HPX) is dissolved in a volatile solvent (water) and then mixed with the inert solid support and the volatile solvent is removed by evaporation and the stationary phase would form films on the surface of the support. In another method reported by Al Saigh and Munk, the support is soaked in polymer solution in several portions for several hours in order to have less loss of the polymer due to coating of the glass flask in the rotary evaporator method. However the film obtained with this method is not as uniform as the first one. Possible non-uniformity of the films may cause uncertainty in the determination of diffusivities [93],[20]. The weight of the polymer coated on the support can be obtained by ashing, using a thermogravimetric method. The polymer loading after coating is usually 3% less than the initial weighted polymer. The optimum loading is reported between 4-13 % wt for chromosorb and approximately 0.5 % wt for glass beads, as below this, there would be some uncoated support which may affect the retention time and above 15% there would be problems due to diffusion through thicker coating. The optimum thickness of the film coating should be 0.5-5 μm . [102]

In another approach, solid particles of the polymer can be used directly. When it is desired to characterize solubility and diffusivity without altering the morphology of the polymer, neat samples with a uniform size can be packed into the column. Unless the particles are very small,

the time required to reach equilibrium may be too long because of small diffusivities in polymers. Large pressure drops and dispersion through the column are some of the difficulties in working with this type of columns [20], [21].

Capillary Columns

In the case of capillary column, the polymer film (stationary phase) is coated as a thin film of the stationary phase on the inside wall of the column which is a capillary tube (typical diameter 0.53 mm). The film thickness in capillary columns is typically 3 to 10 μm thick [92]. Capillary columns are longer columns which provide higher resolution and less pressure drop of the carrier gas compared to packed columns [93], [20]. A more uniform, thin film formed on the wall gives more accurate results for measuring partition and diffusion coefficients compared to packed columns in which the non-uniformity of the coated support and non-uniform packing cause the results require correction.

4.3.3. Detector

The output of the column is measured by the detector which is usually a thermal conductivity detector (TCD) or flame ionization detector (FID). The important factors in selecting the detector are selectivity and sensitivity. Thermal conductivity difference between the probe and carrier gas is the basis of TCD operation while FID measures the concentration of organics (containing carbon atom) through their destruction and formation of ions. Water can be detected by TCD while most hydrocarbons can be detected by FID. A combination of the two detectors can also be used for increasing sensitivity of measurements [88]. In FID the effluent from the column is mixed with hydrogen and air and then ignited electrically. It has advantages of high sensitivity, large linear response range and low response time but the disadvantage of damaging the sample.

TCD is simple, has large linear dynamic range and non-destructive character, but its low sensitivity will be a disadvantage in detecting organic samples.

4.4. Theory of Chromatography

Gas chromatography is based on the distribution of the solvent/probe between the mobile gas phase (carrier gas) and the stationary phase (polymer). A classical definition of chromatography can be defined as [104]:

“A separation process that is achieved by the distribution of the substances to be separated between two phases, a stationary phase and a mobile phase. Those solutes, distributed preferentially in the mobile phase, will move more rapidly through the system than those distributed preferentially in the stationary phase. Thus, the solutes will elute in order of their increasing distribution coefficients with respect to the stationary phase.”

In classical chromatography (when separation of different solutes/solvents by the stationary phase is the main purpose) two processes occur during the separation: First, due to difference in affinities of each solute/solvent with the stationary phase, the solvents are moved apart in the distribution system. Secondly, the tendency of the bands to spread or disperse is controlled to ensure that the achieved separation is maintained. So the system should be able to provide required retention of the solutes and minimize the dispersion while allowing each solute to elute discretely. Chromatography theory provides the basis for these choices by disclosing the mechanisms that control retention, explaining different processes that can cause band dispersion and showing how the solute retention and band dispersion can be affected and controlled by the operating variables of the chromatographic system such as sampling devices, detectors, etc.

In order to understand the chromatographic process it is necessary to be familiar with the two fundamental theories of chromatography: the Plate Theory that deals with solute retention and the Rate Theory that deals with solute dispersion. In plate theory, the column is considered as number of stages or plates (like in distillation column) that there is equilibrium between the two phases in each of the plates [99]. The plate theory was the first effective theory which controlled chromatographic retention and allowed efficiency of the column to be measured. The efficiency of the column is its capacity for containing peak dispersion. Martin and Synge [9] in 1941 were the first to apply plate theory. They used the plate concept from distillation theory as an approach for mathematical examination of elution process in chromatography. The theory is simple and can be used to derive the basic retention equations and other equations used to describe resolution and efficiency of the system. The plate theory was further extended by Mayer and Tomkins (1947) [10], Glueckauf (1955) [11] and later was generated more precise and useful by Said (1956) [12].

Lapidus and Amundson (1952) [13], Glueckauf and Tunitski (1954) were the first who started the work with the Rate Theory which describes dispersion in packed beds [104]. Rate theory considers the actual continuous column in which the two phases are in equilibrium [99]. Van Deemter et al. (1956) [8] described dispersion in packed beds as a function of linear velocity of the fluid passing through the packed bed which is the final form of the Rate Theory equation which is directly applicable to packed gas chromatography columns. They did not consider mobile gas compressibility. Although it does not change the magnitude of dispersion, it affects the method of measurement of linear velocity and resistance to mass transfer terms in the dispersion equation. Giddings [110] applied effect of pressure change along the column in Van Deemter equation and effect of mobile phase compressibility was considered by Ogan and

Scott[111]. Van Deemter equation is proved to be the simplest and most reliable equation used for general column design. Other equations helped in better understanding of the processes that occur in the column. Although the differing views on the theory of packed columns are not yet completely resolved, under normal operating conditions, the simplest modifications of the van Deemter equation give an account of the physical factors determining HETP, which is probably sufficient to satisfy the analytical chemist [112].

4.4.1. Rate Theory and Plate Theory [113]

As mentioned earlier, the Rate Theory and the Plate Theory are the two fundamental theories of chromatography. Before we continue to with these theories and the related equations, some basic definitions regarding peak width are required. The width of a chromatographic peak (peak dispersion) is the result of various processes occurring during the transport of the solvent through the column. As a result the solvent molecules reach the detector at different times which results in a time-dependant Gaussian concentration profile obtained at the detector (Figure 4.3). In fact the peak width is an indication of the processes causing the non-ideal behaviour of elution peak.

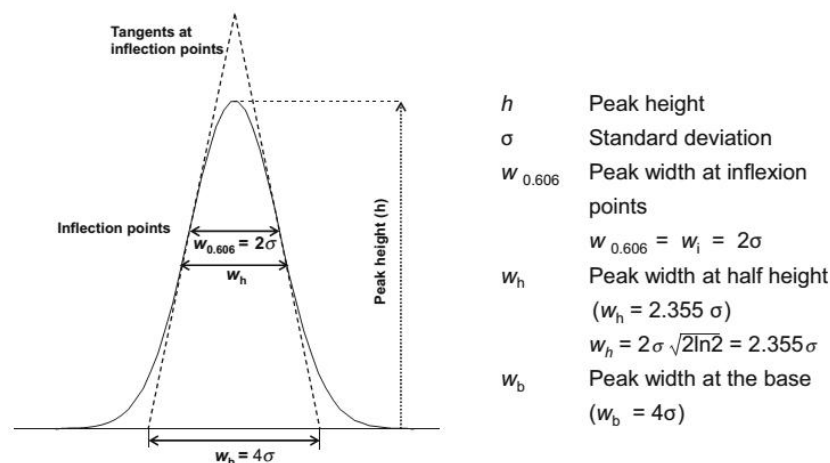


Figure 4.3. Gaussian profile of a peak. Peak widths are given in the dimension of retention (adapted from [113])

Assuming a Gaussian profile, the peak width can be defined at different heights. The peak width at the base of the peak w_b (distance between the intersection of the tangents from the inflection points with the base line) equals four standard deviations (σ), the peak width at half height is $w_h=2.355\sigma$ and the peak width at 60.6% of the peak height (the inflection points) equals $w_{0.606}=w_i=2\sigma$. Peak widths are given in units of volume or time.

4.4.1.1. Plate theory

As mentioned before, the concept of plate theory is obtained from description of performance of distillation column. The column consists of a series of segments called theoretical plates. In each plate equilibrium is assumed between the solute in the stationary phase and the mobile phase. The smaller the height of the theoretical plates the more the number of plates available per unit length of the column. As a result more distribution steps can be achieved and less band broadening in relation to the column length will be observed. N , the number of theoretical plates and H the height of a plate can be obtained using the retention time and peak width of an eluting peak of a solvent in chromatogram:

$$N = \left(\frac{t_r}{\sigma}\right)^2 \quad (4.1)$$

$$N = 16\left(\frac{t_r}{w_b}\right)^2 \quad (4.2)$$

$$N = 5.5545\left(\frac{t_r}{w_h}\right)^2 \quad (4.3)$$

Where σ is the standard deviation, w_b is the peak width at base and w_h is the peak width at half height, as defined before.

And with L being the length of the column, the plate height H or height equivalent to one theoretical plate (HETP) will be:

$$H = L/N \quad (4.4)$$

As mentioned before, plate height is an important property for estimating efficiency of a column or comparing efficiency of several columns. The lower the H (higher N), the higher the efficiency of a column will be. In order for the plate theory to be valid, H and N should be determined under isothermal conditions. Their values depend on temperature, carrier gas velocity and the solvent. Although the plate theory delivers a value to judge the efficiency of a column, it does not explain peak broadening. Van Deemter achieved this issue by rate theory.

4.4.1.2. The Rate Theory According to Van Deemter

In rate theory, several different peak dispersion processes were suggested and expressions were developed that described: the contribution of each of the processes to the total variance of the eluted peak; the final equation that gave an expression for the variance per unit length of the column. In the rate theory introduced by Van Deemter, the separation process in a packed column under isothermal conditions is considered as a dynamic process of independent mass transfer and diffusion process that cause band broadening.

Diffusion is a mass transfer process in which molecules in a mixture move spontaneously due to a concentration gradient. Diffusion of a small molecule like water vapor through a medium made up of polymer can be sketched as the water (solute) molecules move through a tangled mass of polymer chains and holes. The movement occurs due to concentration gradient of the solute plus the action of the surrounding complex of molecules [7]. The nature and magnitude of interaction of the solutes and the polymer under study affects the important parameters of retention and

shape of the peaks. Molecular diffusion describes the random movement of molecules and fluid. In the case of transport (or ordinary) diffusion, where the concentration difference is the cause of the movement, molecules move from the high concentration region to the low concentration region until the concentration difference reaches a balance. The rate of this movement is proportional to the concentration gradient and is expressed as diffusion coefficient (D), which ranges between 10^{-4} to 10^{-5} m^2/s in gases to 4-5 orders of magnitude lower (10^{-9} m^2/s) in liquids.

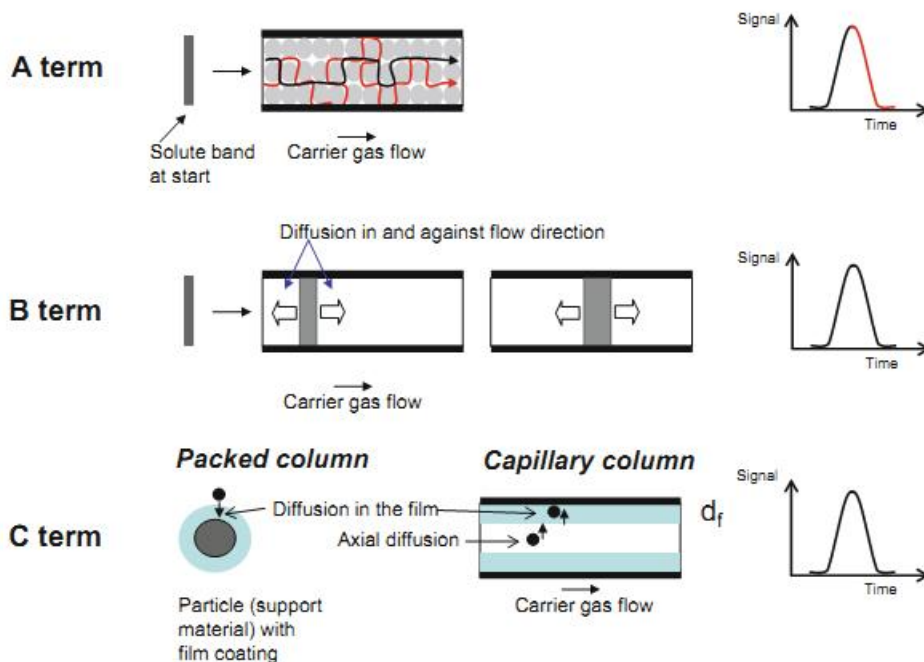


Figure 4.4. Graphical presentation of the A, B, and c terms in van Deemter equation (adapted from [113])

According to Van Deemter equation, diffusion coefficient of the solute through the evenly coated polymer on the surface of solid support can be obtained by the measurement of peak width as a function of carrier gas flow rate, by using the Van Deemter equation. Although, being fairly time consuming, the method is the most popular and relatively simple method from the experimental

point of view. The determination of diffusion coefficient is based on the effect of the carrier gas velocity on a height equivalent to a theoretical plate (HETP). The necessity to know the exact thickness of the coating is the main challenging part of using this method [25]. One important point in using simple Van Deemter equation for polymer diffusion measurements is that comparing to conventional lower molecular weight stationary phases, polymers have higher viscosity which results in formation of more stable and even bead coating. Also, because of lower diffusion rates, the relative contribution to peak spreading is more important. These two factors result in applicability of simple Van Deemter equation for measurement of diffusion coefficients of solutes in polymers. However, care must be taken to do experiments at temperatures above the glass transition of the polymer and with relatively non polar solutes [24]. Otherwise, due to strong polymer-solute interaction the diffusion coefficient will be dependent on both time and solute concentration which will result in thermodynamic peak spreading. In order to relate the diffusion coefficient with peak shape by using the Van Deemter equation, care must be taken for the main source of peak spreading to be just due to equilibration through the stationary phase. Therefore, the isotherms relating the vapor and stationary phase concentration should be linear; the instrumental dead volume and detector response time should be minimized. The other important point is to determine geometric distribution of the polymer (film thickness and uniformity) on the support or column precisely as it has direct effect on peak shapes. So, more accurate experimental and theoretical methods should be considered for determining geometric distribution of the polymer on the column and its effect on the peak shapes. The most difficult problem in working with packed columns is determining the film thickness. By using regular surfaces like glass beads, this effect may reduce; however, it is still difficult to obtain uniform thickness [98], [19], [115].

The mentioned kinetic factors have been related to column properties by Van Deemter using the following equation for eluted peaks which describes the relation between the HETP and the average carrier gas velocity [22], [6]:

$$H = A + (B/u) + Cu \quad (4.5)$$

where H is the height equivalent to theoretical plate which would be determined from the widths of the eluting peaks for different carrier gas flow rates; u is the average linear carrier gas flow rate (usually between 8-12 cm/s, depending on relative molecular mass of the carrier gas) [23]. A and B are constants that are independent of flow rate but are related to instrument performance and gas phase spreading. Indeed, A is attributed to eddy diffusion that is defined as $2\lambda d_p$. Here, d_p is the diameter of inert support and λ is a packing factor. In fact packing nonuniformity causes scattering in the distance traveled by the solvent molecules resulting in peak dispersion describing parameter A . Parameter B is defined as $2\gamma D_g$ for longitudinal molecular diffusion describing peak broadening associated with the diffusion of the solvent in the mobile phase. D_g is the diffusion coefficient of the solute in the carrier gas and γ (labyrinth factor) is a constant, less than unity, signifying the curved path followed by the gas in a packed column. C_T corresponds to the mass transfer resistance between the stationary phase and the mobile phase. C_T consists of two components: $C_T = C_M + C$ where C_M is the resistance to mass transfer in mobile phase defined as: $C_M = \omega d_p^2 / D_M$. Where ω is a constant and d_p^2 is the solvent particle size and D_M is the solvent diffusion coefficient in the mobile phase. It is worth noting that C , the resistance to mass transfer in stationary phase, is independent of the flow rate but depends on a number of factors including the diffusion coefficient of the solute molecule in the stationary phase D_p . Plotting Equation $H = A + (B/u) + Cu$ (4.5 at higher gas flowrates

$((B/u) \rightarrow 0)$, the slope C_T of the linear portion is obtained. Considering the very slow diffusion in solid stationary phase compared to the large diffusion coefficient in the mobile phase, the resistance to mass transfer in the mobile phase can be negligible ($C_M \rightarrow 0$, so, $C_T \cong C$). Then D_p (diffusion coefficient of solute through the polymer) is obtained:

$$C = \left(\frac{8}{\pi^2}\right) \left(\frac{d_f^2}{D_p}\right) \left(\frac{k}{(1+k)^2}\right) \quad (4.6)$$

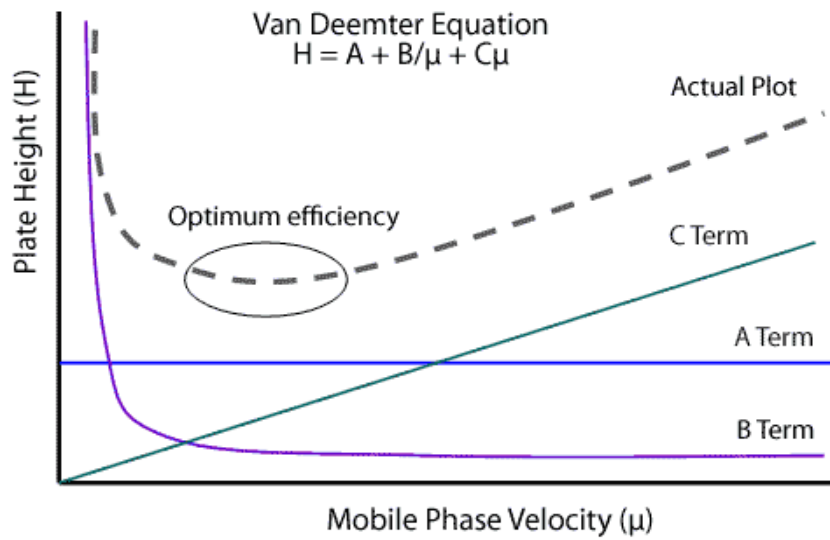


Figure 4.5. Relationship between gas flow rate and peak efficiency [93]

where k is partition ratio; d_f is the thickness of the stationary phase and is determined by the following equation:

$$d_f = \left(\frac{1}{3}\right) W \left(\frac{\rho_s}{\rho_p}\right) r_s \quad (4.7)$$

where W is the fraction loading of the polymer; ρ_s and ρ_p are the density of inert support and polymer, respectively; r_s is the average radius of inert support particles.

The partition ratio, k , is calculated from the equation:

$$k = (t_r - t_f)/t_f \quad (4.8)$$

where t_r and t_f are the retention times of solvent and non-interacting indicator, such as air, respectively.

H in the Van Deemter equation can be obtained from peak parameters by:

$$H = \left(\frac{L}{5.54}\right)\left(\frac{W_{1/2}}{t_r}\right)^2 \quad (4.9)$$

where L is the column length; $W_{1/2}$ is the peak width at half the peak height.

Also, u is the linear velocity of carrier gas which can be obtained by:

$$u = \frac{jV_0}{\bar{a}} \frac{T_{col}}{T_{flow}} \quad (4.10)$$

where T_c is the temperature of the column; T_{flow} is the temperature of the flow meter; \bar{a} is volume of gas phase per unit length determined by dividing the retention volume² of air by the column length; V_0 is the corrected flow rate; As the pressure drops along the length of the column, the velocity changes. Also, as the solute diffusion coefficient is inversely proportional to the pressure, modification for effect of pressure on velocity and consequently diffusivity should be applied considering the compressibility factor, j , (James Martin correction):

$$j = \frac{3}{2} \frac{\left[\left(\frac{P_i}{P_0}\right)^2 - 1\right]}{\left[\left(\frac{P_i}{P_0}\right)^3 - 1\right]} \quad (4.11)$$

² Retention volume: the volume of gas phase that passes through the column from the time of injection to the elution time of the peak maximum.

P_i and P_o are the inlet and outlet pressures of the column.

Temperature dependence of diffusion coefficient can be shown by a plot of log diffusion coefficient versus $1/T$.

$$D_p = D_0 e^{\frac{-E_a}{RT}} \quad (4.12)$$

where E_a is the activation energy for diffusion, R is the gas constant and D_0 is a constant.

In summary, the following assumptions should be considered to make the model equations of packed column applicable for the current system:

1. The system is isothermal.
2. The particles are spherical and have the same radius. Also, size of the support particles is important. The smaller the particles, the less will be the contribution of eddy diffusion to peak broadening, as the distribution of path length of a set of molecule traveling through the packed bed will be more uniform.
3. The average film thickness is constant for all the support particles in each column $<1 \mu\text{m}$.
4. The gas velocity is constant.
5. The pressure drop over the column is small and the gas phase can be treated as an incompressible fluid. In order for the parameters B and C to be independent of pressure, the pressure drop across the column should not exceed 1 atm.[116]
6. The diffusion coefficient of the solute through the polymer is constant in the concentration range.
7. The partition coefficient of the solute between the carrier gas and the polymer is constant in the concentration range.

8. The carrier gas does not interact with the polymer.
9. There are no chemical reactions in the system.
10. The sorption of the solute does not cause the swelling of the polymer.

4.5. Solubility Coefficient

Braun and Guillet (1976), proposed a model to describe sorption behaviour of polymers near the glass transition temperature under different chromatographic conditions. In the diagram of the specific retention volume vs temperature (Figure 4.6), they identified three temperature regions [96], [114], [117]:

- Glassy state of the polymer (well below T_g) (AB), which corresponds to the adsorption at the gas phase/polymer interface. In this region diffusion of solvents in the polymer occurs at a very slow rate as the solute interacts only with the surface of the polymer and no significant bulk interaction will happen. Thus, the corresponding retention diagram is linear.
- An intermediate region (BC), where the sorbate/polymer contact time is too short and bulk sorption has no time to settle. At point B, glass transition, the solute starts to penetrate in the bulk of polymer which results in increase in retention volume, but because of slow diffusion rate nonequilibrium conditions exist. At temperatures close to glass transition both bulk and surface interaction affect the retention volume. The location of point C on the temperature axis depends both on the polymer solute system, experimental conditions, film thickness and flow rate.
- And above T_g (rubbery state for amorphous polymers) (CD), which corresponds to volume and surface sorption.

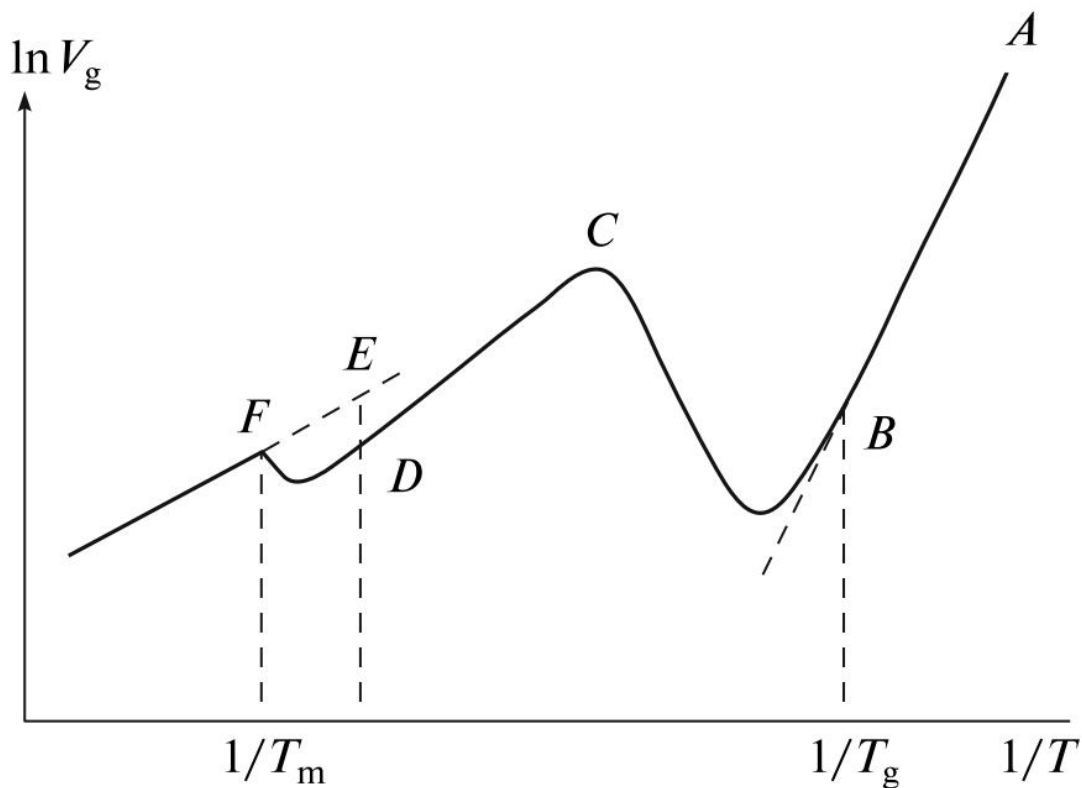


Figure 4.6. Retention diagram for semicrystalline polymer [96]

For semicrystalline polymers the region (DF) will be observed where the crystalline phase melts and increases specific retention volume. After the polymer starts to melt at melting point the solute-polymer interaction occurs in the bulk of amorphous polymer and a linear retention diagram is obtained (FG). The linear parts of the retention diagram can provide useful physicochemical information in different temperature ranges. The CD region is useful for determining the absorption capacity of the polymer and/or intermolecular interactions between sorbate/polymer molecules.

As mentioned before, like any sorption method, the main purpose of IGC is to determine the partition constant, K , of the solvent between the polymer and gas phase which can be obtained from concentration of the solvent in the polymer and the gas phase at equilibrium conditions:

$$K = \frac{C_p}{C_g} \quad (4.13)$$

Where C_p and C_g are the concentration of the sorbate/solvent in polymer and gas phase, respectively.

The concentrations of the solvent can be replaced as [118], [96]:

$$K = \frac{n_p/V_p}{n_g/V_g} \quad (4.14)$$

Where n_p and n_g are the number of moles of the solvent in polymer phase and gas phase and V_p and V_g are the volumes of polymer and gas phase, respectively.

Using the ideal gas equation, the concentrations in the gas phase and polymer phase can be estimated as:

$$n_p/V_p = cp^0/RT^0 \quad (4.15)$$

Where $P^0 = 1 \text{ atm} = 101325 \text{ Pa}$, $T^0 = 273.2 \text{ K}$.

And

$$n_g/V_g = p/RT \quad (4.16)$$

The solubility coefficient, S , is defined as:

$$c = S * p \quad (4.17)$$

Where c is the concentration expressed in $\text{m}^3(\text{STP})$ of probe/solvent/solute dissolved per m^3 of the polymer.

Consequently, the partition coefficient can be defined as:

$$K = \frac{T}{T^0} \frac{p^0}{p} c = \frac{T}{T^0} p^0 S \quad (4.18)$$

Where p is the equilibrium partial pressure of the solute/solvent and T is the column temperature.

On the other hand when Henry's law holds between the concentration of the solvent in the stationary phase and the gas phase and gas phase imperfection can be neglected, the net retention volume, V_N , can be related to partition coefficient by:

$$V_N = KV_P \quad (4.19)$$

Thus

$$S = \frac{T^0}{T} \frac{1}{P^0} \frac{V_N}{V_P} \quad (4.20)$$

Depending on the partition coefficient, different volumes of carrier gas are required to elute the solvent/probe expressing the results as retention volumes. The specific retention volume which is the volume of the carrier gas to elute the solvent/probe per unit mass of stationary phase is the basic parameter for determining results from IGC [90].

$$V_g^0 = \left(\frac{T^0}{T}\right) \left(\frac{V_N}{w}\right) \quad (4.21)$$

Where V_g^0 (ml g⁻¹) is the specific retention volume

Substituting Equation $V_g^0 = \left(\frac{T^0}{T}\right) \left(\frac{V_N}{w}\right)$ (4.21) into Equation

$$S = \frac{T^0}{T} \frac{1}{P^0} \frac{V_N}{V_P} \quad (4.20)$$

$$S = \frac{1}{p^0} \rho_p V_g^0 \quad (4.22)$$

Where ρ_p is the density of the polymer phase.

To determine the value of specific retention volume experimentally, it is required to measure the retention time of the sorbed/solute/solvent molecule and a non-sorbed component such as air, methane or nitrogen. At infinite dilution, since no interaction is assumed between the probe molecules, a symmetrical Gaussian peak is expected. The gross retention time, t_r , which is the time that takes long from the injection time until when the probe exits the column is the time shown at maximum peak height. In order to obtain the net retention time which is the time it takes for the probe molecules to interact with the stationary phase, dead time should be deducted from the gross retention time. The retention time of the non-sorbed molecule, t_m , is used to estimate the dead volume of the chromatograph. By calculating net retention volume as below,

$$V_{g0} = (TOT) V_{NW} \quad (4.21. [88])$$

$$V_N = j F_c (t_r - t_m) \quad (4.23)$$

Where F_c is the corrected volume flow rate of the carrier gas at average pressure of the length of the column and temperature of the experiment.

Where j is James-Martin compressibility correction factor and F_c is the corrected flow rate of the carrier gas (ml min^{-1}) at the column operating conditions.

$$j = \frac{3}{2} \frac{\left[\left(\frac{P_i}{P_o} \right)^2 - 1 \right]}{\left[\left(\frac{P_i}{P_o} \right)^3 - 1 \right]} \quad (4.24)$$

P_i and P_o are the inlet and outlet pressures of the column.

$$F_c = \frac{T_c}{T_{fl}} * \frac{P_0 - P_w}{P_0} * F \quad (4.25)$$

where F is the measured flow rate of the carrier gas (ml/min). And T_c and T_{fl} are the column and flow meter temperatures (K), respectively, and P_w is the vapour pressures of the probe inside the flow meter (atm).

Where V_g^0 can be calculated as:

$$V_g^0 = \frac{(t_r - t_m)}{w_p} * \frac{(p_0 - p_w)}{p_0} * \frac{T^0}{T_{fl}} * j * F \quad (4.26)$$

According to Everett and Stoddart [119] and later Cruickshank et al.[120] the net retention volume is related to the partition coefficient at zero total pressure, K_0 , when gas imperfection is not negligible:

$$V_N = K_0 V_p \exp(\beta p_0 j) \quad (4.27)$$

Where

$$\beta = \frac{2B_2 - v_1}{RT} \quad (4.28)$$

where p_0 is the standard pressure (1 atm); ρ is the polymer density (g/cm^3); B_2 is the second virial coefficient of the probe (cm^3/mol) which characterizes the interaction between the probe molecules; v_1 is the solvents partial molar volume (cm^3/mol) at infinite dilution at the column temperature T (K) and R is the gas constant ($\text{cm}^3 \text{ atm K}^{-1} \text{ mol}^{-1}$). Thus, the solubility coefficient at zero pressure is related to K_0 by:

$$S = V_g^0 \frac{\rho}{p_0} \exp \left[(2B_2 - v_1) j \frac{p_0}{RT} \right] \quad (4.29)$$

Chapter 5

5. Diffusion Behavior of Water at Infinite Dilution in Hydroxypropyl Xylan Films with Sorbitol and Cellulose Nano Crystals

5.1. Introduction

In recent years, increasing awareness of sustainability has driven the society to increase its effort to replace petroleum-based polymers by natural polymers [3]. Given that 40% of all plastics consumed are used for packaging purposes, it is not unreasonable to focus such effort on determining whether polymers from bio resources could be used as packaging materials [2]. Among the natural polymers, xylan is a prime candidate, as xylan, one principal component of hemicelluloses, is a film forming polymer and the second most abundant polysaccharide after cellulose [62],[121]. It is worth noting that not all natural polymers are able to form films, an obvious requirement for packaging applications. Cellulose and cellulosic derivatives have found their ways in the paper production industry and many other applications while hemicelluloses, xylan in particular, have not because of their high heterogeneity, low water solubility and source dependent composition. However, recently, chemically modified xylan such as xylitol, xylooligosaccharides, xylose, to name a few, have gradually been used in improving nutritional properties of food, as prebiotics or as additive to film forming biopolymers [65], [122], [123]. Also, there has been increasing effort on turning xylan from different sources into biodegradable films by using additives [4], [65] (e.g., pretreating xylan before the extraction process [124] or chemically modifying xylan [62], [125], [126]).

In terms of chemical modification of xylan, Jain *et al.*, found that when the hydroxyl groups of xylan are substituted by alkoxy substituents, water-soluble hydroxypropyl xylan (HPX) (see Figure 5.1) is obtained. HPX forms transparent, rigid films upon precipitation from its aqueous solution, a potential material for packaging applications [62]. Being water soluble, HPX is expected to be used as an internal layer of coating when a layer of good water barrier is available. It means that there would be very low concentration of water present. To use HPX for certain packaging applications, its flexibility has to be increased. Plasticizers are normally used for such purpose. In fact, this is commonly practised on hemicellulose-based materials [8]. However, this is accomplished at the expense of negatively affecting the barrier properties of the films (e.g., water vapor transmission rate (WVTR) and oxygen permeability) [127], [128], obviously not acceptable for the target applications. Naturally, most of the biopolymers, do not exhibit desired barrier properties, especially to water vapor, due to the presence of a large number of hydroxyl groups in their structure which makes them hydrophilic [9]. Fillers are expected to improve their barrier properties by reducing the water vapor permeability in the polymer. In this regard, adding nano-sized fillers may help but such fillers will inevitably increase the rigidity of the films. Therefore, it is of great interest to investigate whether there exist optimal concentrations of plasticizer and nano-sized filler in HPX films that would exhibit acceptable flexibility and barrier properties. In particular, we used sorbitol (see Figure 5.1), a commonly used plasticizer for hemicellulose, and a cellulosic-based, nano-sized filler namely cellulose nanocrystal (CNC). CNC is produced from the acid hydrolysis of cellulose [8], compared to inorganic fillers, it is easily recyclable even at high filling levels [10]. According to Bulota *et al.*, [10] in contrast to other chemically modified nanoparticles, where there are still toxicity issues, no indications of toxicity has been found with regard to CNC. Also, CNC is

expected to be compatible with HPX. Typical CNC has a diameter of 5-10 nm and a length of 50-200 nm (i.e., aspect ratios $\sim 5 - 40$) [9]. It is expected that such aspect ratios would significantly improve the barrier properties of the HPX films [129], as the tortuosity of the penetrating molecules and the mobility of the polymer chains will be increased and decreased, respectively. Several studies have shown enhancement of barrier properties of biopolymers in the presence of CNC. Addition of 1-10% CNC has reduced water vapor permeability in various biopolymers from 20 to even 70% compared to the neat polymer as the filler is less permeable and disperses well in the matrix [8], [9], [130].

Studying moisture permeability or WVTR is an important issue for food packaging applications that includes study of the thermodynamic process of solubility and diffusivity of the moisture through the polymer film. The penetrant (water) first dissolves on the surface of the polymer and then penetrates through the film by molecular diffusion and then exits the film [49]. Diffusivity of water is of major interest of this work especially in the case of low water concentrations. In order to study diffusivity of water molecules through HPX films, infinite dilution was chosen as the region of study to minimize the interactions between water molecules. In this work, changes in the glass transition temperatures of the HPX films with addition of sorbitol and CNC were measured by the differential scanning calorimetry and the corresponding diffusivity behaviours were characterized by measuring the diffusion coefficients of water in HPX films with various amounts of sorbitol and CNC using the technique of inverse gas chromatography (IGC). In order to meet the conditions for the applicability of the method, infinite dilution was used as the absorption isotherm is linear. Also, activation energy of diffusion of water in the HPX films with or without sorbitol and CNC was calculated at temperatures above the glass transition. The reasons that IGC is used are: fast analysis (minutes),

reliability and simplicity, sensitivity to even low concentrations (infinite dilution) and accuracy for low diffusion coefficients.

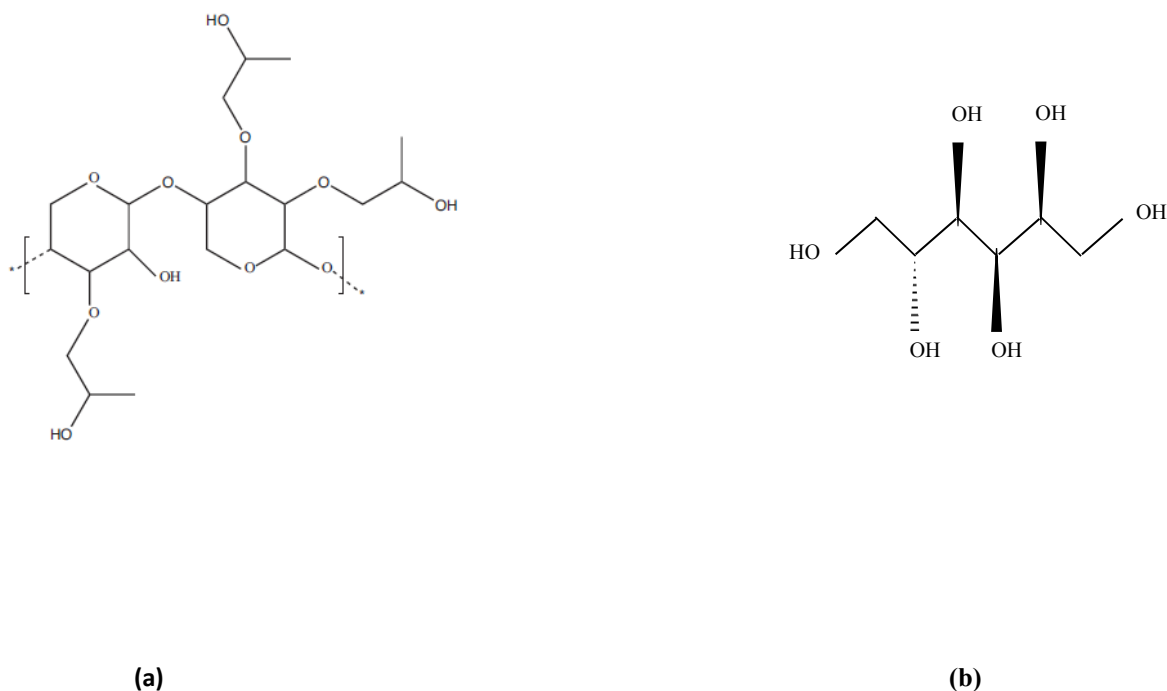


Figure 5.1. Molecular structures of a) the repeating unit of HPX [131] b) Sorbitol ($C_6H_{14}O_6$).

5.2. Inverse Gas Chromatography Theory

As mentioned, IGC was used to measure the diffusion coefficients of water at infinite dilution in a series of HPX films. At infinite dilution, retention time of the probe is independent of concentration and concentration of probe molecules in stationary phase is in equilibrium with that of the gas phase. In order to measure diffusion coefficient at infinite dilution, Equation 5.3 from Van Deemter method was used [132], [133].

$$H = A + (B/u) + Cu \quad (5.1)$$

where H is the equivalent theoretical plate height which is determined from the widths of the eluting peaks for different carrier gas flow rates; u is the average linear carrier gas flow rate. A is attributed to the eddy diffusion that is defined as $2\lambda d_p$. Here, d_p is the diameter of inert support and λ is a packing factor. The B term denotes the longitudinal molecular diffusion that is given by $2\gamma D_g$. Here, D_g is the diffusion coefficient of the solute in the carrier gas and γ is a constant, less than unity, signifying the curvy path experienced by the gas in a packed column. The C term corresponds to the mass transfer in the stationary phase. It is worth noting that C is independent of the flow rate but depends on a number of factors including the diffusion coefficient of the solute molecule in the stationary phase D_p . By plotting Equation 5.1 at a higher gas flow rates ($B/u \rightarrow 0$), the slope of the linear portion is equal to C . Then, D_p can be obtained:

$$C = \left(\frac{8}{\pi^2}\right) \left(\frac{d_f^2}{D_p}\right) \left(\frac{k}{(1+k)^2}\right) \quad (5.2)$$

where k is the partition ratio; d_f is the thickness of the stationary phase that is determined by the following equation:

$$d_f = \left(\frac{1}{3}\right) W \left(\frac{\rho_s}{\rho_p}\right) r_s \quad (5.3)$$

where W is the percentage loading of the polymer; ρ_s and ρ_p are the density of inert support and polymer, respectively; r_s is the average radius of inert support particles.

The partition ratio, k , is calculated from the following equation:

$$k = (t_r - t_f)/t_f \quad (5.4)$$

where t_r and t_f are the retention times of solvent and non-interacting indicator, such as air, respectively.

H in the Van Deemter equation can be obtained by equation:

$$H = \left(\frac{L}{5.54}\right)\left(\frac{W_{1/2}}{t_r}\right)^2 \quad (5.5)$$

where L is the column length; $W_{1/2}$ is the peak width at half of the peak height.

Also, u is the linear velocity of carrier gas which can be obtained by:

$$u = \frac{jV_0}{\bar{a}} \frac{T_{col}}{T_{flow}} \quad (5.6)$$

where T_{col} is the temperature of the column; T_{flow} is the temperature of the flow meter; \bar{a} is volume of gas phase per unit length determined by dividing the retention volume³ of air by the column length; V_0 is the corrected flow rate; and j is the compressibility (James Martin correction) factor which is defined from:

$$j = \frac{3}{2} \frac{\left[\left(\frac{P_i}{P_o}\right)^2 - 1\right]}{\left[\left(\frac{P_i}{P_o}\right)^3 - 1\right]} \quad (5.7)$$

Here, P_i and P_o are the inlet and outlet pressures of the column.

³ Retention volume: the volume of gas phase that passes through the column from the time of injection to the elution time of the peak maximum.

5.3. Materials and Method

5.3.1. Materials

Xylan from beechwood, propylene oxide, sodium hydroxide and sorbitol were purchased from Sigma Aldrich (Oakville, ON, Canada) and used as received. Cellulose nanocrystal (CNC) with diameters of 5-10 nm and a length of 150 nm was provided by Alberta Innovates Technology Future (AITF). Acid washed glass beads with a diameter range of 150-212 μm , also purchased from Sigma Aldrich, were used as the solid support for HPX. And a 0.5 μl Hamilton syringe was used for the injection of water.

5.3.2. Preparation of Hydroxylpropyl Xylan

Hydroxylpropyl xylan (HPX) was prepared by reacting xylan with propylene oxide according to the method of Jain *et al.* [62] Xylan (5 g) was first dissolved in 20 ml sodium hydroxide solution (pH 10) at ambient temperature and with constant stirring in a three neck flask under nitrogen for 2 hours. Upon the complete dissolution of xylan, the solution was cooled down by placing the flask in an ice bath. While stirring under nitrogen, 10 ml of propylene oxide was added drop-wise using an addition funnel. The reaction was left stirring under nitrogen for 12 hours at ambient temperature. Then the reaction was precipitated with 150 ml acetone with brisk stirring. The suspension was let to settle and removed, then washed with fresh acetone. The precipitate was finally collected by filtration and dried in vacuum for 24 hours.

5.3.3. Differential Scanning Calorimetry

Differential scanning calorimetry (DSC) experiments were carried out to determine the glass transition temperatures of the neat HPX film and those with the addition of different amounts of sorbitol and CNC. All experiments were carried out using a DSC 2910 (TA instruments, USA),

calibrated with indium and zinc standards. Aluminum hermetic pans and lids were used for experiments with an empty pan used as reference. For preparing the films, HPX, sorbitol and CNC were dissolved in distilled water according to the amounts described in Table 5.1. The solution was stirred for an hour and then was filtered to remove any insoluble materials. Fifteen ml of each solution was poured in a plastic petri dish (diameter 9 cm) covered with teflon papers. The films were left at ambient temperature and pressure for one week to dry. Approximately 2 mg of the dried films were sealed in the pans with the lid on top. To ensure that all samples had the same thermal history, each sample was heated to 150 °C with a heating rate of 10 °C/min under nitrogen, then it was cooled down to room temperature. The same heating and cooling steps were repeated. Results of the third heating with a heating rate of 5 °C/min are reported and used for comparison. The first heating was used to get rid of the water in the films while the second heating was carried out to ensure that the polymers went through the same thermal history without water. Midpoint temperatures were reported as glass transition temperature for each sample. The measurements were repeated three times for each sample and the corresponding means and standard errors are reported.

5.3.4. Inverse Gas Chromatography Procedure

Chromatographic measurements were carried by an Agilent 7890A Series GC equipped by a thermal conductivity detector (TCD). Helium was used as the carrier gas. The injector and TCD temperature were set 200 °C and 250 °C, respectively (50 °C above the column temperature) to prevent condensation in the injector and detector.

The chromatographic columns were 90-100 cm long, 1/4-in o.d., stainless steel tube, packed with glass beads (150-212 μm diameter) coated with HPX films. For preparing the column, weighted quantity of the HPX, sorbitol and/or CNC were dissolved in distilled water (Table 5.1)

and stirred for an hour and filtered to remove insoluble materials. A known amount of glass beads (20 g) was added to a known amount of the solution (10 ml). Using the rotary evaporator, the solvent was evacuated and the polymer film was coated on the glass beads. The percentage loading of the coating was <5% determined by thermal gravimetric analysis (TGA). The column was filled with the coated support and both ends were blocked with glass wool. The column characteristics are shown in Table 5.2.

Small amounts of water vapor (0.01-0.05 μl .) was injected in the column through the column injector using a 0.1 μl Hamilton syringe to have infinite dilution of the solvent. Changing the sample concentration would not change retention time when working in the infinite dilution region. A small amount of air was also injected with the sample to determine the dead volume of the column. Each measurement was repeated at least 5 times to verify infinite dilution conditions. Most of the retention times were reproducible with less than 5% difference with their average, meeting infinite dilution conditions. Measurements of diffusion coefficient were done using the average of retention times and peak width for each flow rate. The diffusion data are presented with the standard deviations regarding the uncertainties from the slope of the Van Deemter curves. The experiments were carried out from 120 to 170 $^{\circ}\text{C}$ at a 10 $^{\circ}\text{C}$ interval. The column temperatures were chosen to be higher than the T_g of HPX to minimize the adsorption of the injected water.

Table 5.1. Concentrations of HPX solutions used for the preparation of the films and coating of the glass beads

Polymer solution	HPX (g)	Sorbitol (g)	CNC (g)	Water (ml)	Wt % (HPX/Sorbitol/CNC)
1	1	-	-	33	100
2	0.8	0.2	-	33	80/20/0
3	0.7	0.3	-	33	70/30/0
4	0.6	0.4	-	33	60/40/0
5	0.6	0.39	0.01	33	60/39/1
6	0.6	0.37	0.03	33	60/37/3
7	0.6	0.35	0.05	33	60/35/5

Table 5.2. Specifications of the packed columns

Polymer coating	Mass of glass beads in the column (g)	Mass of coating in the column (g)	Column length (cm)
Solution 1	16.2	0.057	90
Solution 2	17	0.062	90
Solution 3	16.4	0.057	90
Solution 4	17.9	0.064	100
Solution 5	16	0.061	100
Solution 6	16.2	0.055	100
Solution 7	17.1	0.056	90

5.4. Results and Discussion

DSC curves of the third heating of HPX films containing various amounts of sorbitol are shown in Figure 5.2. The glass transition temperature (T_g) of each film is also given in the figure. As expected, addition of sorbitol to HPX films decreased their T_g , thereby increasing their flexibility. In particular, the T_g of the films decreased from 137.4 °C (no sorbitol) to 103.7 °C (40 wt% sorbitol). However, it is worth mentioning that the effect of sorbitol on the T_g (i.e., $dT_g/dC_{\text{Sorbitol}}$) diminished with increasing sorbitol concentration, a somewhat expected observation. As some of the sorbitol molecules at high concentrations do not participate in breaking the HPX-HPX hydrogen bonds, a mechanism that increases the free volume and chain mobility of HPX, thereby the glass transition temperature reduction decreases [134]. There exist mathematical models that correlate T_g of a plasticized polymer with the plasticizer content. However, most of them are empirical and are only applicable over a narrow range of concentrations especially when the polymer and plasticizer have limited compatibility. Also, the kinetic aspect of the T_g measurements is not considered in such models that makes the results rough estimates of the plasticizer effect on the T_g of the polymer [135]. In the range of concentrations of interest in the present work, we used the results of two models to compare with our experimental results. One is the modified equation of Couchman and Karasz (C-K) which can be used for polymer-plasticizer mixtures when the ΔC_p of the polymer and plasticizer is not available [136].

$$\ln\left(\frac{T_g}{T_{g1}}\right) = \frac{w_2 \ln\left(\frac{T_{g2}}{T_{g1}}\right)}{w_1 \left(\frac{T_{g2}}{T_{g1}}\right) + w_2} \quad (5.8)$$

The other model is the simple empirical model which predicts glass transition temperatures that yielded results that are less than 5% different from our the experimental results [135]:

$$\frac{1}{T_g} = \frac{1}{T_{g1}} + \left(\frac{1}{T_{g2}} - \frac{1}{T_{g1}}\right)\sqrt{w_2} \quad (5.9)$$

In the above equations, T_g is glass transition temperature of the plasticized polymer; T_{g1} is the glass transition of plasticizer; T_{g2} is the glass transition of the bare polymer. And w_1 and w_2 are weight fractions of the plasticizer and the polymer, respectively. As shown in Figure 5.3, Equation 5.8 yielded results that are significantly lower than the experimental results. However, Equation 5.9 shows a much better agreement.

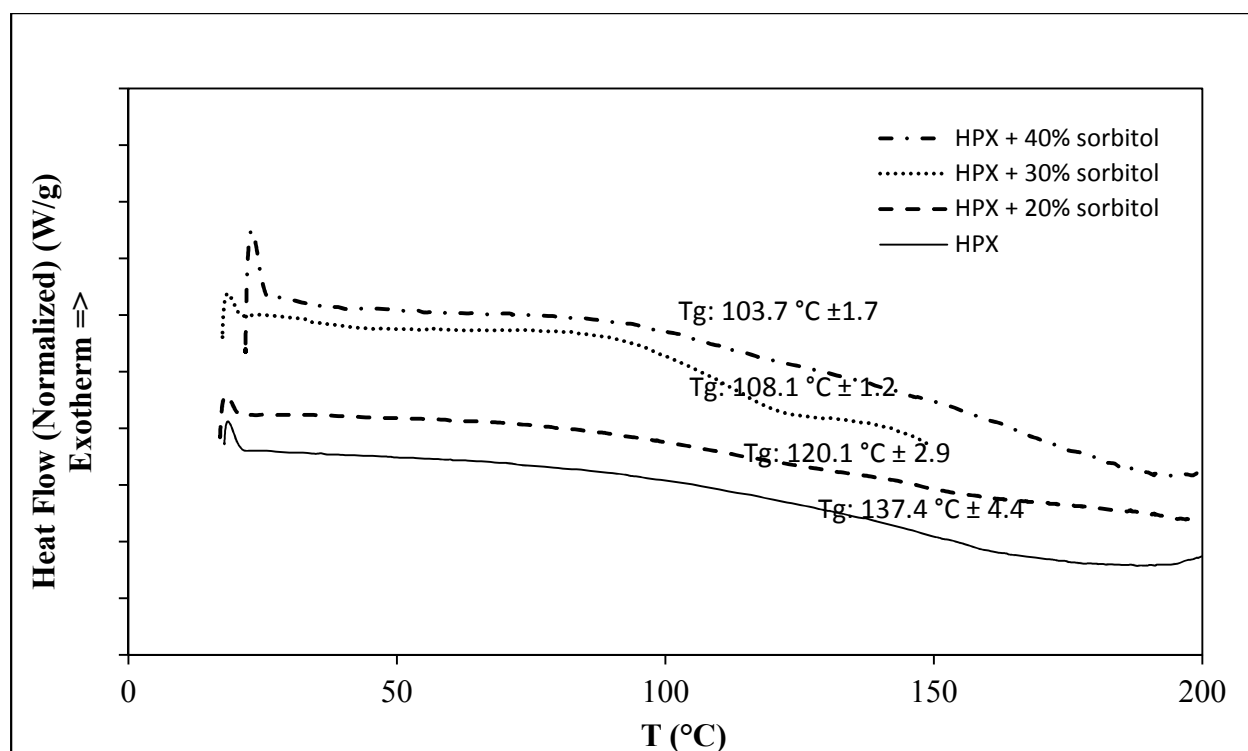


Figure 5.2. DSC curves for HPX films with sorbitol

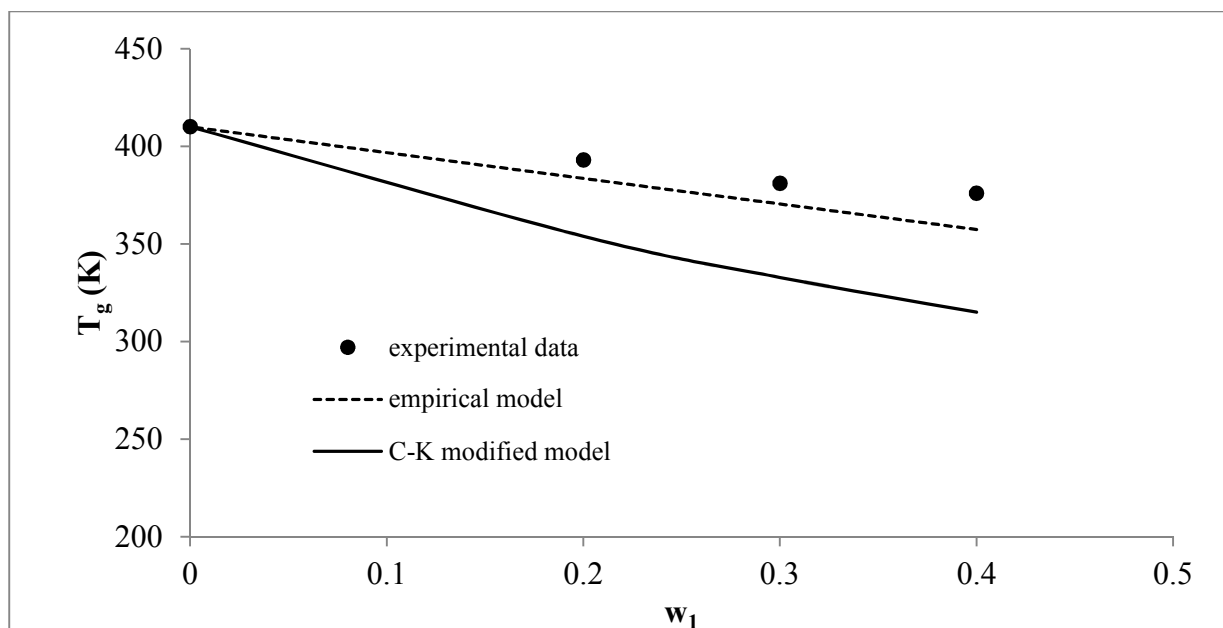


Figure 5.3. T_g of plasticized films as a function of weight fraction of sorbitol compared with two mathematical models

Figure 5.4 shows the effect of adding CNC to the plasticized HPX films with 20 to 40 wt % of sorbitol. As expected, adding CNC to the plasticized films increased their T_g except the case in which 1 wt % of CNC was added to the film with 60 wt % HPX and 39 wt % of sorbitol. Compared to the film with 60 wt % HPX and 40 wt % of sorbitol, the T_g decreased from 103.7 to 98.6 °C. In fact, similar behaviour was observed for plasticized starch-based composites that addition of CNC up to 3.2 wt % decreased the T_g of the composite [137]. The reason is not known and further investigation is needed. Nevertheless, our data show that the effect of adding 1 wt % of CNC on the T_g of the plasticized HPX films depends on the amounts of HPX and sorbitol. In general, adding CNC to a hydrophilic polymer such as HPX reduces its chain mobility and free volume, thereby increasing T_g . This is because there are strong interactions between the hydroxyl groups of CNC and those of HPX [138]. And it seems that effect of such

interactions on the T_g (i.e., dT_g/dC_{CNC}) is more or less linear over the range of 1 to 5 wt % and independent of the sorbitol concentration.

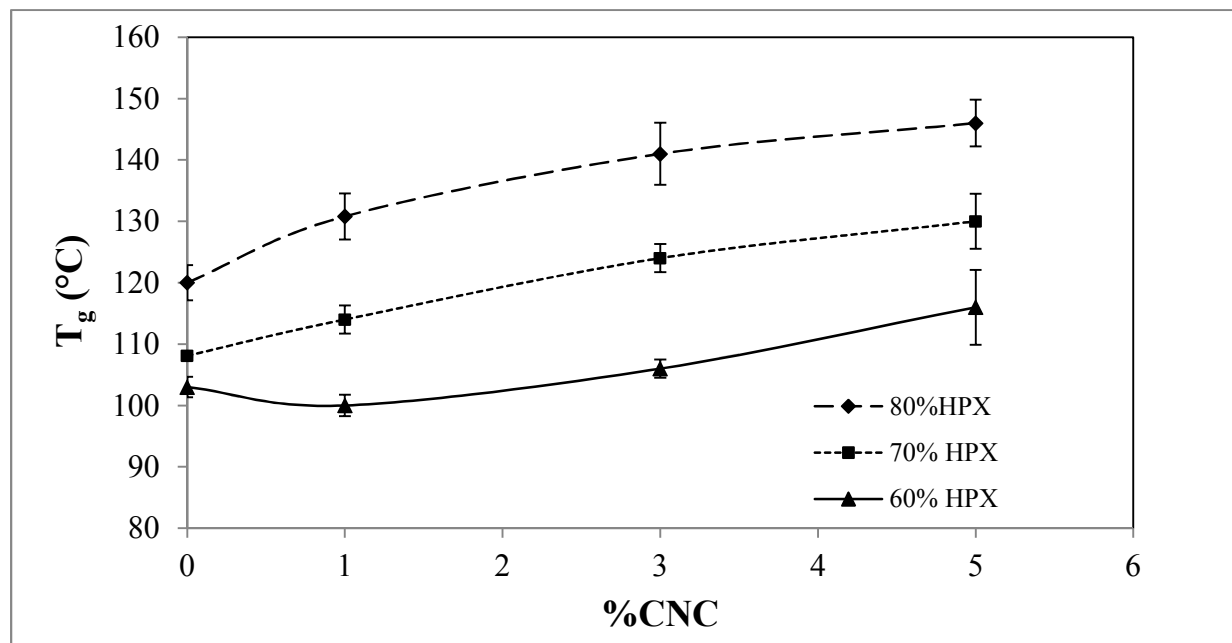


Figure 5.4. Effect of adding 1-5% CNC to plasticized HPX films on T_g (Data is presented as mean+ standard error for n=3)

To quantify the water diffusivity for the aforementioned HPX films, IGC was used. It should be pointed out that the profile of the elution peaks is not perfectly symmetrical as required by Equation 5.5. In fact, the peaks tend to have a long tail (due to the adsorption of water molecules). Same phenomenon has been reported for cellulosic type of materials [139]. To reduce the adsorption effect, high flow rates but without severe pressure drop were used.

The van Deemter equation plots of plate height (H) versus carrier gas linear velocity (u) over the temperature range of 120-170 °C for the neat HPX film are shown in Figure 5.5. We omit the corresponding plots of the HPX films with different amounts of sorbitol and/or CNC as they resemble to those of neat HPX. It is obvious from Figure 5.5 that the carrier gas flow rate used

met the condition. The curves are linear showing that the first two terms of the van Deemter equation could be ignored. Estimated diffusion coefficients of water in different HPX films are listed in Table 5.3. It shows that diffusion coefficient at infinite dilution increases with increasing temperature, as expected, in all cases. Also, diffusion coefficient varies with the concentration of additives, sorbitol and/or CNC, added to the HPX film. However, all such changes are more or less within the same order of magnitude.

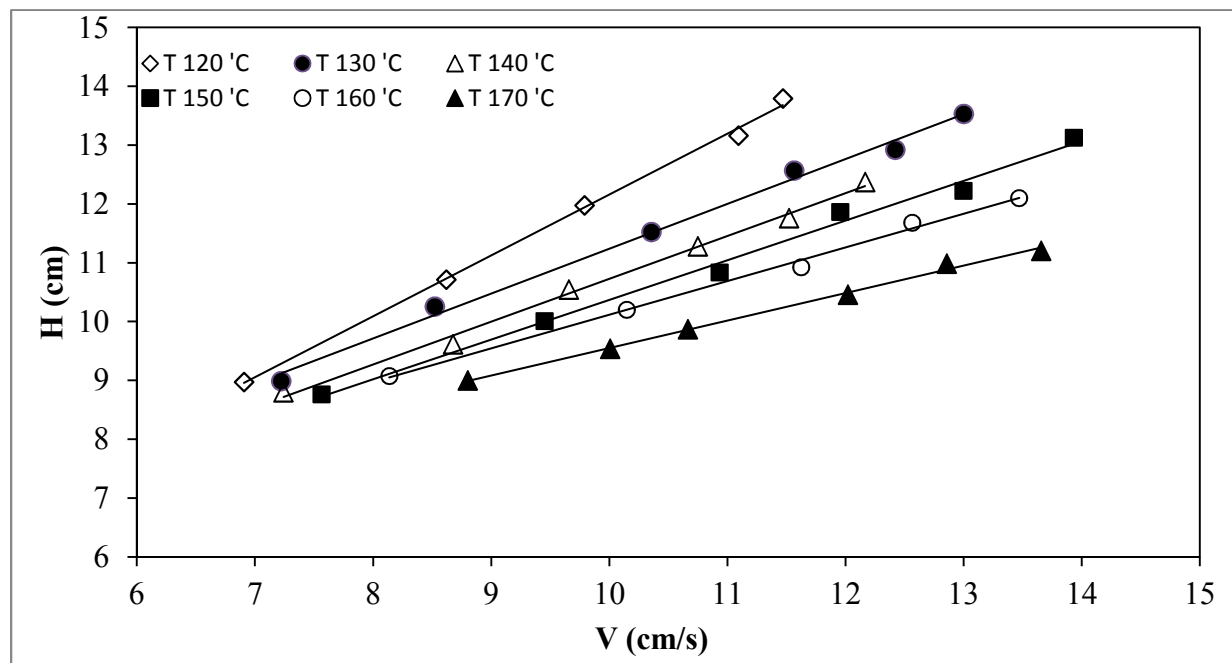


Figure 5.5. Van Deemter Plots for the neat HPX film at various temperatures from 120 °C to 170 °C

Table 5.3. Infinite dilution diffusion coefficients of water in HPX films with different amounts of sorbitol and CNC at various temperatures

T (K)	HPX	$D^\infty (\times 10^7 \text{ cm}^2/\text{s})$					
		20% sorbitol	30% sorbitol	40% sorbitol	39% sorbitol+ 1% CNC	37% sorbitol+ 3% CNC	35% sorbitol+ 5% CNC
394	1.94±0.12	4.30±0.95	5.74±1.28	7.63±0.23	5.96±0.69	4.19±0.59	3.21±1.85
404	3.13±0.29	6.43±1.46	6.91±0.55	10.55±2.15	8.16±0.25	5.55±0.61	3.92±0.33
414	4.68±0.94	7.72±0.49	8.63±2.06	11.42±3.27	10.01±1.11	7.63±0.3	5.97±0.45
424	6.77±0.95	11.89±2.1	13.44±1.19	16.70±1.36	16.48±0.57	10.61±0.81	7.39±0.78
434	9.41±2.4	15.16±0.87	18.68±3.12	19.53±2.87	18.91±3.60	15.20±2.21	10.99±1.56
444	11.58±2.41	20.40±3.01	25.15±4.06	28.74±1.63	24.08±2.9	16.01±1.08	14.03±3.56

As mentioned earlier, sorbitol molecules reduce the number of hydrogen bonds between the HPX chains leading to more free volume available for the diffusion of water [134]. In fact, Figure 5.6, logarithmic plots of diffusion coefficient versus the sorbitol concentration in HPX over the range of 0 to 40 wt % support such an idea. According to free volume theory, there exist a logarithmic relationship between diffusion coefficient and free volume. However, other researchers proposed that increasing mobility of HPX chains due to the increasing amount of sorbitol would lead to higher rates of free volume redistribution, thereby increasing the rate of diffusion [133].

Adding a small amount of CNC to the plasticized films decreases diffusion coefficient. Generally, increase in barrier properties of polymers due to the addition of nano-sized fillers is attributed to three reasons: 1) induced crystallization of the polymer, 2) increase in tortuosity due to fractionation and alignment of crystals in the diffusing direction and 3) decrease in the free

volume of the amorphous phase [49]. Several studies have related the reduction in water transport through biocomposites filled with CNCs (with average aspect ratios of 10-50) to the increase in the tortuosity in the films [8], [127], [9], [10], [129], [130]. Our DSC results did not suggest the existence of crystalline phase in HPX films upon addition of CNC. On the other hand, Figure 5.7 suggests that it is the decrease in the free volume that leads to the decrease in the water diffusivity as the data shows a linear relationship between logarithm of diffusion versus concentration of CNC in the films (i.e., the free volume theory). Cellulose-based fillers are able to form strong hydrogen bonds with hydrophilic biopolymer resulting in a less mobile structure (i.e., lower free volume) and therefore reduce the diffusivity of water in the composite environment [9]. In the present study interaction of CNC with HPX decreased diffusion coefficient by 10-50% at different temperatures as a result of reduction in free volume and chain mobility. This is somewhat unexpected as the CNC added did not increase the tortuosity of the water molecules. However, Dufresne *et al.* [140] had a similar observation that adding 30% CNC to starch-based bio-composites reduced diffusion coefficient of water only by about 65% in their study. It seems that sorbitol increases while CNC decreases the free volume in the HPX matrix leading to the result that the water diffusivity of the HPX film with 35 wt % sorbitol and 5 wt % is comparable to that of the neat HPX film.

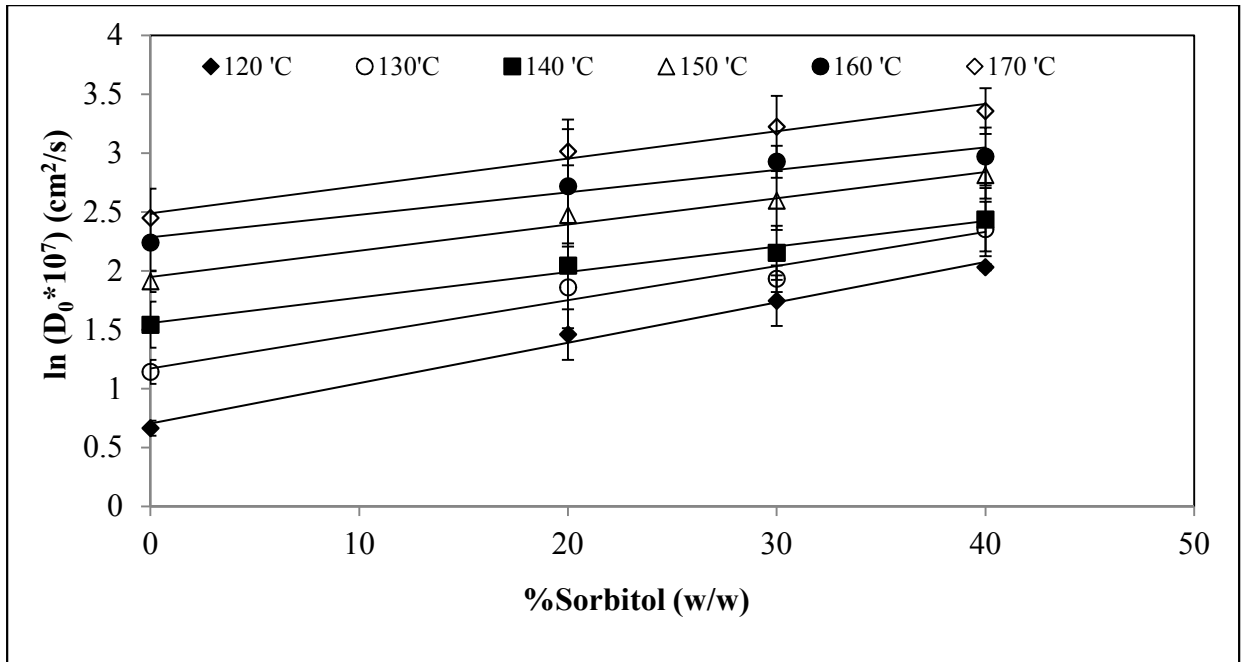


Figure 5.6. Effect of sorbitol concentration on the diffusion coefficient of water at various temperatures.

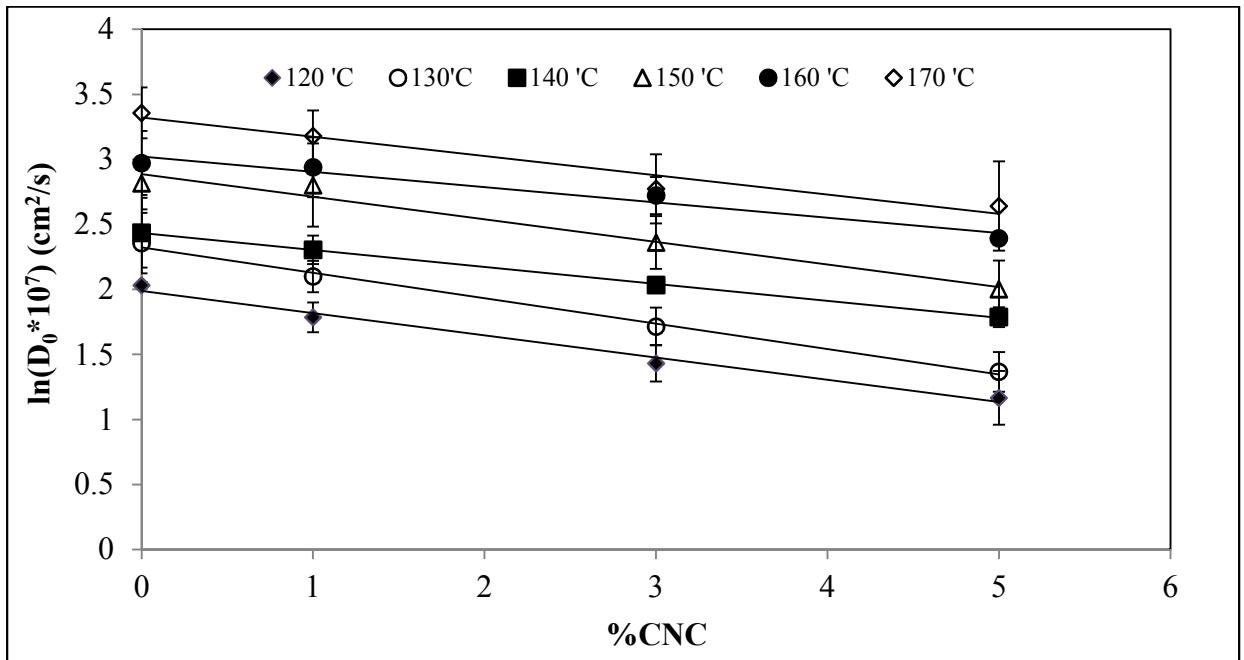


Figure 5.7. Effect of adding CNC to HPX films with 60%w/w HPX (40%w/w Sorbitol) on diffusion coefficient of water at various temperatures

Figure 5.8 Figure 5.9 show the inverse temperature dependence of the logarithm of the diffusion coefficient of water for the HPX films at various concentrations of sorbitol and CNC. Obviously, the data follow a linear relationship in the two plots, indicating that the data follow the Arrhenius equation of the temperature dependency of diffusion coefficient (D):

$$D = D_0 e^{\frac{-E_a}{RT}} \quad (5.10)$$

where D_0 is pre-exponential constant and E_a is the activation energy. R and T are the universal gas constant and temperature, respectively. Here, the activation energy signifies the energy required for free volume hole formation against the attractive forces between the polymer chains as well as that required for the water molecules to jump from one free volume hole to a nearby one [133]. Following the Arrhenius behaviour simply suggests that the water molecules exhibited a hopping diffusion mechanism as described in the free volume theory [132].

Table 5.4 summarizes the activation energy values determined based upon the data shown in Figure 5.8 Figure 5.9. Over the temperature range of interest, activation energy decreases with increasing concentration of sorbitol. As discussed before, adding sorbitol reduces inter-chain interactions, thereby decreasing the activation energy required for the free volume hole formation and for the hopping of the water molecules [133].

On the other hand, adding CNC to plasticized films increases activation energy. Once again, the increase in the activation energy is attributed to the adsorption of HPX chains on to the CNC surfaces. It is obvious that most significant increase in the activation energy occurs at 1 wt % CNC. Further increase in the CNC concentration does not increase the activation energy much. It means that increasing CNC concentration reduces diffusion coefficient by reducing fractional

free volume but not by decreasing the corresponding activation energy. This is probably due to insignificant change in the environment experienced by the water molecules.

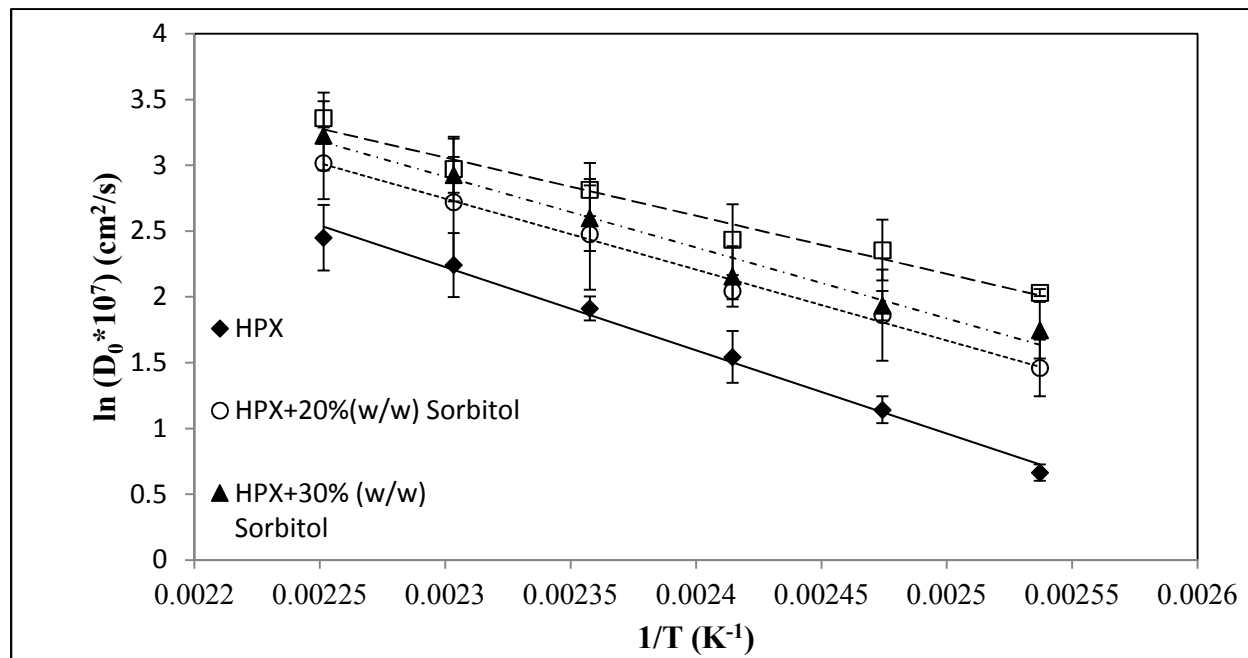


Figure 5.8. Inverse temperature dependence of the diffusion coefficient of water in HPX films with various concentrations of sorbitol.

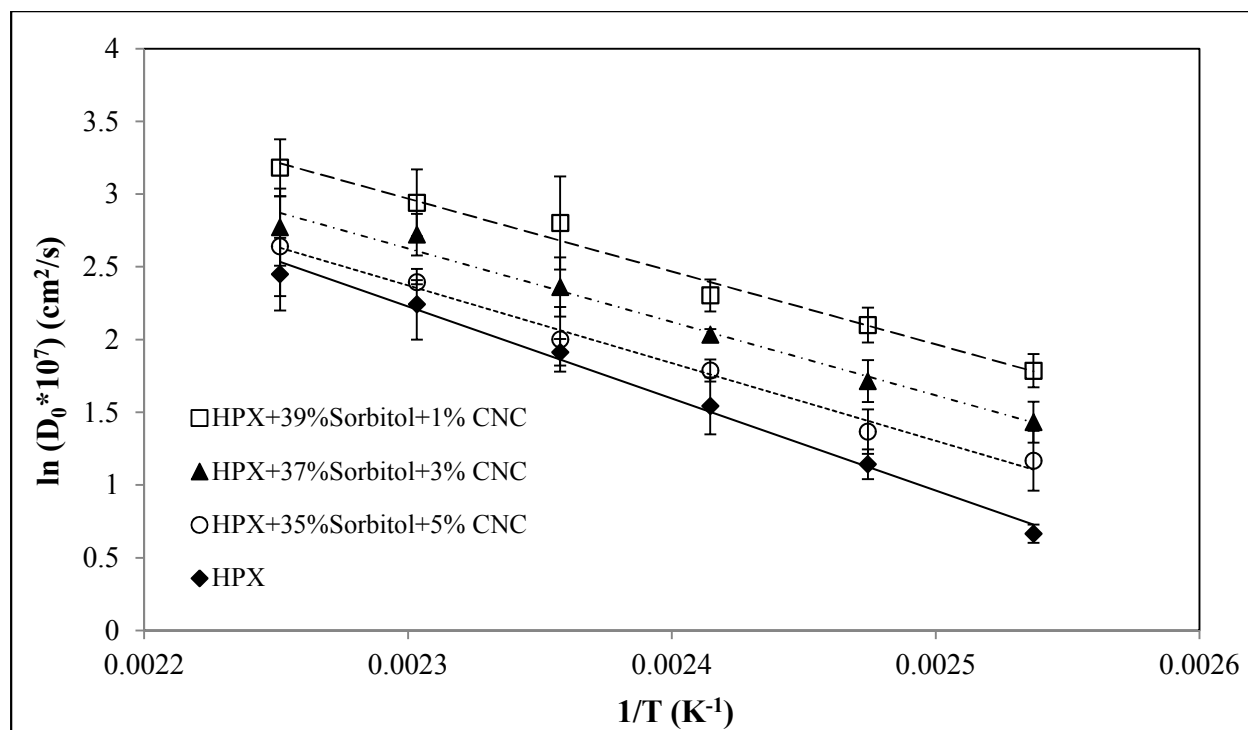


Figure 5.9. Inverse temperature dependence of the diffusion coefficient of water in HPX films with 60 wt % of HPX and various concentrations of sorbitol and CNC.

Table 5.4. Dependence of the activation energy of water diffusion in HPX films on the sorbitol and CNC concentrations (films contained 60 wt % HPX).

Sorbitol	E_a	CNC	E_a
% (w/w)	(kJ mol⁻¹)	%(w/w)	(kJ mol⁻¹)
0	52.6±0.3	0 (40% Sorbitol)	36.8±0.4
20	44.9±0.2	1 (39% Sorbitol)	41.6±0.3
30	44.8±0.4	3 (37% Sorbitol)	41.9±0.3
40	36.8±0.4	5 (35% Sorbitol)	44.4±0.3

5.5. Conclusion

To determine the suitability of using HPX as an internal layer for packaging material, the effect of adding sorbitol, a commonly used environmentally friendly plasticizer, and a nano-sized filler namely cellulose nanocrystals, on the film glass transition temperature (T_g) and water diffusivity was studied. Adding sorbitol to the HPX film decreased T_g as a result of increasing free volume in the material. This is because sorbitol reduces the number of hydrogen bonds formed between the HPX chains. The diffusivity of water in such plasticized HPX films was increased 2-5 times by adding 20 to 40 wt % of sorbitol. The concentration dependence of the water diffusivity indicates that the diffusion of water follows the free volume theory. Adding CNC to the plasticized films increased T_g of the films while decreasing the water diffusivity. Once again, the free volume theory is able to explain the data. And the expected increased tortuosity due to the presence of CNC with high aspect ratios did not slow down the diffusion of water molecules. Addition of 5% CNC to plasticized films would neutralize effect of sorbitol on increase of diffusion coefficient. However, the films are still poor barriers to water.

Chapter 6

6. Inverse Gas Chromatography Study of the Permeability of Aroma through Hydroxypropyl Xylan Films

6.1. Introduction

Owing to their superior barrier properties to water and oxygen, synthetic polymers have been the choices as the packaging materials for packaged food to preserve food quality. Over the years, disposal of such non-biodegradable polymers has led to various environmental issues. Replacing such synthetic polymers by natural polymers seems to be a sensible approach to the problem. In addition to their biodegradability, natural polymers are renewable and inexpensive [3]. Extensive efforts have been devoted to developing packaging materials using such natural polymers with a good balance of mechanical, thermal, optical and barrier properties [77]. Hydroxypropyl xylan (HPX), a water soluble derivative of xylan which is a major component of hemicelluloses, is a natural polymer which forms rigid, transparent films from its aqueous solution and has a potential to be used in certain food packaging applications. Diffusivity of water at infinite dilution in HPX films modified by adding sorbitol, a commonly used food grade plasticizer, and cellulose nanocrystalline (CNC), a nano-sized filler, was studied in previous work to evaluate its potential as a food packaging material [74]. The results showed that HPX films containing 35 wt % sorbitol and 5 wt % CNC exhibited the required mechanical, thermal and optical properties but poor water barrier properties. The results implied that HPX, being water soluble, has the potential to be used as an intermediate layer in a multi-layer film to retain aroma, a vital component to the taste and smell of the food. It is worth noting that most multi-

A modified version of this chapter has been published as: "Inverse Gas Chromatography Study of the Permeability of Aroma through Hydroxypropyl Xylan Films" Fatemeh Bayati, Yaman Boluk, and Phillip Choi, ACS Sustainable Chem. Eng., 3 (12), 2015, 3114-3122

layer films are made up of moisture barrier materials (e.g., polyethylene) which exhibit poor aroma but good water barrier properties [141]. CNC, being a recyclable organic filler, is expected to improve barrier and mechanical properties of the HPX films due to their high surface area and aspect ratio, excellent mechanical, chemical and thermal properties [10], [142]. Several studies have shown the improvement of barrier properties of biopolymers by the addition of CNC to the polymer matrix [8], [9]. Decreasing polymer chain mobility and increasing the transport path of the permeating molecules, as a result of using CNC, can enhance barrier properties [129].

The extent of the leaking of food aroma depends on several factors [143]. First, it is the composition of the packaged food (e.g., water content, fat content, aroma composition, etc.) that governs the partition of the aroma molecules between the food and the packaging material that is normally in close contact with the food. In other words, having knowledge of the solubility of different types of aroma molecules in food and the packaging material is imperative. The second factor is the diffusivity of the aroma molecules through the packaging material [19], [144]. In particular, if a polymer is used, its molecular weight averages, glass transition temperature, degree of crystallinity and morphology will determine the diffusivity of the aroma molecules. Since additives are frequently used in polymers, types and concentrations of the additives (e.g., plasticizer and fillers) are the other factors that can affect the rate of diffusion. Thirdly, external factors such as temperature and humidity of the surroundings also influence the leaking of aroma [145]. The aroma leakage can happen for all flavors simultaneously which results in weak flavors left for the food or even worse, selective leakage of the flavors, which may change the balance of flavors in the food resulting in unpleasant flavors of the food [146].

Since leakage is related to the permeability of aroma, in this work, permeability of a series of aroma through a neat HPX film and HPX films containing 40 wt % of sorbitol and 35 wt % sorbitol and 5 wt % CNC was studied. Primary alcohols (methanol, ethanol, propanol and butanol) were selected as permeates, as they are known to be responsible for food aroma. For examples, butanol and hexanol are detected in cheese [147] and cooked rice [148]; methanol, ethanol, propanol and butanol are found in southern pea seed [149]. Methanol, ethanol and propanol are also some of the aroma found in peanut [150].

To study solubility and diffusivity, we used the technique of inverse gas chromatography (IGC), as the technique yields information about the two processes readily. In fact, IGC has shown to be a reliable and efficient method for obtaining solubility and diffusivity of solvents in polymers at different temperatures when the solvents are at finite concentrations or infinite dilution. IGC results have shown to be within a good agreement with data from gravimetric sorption [92], [95], [96]. The high sensitivity of IGC detectors ($\sim 10^{-9}$ mol) makes the technique more applicable compared to other techniques [88]. From the characterization perspective, doing experiments at infinite dilution is advantageous as the dissolution and diffusion are mainly controlled by the interaction between the aroma and the chosen polymer and not by that of the aroma-aroma interaction. Solubility coefficients and diffusion coefficients of the aroma at infinite dilution were then used to calculate the corresponding permeability coefficients [151].

6.2. Theory

Permeation of small molecules in a polymer takes place by a multistep process in which the small molecules: (1) adsorb on the polymer surface, (2) dissolve in the polymer and diffuse through the polymer and (3) desorb from the other side of the surface of the polymer. In general, the dissolution and diffusion processes control the rate of permeation. Therefore, permeability

coefficient (P), in the context of the present work, is defined as the product of solubility coefficient (S) and diffusion coefficient (D) of the permeate in a polymer/permeate system [146]:

$$P = S \times D \quad (6.1)$$

In this work, we used the technique of inverse gas chromatography to measure both S and D .

In gas chromatography, interactions between injected probes (i.e., the aroma compounds and water in this work) and the stationary phase (i.e., HPX 'with and without additives) is quantified by the specific retention volume V_g^0 (ml/g) [88], [90], [93], [152]:

$$V_g^0 = \frac{V_N}{w_s} * \frac{27315}{T} \quad (6.2)$$

where w_s is the weight of stationary phase (g) and T is the absolute temperature of the column (K). V_N is the net retention volume of the probe (ml) estimated by:

$$V_N = F_c(t_r - t_m) \quad (6.3)$$

where t_r and t_m are the retention times of probe and the marker (min). The marker is either non-adsorbing or non-absorbing compound. F_c is the corrected carrier gas flow rate under the column operating conditions (ml/min):

$$F_c = \frac{T_c}{T_{fl}} * \frac{P_0 - P_w}{P_0} * j * F \quad (6.4)$$

where F is the measured flow rate of the carrier gas (ml/min). And T_c and T_{fl} are the column and flow meter temperatures (K), respectively. P_0 is the pressure at the outlet of the column and P_w is the vapour pressures of the probe inside the flow meter (atm). And j is the compressibility factor which is defined as:

$$j = \frac{\left(\frac{P_i}{P_o}\right)^2 - 1}{\left(\frac{P_i}{P_o}\right)^3 - 1} * \frac{3}{2} \quad (6.5)$$

where P_i is the inlet pressure of the column.

Retention of the probe may be a result of the pure adsorption on the stationary phase surfaces or the mixed retention mechanism involving both adsorption and bulk absorption. Adsorption occurs when the stationary phase, in the case of polymer, is below its glass transition temperature T_g . Once it is above its T_g , the retention mechanism is dominated by the bulk absorption [153]. In this work, we carried out all measurements at temperatures mostly above the T_g of HPX to minimize the effect of adsorption on the peak width that is important in determining the diffusion of the probe in the polymer. In order to confirm that the sorption data obtained correspond to equilibrium condition, the specific retention volume should not have any dependence on the carrier gas velocity. This behaviour is most expected when the polymer is in rubbery state. In the case of weak dependence, the retention parameters can be extrapolated to zero velocity of carrier gas. At infinite dilution, the sorption isotherms must meet Henry's law. Therefore, the corrected retention volume should not be depended on the amount of the solvent injected. If these requirements are fulfilled, the sorption data obtained correspond to equilibrium condition at infinite dilution [96].

To obtain solubility coefficients, S ($\text{cm}^3[\text{STP}]/\text{cm}^3 \cdot \text{atm}$), from the IGC measurements, one uses the following equation [151]:

$$S = V_g^0 \frac{\rho}{p_0} \exp \left[(2B_2 - V_1) j \frac{p_0}{RT} \right] \quad (6.6)$$

where p_0 is the standard pressure (1 atm); ρ is the polymer density (g/cm^3); B_2 is the second virial coefficient of the probe (cm^3/mol) which characterizes the interaction between the probe molecules; V_l is the solvents molar volume (cm^3/mol) at the column temperature T (K) and R is the gas constant ($\text{cm}^3 \text{ atm K}^{-1} \text{ mol}^{-1}$).

The diffusion coefficients of the probe (D) can be obtained at various temperatures using the plate height theory established by van Deemter et al. [30], [93], [154]:

$$H = A + \frac{B}{u} + Cu \quad (6.7)$$

where H is the height equivalent to a theoretical plate (cm). A , B and C are constants independent of flow rate and u is the average linear velocity of the carrier gas (cm/min).

$$u = \frac{jl}{t_m} \quad (6.8)$$

Using the eluted peak for each probe, H can be calculated from:

$$H = \left(\frac{l}{5.54} \right) \left(\frac{d}{t_r} \right)^2 \quad (6.9)$$

where l is the column length (cm) and d is the measured peak width at half height (cm).

When carrier gas flow rate is high, the term B/u is usually negligible and a plot of H vs u yields a straight line with a slope of C .

From C , diffusion coefficient, D , can be calculated as follows:

$$D = \frac{8}{\pi^2} \frac{k}{(1+k)^2} \frac{d_f^2}{C} \quad (6.10)$$

where k is partition ratio defined as:

$$k = \frac{t_r - t_m}{t_m} \quad (6.11)$$

And d_f is the thickness of the polymer coating on the inert support (cm) determined by the following equation:

$$d_f = \left(\frac{1}{3}\right) \frac{w_p}{w_s} \left(\frac{\rho_s}{\rho_p}\right) r_s \quad (6.12)$$

where w_p is the weight of polymer (gr); w_s is the weight of coated support (gr); ρ_s and ρ_p are the density of inert support and polymer (gr/cm^3), respectively; r_s is the average radius of inert support particles (cm).

6.3. Materials and Method

6.3.1. Materials

Xylan, propylene oxide, sodium hydroxide and sorbitol were purchased from Sigma Aldrich (Oakville, ON, Canada) and used without further purification. The probes (methanol, ethanol, propanol, and butanol-HPLC grade >99.8%) were also from Sigma Aldrich and propanol-HPLC grade >99.8% was from Baxter. The alcohols and water were injected in the vapor form. Cellulose nanocrystal (CNC) with diameters of 5-10 nm and an average length of 150 nm was provided by Alberta Innovates Technology Future (AITF).

6.3.2. Column preparation

Hydroxypropyl xylan was prepared according to the method introduced by Jain et al. [62] To prepare the columns, a weighted amount of the polymer with or without sorbitol and/or CNC (a total of 1 gram with or without additives) was dissolved in 33 ml water by stirring for an hour and then the non-dissolved materials were removed by filter. Then 10 ml of the solution was

added to 20 grams of glass beads in a rotary evaporator to coat the polymer on the beads. The coated glass beads were packed into 1/8 in. outer diameter stainless steel column. Both ends were blocked with glass wool. Column characteristics are shown in Table 6.1. Scanning electron microscopy (SEM) was used to scan the surface of the coated glass beads to confirm uniformity of the coatings (Figure 6.1). It also gives a visual estimation of the average coating thickness as calculated by Equation 6.12 which is less than 1 μm . Confirmation of the beads being coated and mass of the column loading was determined by thermal gravimetric analysis (TGA).

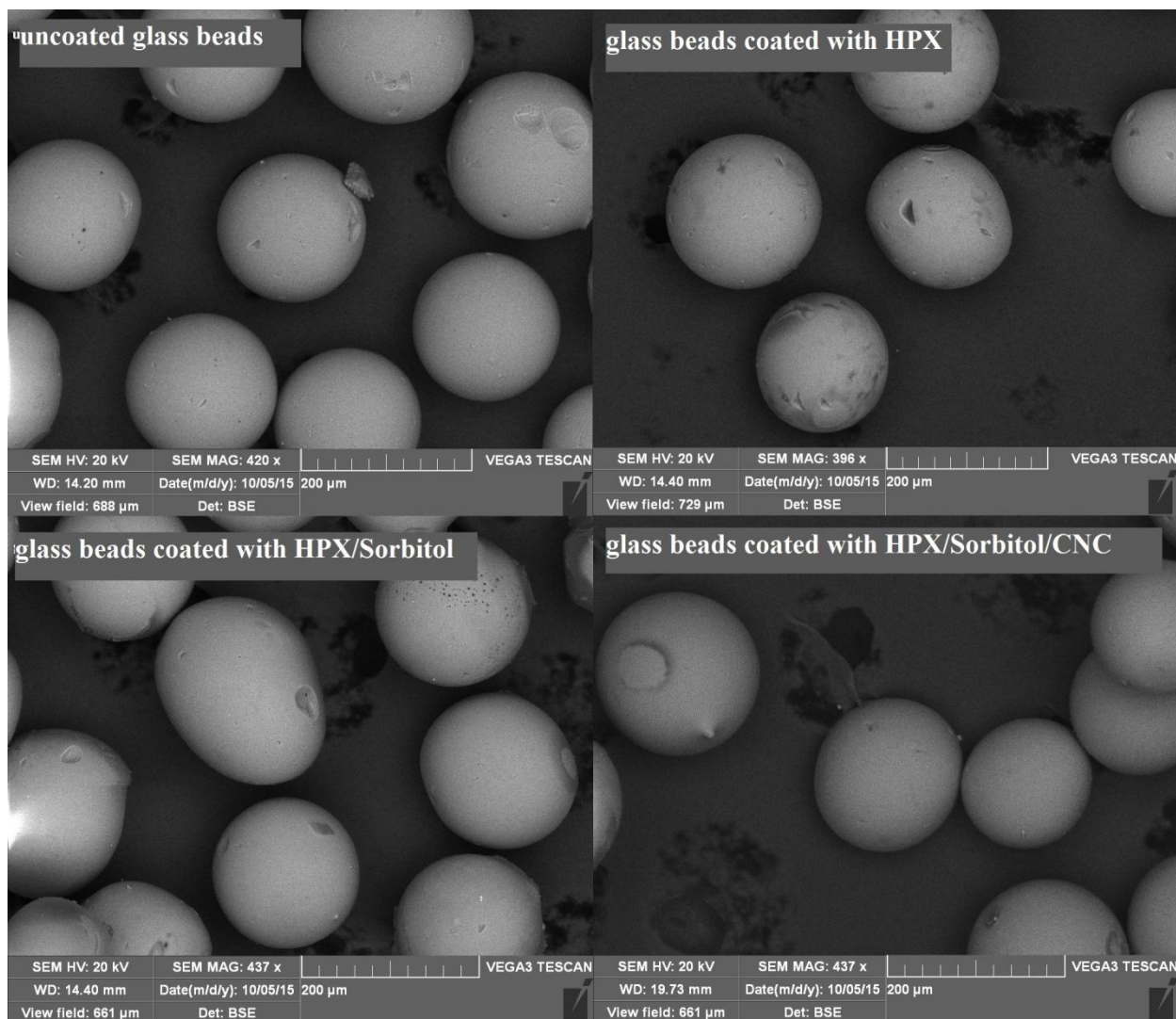


Figure 6.1. SEM of glass bead supports coated with HPX films.

6.3.3. Inverse gas chromatography procedure

The column was installed in the oven of an Agilent 7890A Series GC equipped with two types of detectors – flame ionization detector (FID) and thermal conductivity detector (TCD). Here, FID and TCD were used to detect alcohols and water, respectively. Helium and methane were used as the carrier gas and marker, respectively. Methane was used as the marker to determine dead volume of the column, thereby the average linear velocity of the carrier gas in the column. For the solubility and diffusion coefficient measurements, the experiments were run over a wide range of flow rates at temperatures 120 – 160 °C (393 – 433 K), with increments of 10 °C. The injector and detector temperatures were maintained at 250 and 300 °C, respectively, well above the column temperatures to prevent condensation. The measurements were done at infinite dilution concentration of the alcohols and they were injected in the vapour form and in the quantity of less than 0.5 µl using a 0.5 µl Hamilton syringe. Injections were repeated five times. Subsequent calculations using the five repeated retention times, resulted in related errors being less than 5%. The diffusion data are presented with the standard deviations regarding the uncertainties from the slope of the Van Deemter curves. The solubility data are presented as the average from five repeated measurements with the corresponding standard deviations.

Table 6.1. Specifications of the IGC columns

HPX/Sorbitol/CNC (wt %)	Mass of glass beads (g)	Mass of stationary phase (g)	Polymer film thickness (µm)	Column length (cm)
100/0/0	5.2	0.0273	0.33	150
60/40/0	5.9	0.0332	0.82	150
60/35/5	4.5	0.0341	0.61	150

6.4. Results and Discussion

6.4.1. Infinite dilution solubility coefficient

Figure 6.2 shows the measured solubility coefficients as a function of the molecular weight of the alcohols used in this work (methanol: 32.04, ethanol: 46.07, propanol: 60.1 and butanol: 74.12 g/mol) over the temperature range of 120 to 160 °C (i.e., 393 – 433 K) for the neat HPX film and those HPX films containing sorbitol (40 wt %) as well as sorbitol (35 wt %) and CNC (5 wt %). And their values are reported in Table 6.2. In general, solubility of small molecules in a polymer is determined by their condensability (i.e., volatility) and compatibility with the polymer. The observed minima in Figure 6.2 are simply a result of the balance between the two aforementioned factors. In particular, as the molecular weight of alcohol increases, volatility and polarity decrease. Decrease in volatility is in favor of increasing solubility while decrease in polarity has the opposite effect. Gavara et al. observed similar behaviour for the solubility of alcohols in ethylene-vinyl alcohol (EVOH), a common biodegradable polymer used for food packaging [155].

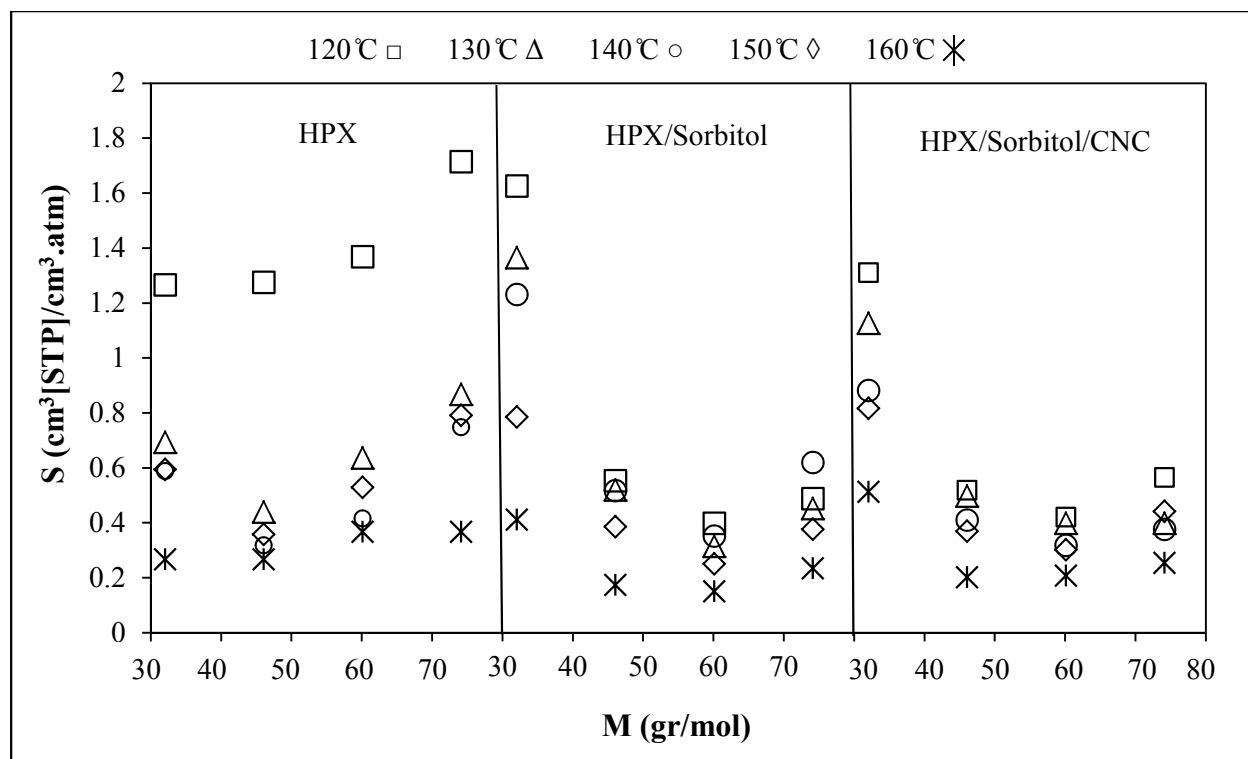


Figure 6.2. Dependence of infinite dilution solubility coefficient of alcohols in HPX films with and without additives on molecular weight of alcohols at 120 °C □, 130 °C Δ, 140 °C ○, 150 °C ◇ and 160 °C * .

It seems that adding sorbitol reduces the solubility of alcohols, especially at 120°C and replacing 5 wt % of sorbitol by CNC did not have a significant effect on the solubility behaviour of the alcohols. This is because adding sorbitol to HPX reduces the number of hydrogen bonds formed between HPX chains [156]. This will in return improve HPX chain mobility, resulting in a reduction in its glass transition temperature [74]. However, it will also decrease the number of hydrogen bonds formed between the alcohols and HPX, thereby reducing the solubility of the alcohols. Figure 6.3 shows that the HPX films exhibit similar behaviour when water was used. However, in the case of water, addition of CNC further decreases the solubility of water, especially at high temperatures. The current results are somewhat comparable to the results

obtained for the effect of sorbitol on water sorption in hydrophilic starch-based films at low water activity studied by Talja et al. [156] that is, films without sorbitol had higher water content than films with sorbitol. Several other studies also reported that higher water content for un-plasticized films of wheat starch [157], amylose and amylopectin [158] and waxy maize starch [159] than their plasticized films.

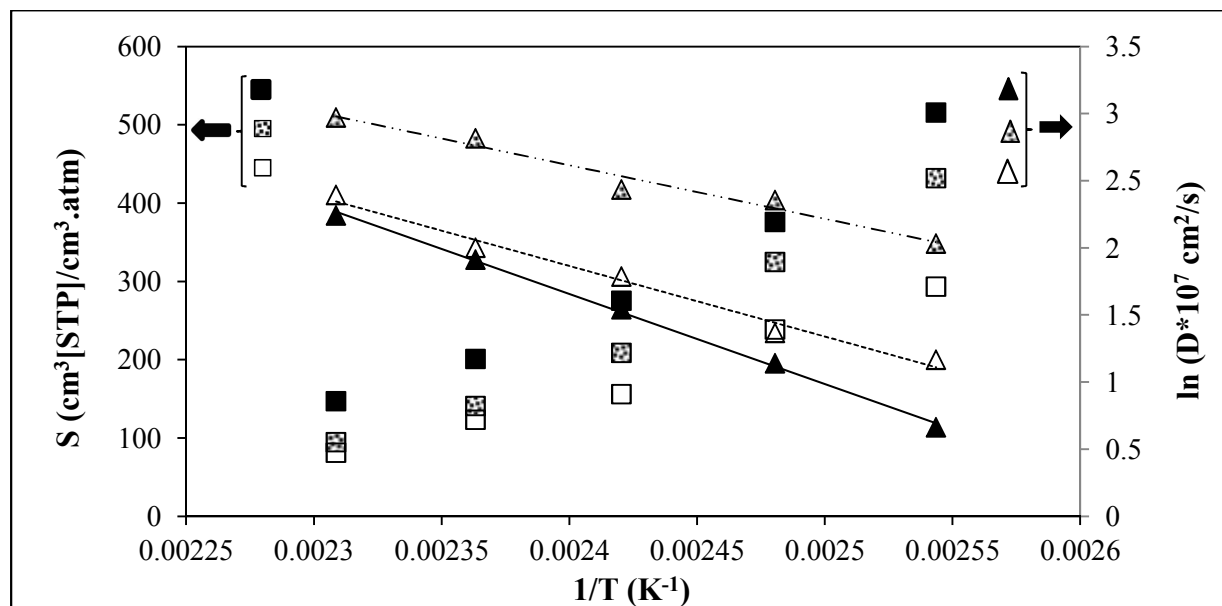


Figure 6.3. Temperature dependence of solubility and diffusion coefficients of water in HPX films. (symbols representing data for HPX: solid, HPX/Sorbitol: patterned and HPX/Sorbitol/CNC: open)

Figure 6.4 shows the effect of temperature on the measured solubility coefficients of the selected alcohols and water in HPX films with and without additives. Temperature can either increase or decrease solubility coefficient [151], [155], [160]. However, since our systems involved hydrogen bonds formed between HPX and the injected solutes, increasing temperature was expected to decrease solubility. And this was exactly what was observed. Another noteworthy point is that methanol exhibits the highest solubility and the greatest decrease in solubility over the temperature range of the experiments. This is because compared to other alcohols, it has the highest ability to form hydrogen bonds with HPX and the additives used.

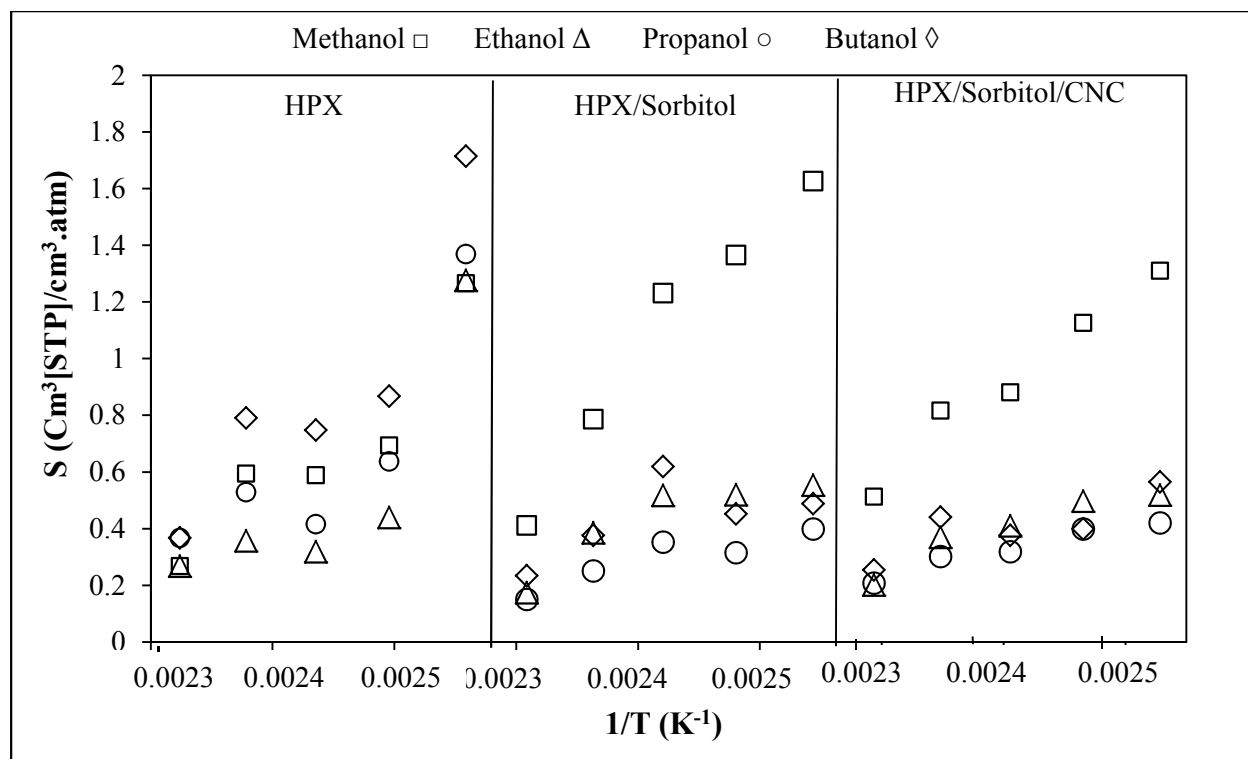


Figure 6.4. Temperature dependence of the solubility coefficient of selected alcohols (Methanol \square , Ethanol Δ , Propanol \circ , Butanol \diamond) in HPX films.

Table 6.2. Measured infinite dilution solubility coefficients (cm^3 [STP]/ cm^3 .atm), infinite dilution diffusion coefficients ($\times 10^{-11}$ cm^2/s) and calculated infinite dilution permeability coefficients ($\times 10^{-11}$ cm^3 [STP]/ cm .atm.s) of alcohols and water in HPX films with and without additives at 120-160 °C.

T (°C)	Methanol			Ethanol			Propanol			Butanol			Water			
	S	D	P	S	D	P	S	D	P	S	D	P	S	D (*10 ⁻⁷ cm ² /s)	P (*10 ⁻⁷ cm ³ [STP]/cm.atm.s)	
HPX	120	1.27±0.06	13.4±1.3	16.9	1.28±0.21	9.42±1.52	12.0	1.37±0.18	7.79±0.55	10.6	1.71±0.16	6.63±0.49	11.4	515±10.5	1.94±0.12	1001
	130	0.693±0.037	15.0±0.91	10.4	0.439±0.022	11.7±0.09	5.14	0.637±0.037	8.97±0.04	5.71	0.868±0.048	8.00±0.84	6.94	376±22.0	3.13±0.29	1177
	140	0.588±0.03	15.7±1.36	9.24	0.319±0.010	13.7±0.75	4.37	0.416±0.011	11.7±1.25	4.86	0.745±0.11	8.78±1.62	6.57	275±9.7	4.68±0.94	1289
	150	0.594±0.07	17.9±0.62	10.6	0.358±0.013	15.3±0.64	5.47	0.529±0.019	12.9±1.54	6.84	0.791±0.13	11.4±1.41	9.06	201±15.3	6.77±0.95	1361
	160	0.486±0.031	18.9±0.82	9.22	0.268±0.043	16.0±0.48	4.28	0.256±0.007	13.8±2.09	3.53	0.368±0.013	11.7±1.33	4.30	147±12.1	9.41±2.4	1385
HPX/Sorbitol	120	1.63±0.07	366±53.2	595	0.554±0.09	286±33.8	158	0.399±0.05	188±17.7	74.9	0.488±0.06	124±19.1	60.3	432±51.0	7.63±0.23	3297
	130	1.36±0.04	393±35.6	537	0.520±0.013	310±20.4	161	0.315±0.041	210±9.67	66.3	0.452±0.01	145±5.45	65.4	325±22.3	10.5±2.15	3429
	140	1.23±0.11	408±24.8	502	0.517±0.06	337±14.5	175	0.353±0.012	213±6.33	75.2	0.620±0.022	150±5.25	93.2	209±9.01	11.4±3.27	2387
	150	0.786±0.07	468±24.2	368	0.386±0.043	382±48.5	147	0.251±0.008	258±8.04	64.7	0.376±0.038	161±2.44	60.6	141±13.6	16.7±1.36	2356
	160	0.411±0.04	506±76.9	208	0.174±0.022	402±41.5	70.2	0.151±0.02	269±25.8	40.6	0.235±0.03	186±6.80	43.7	95±3.8	19.5±2.87	1856
HPX/Sorbitol/CNC	120	1.31±0.08	159±17.7	209	0.518±0.04	96.4±8.4	49.9	0.421±0.027	79.7±2.35	33.5	0.565±0.03	59.5±6.8	33.6	293±41.5	3.21±1.85	942
	130	1.12±0.02	172±8.17	193	0.498±0.069	124±10.7	61.9	0.399±0.046	99.5±2.4	39.7	0.399±0.026	65.9±9.7	26.3	239±29.0	3.92±0.33	935
	140	0.882±0.05	211±9.83	186	0.410±0.055	140±5.48	57.2	0.318±0.04	120±14.4	38.3	0.376±0.04	92.2±6.07	34.7	156±11.7	5.97±0.45	932
	150	0.817±0.04	239±6.92	195	0.369±0.048	158±20.4	58.4	0.302±0.03	143±4.88	43.3	0.441±0.05	127±14.5	56.0	123±6.0	7.39±0.78	912
	160	0.512±0.06	270±9.01	138	0.202±0.018	230±25.5	46.3	0.205±0.026	189±14.6	39.2	0.255±0.008	153±16.7	38.9	81.5±10.4	10.9±1.56	892

6.4.2. Infinite dilution diffusion coefficient

Molecular weight dependence of infinite dilution diffusion coefficients of the primary alcohols in HPX films at temperatures 120 to 160 °C is shown in Figure 6.5. The values for infinite dilution diffusion coefficient are also tabulated in Table 6.2. T_g of HPX, HPX/Sorbitol and HPX/Sorbitol/CNC were reported to be 137.4 °C, 103.7 °C and 116.0 °C, respectively [74]. The diffusivity of the alcohols decreases in the order of methanol>ethanol>propanol>butanol. Based on the size of the alcohols, this result was expected as the free volume theory would predict [22], [161]. This behaviour suggests that size rather than intermolecular interaction (hydrogen bonds in particular) dominates the diffusion process [151]. Here, it was expected that methanol would diffuse slower as it has the highest ability to form hydrogen bonds.

Comparing the infinite dilution diffusion coefficients of HPX, HPX/Sorbitol and HPX/sorbitol/CNC films for each alcohol, it was observed that addition of sorbitol to HPX increased diffusivity significantly while replacing 5 wt % of sorbitol by CNC only decreased their diffusivity slightly. The data also shows that the effect of sorbitol on the infinite dilution diffusion coefficients of the alcohols depends on the size of the molecules. In particular, the effect is larger for methanol and ethanol (30 times) than for propanol and butanol (18 times). This may be due to differences in the abilities to form hydrogen bonds with the polymer for alcohols with different sizes [133]. Adding CNC to the plasticized films decreased diffusion coefficient of the solvents almost 50%. It is believed that addition of CNC to hydrophilic biopolymers results in the formation of strong hydrogen bonds with the biopolymer. As a result, mobility of the polymer chains is suppressed, as the T_g data suggests, thereby lowering the free volume redistribution rate [9].

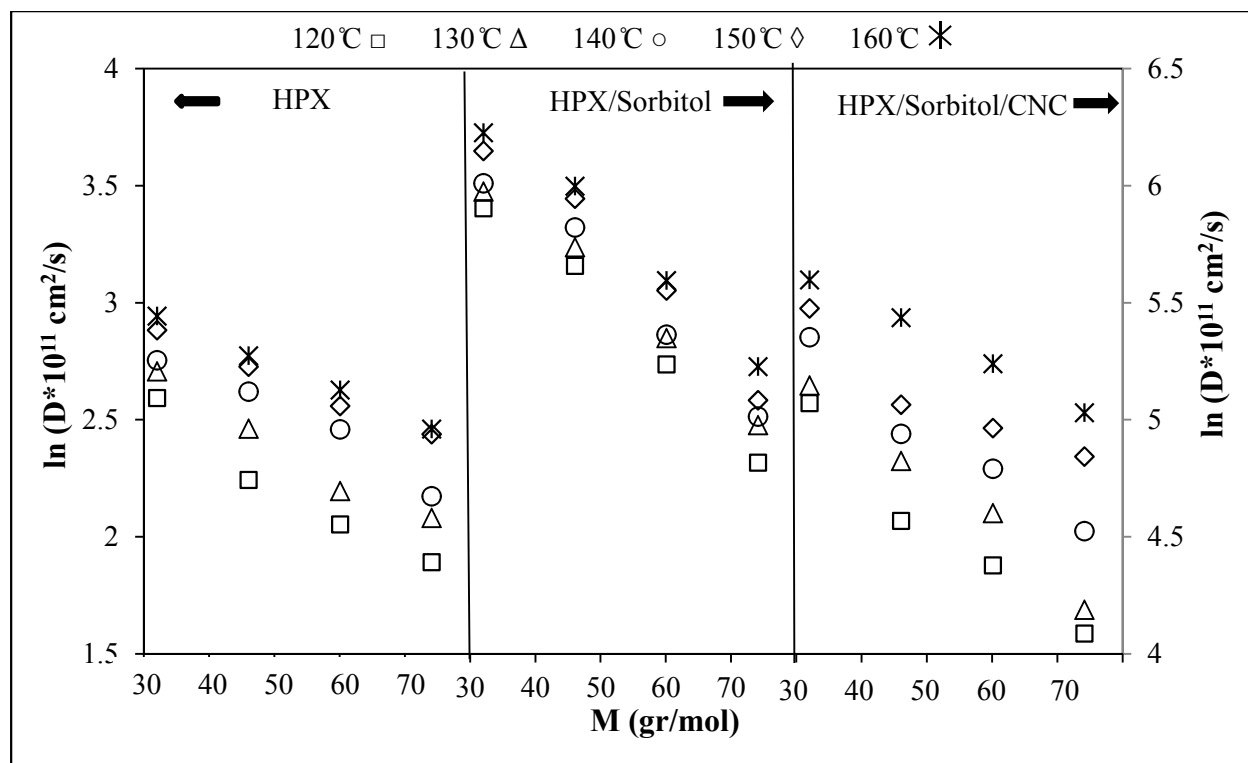


Figure 6.5. Dependence of infinite dilution diffusion coefficient of alcohols in HPX films with and without additives on molecular weight of alcohols at 120 °C □, 130 °C △, 140 °C ○, 150 °C ◇ and 160 °C *.

Temperature dependence of the diffusion coefficient of each alcohol is shown in Figure 6.6 indicating that diffusion coefficients for all the alcohols follow the Arrhenius law [162]:

$$D = D_0 e^{(-\Delta E_a/RT)}$$

where D_0 is the diffusion constant which is independent of temperature and ΔE_a is the activation energy required for the penetrant to escape from its current free volume hole and to move to the next free volume hole as well as the energy required for free volume hole formation against the attractive forces between the polymer chains. The linear dependence of $\ln D$ vs. $1/T$ suggests that ΔE_a is insensitive to temperature over the temperature range used. The calculated values of

ΔE_a are given in Table 6.3. Data shows that ΔE_a of the alcohols in the modified HPX films increases in the order of butanol>propanol>ethanol>methanol. This trend is consistent with the order of the corresponding diffusion coefficients.

It is known that diffusion of large molecules in polymer depends significantly on the chain segmental dynamics. Adding plasticizer enhances the chain segmental mobility, thereby increasing the probability of the formation of larger free volume holes that are crucial for the diffusion of larger molecules. Therefore, it is expected that the effect of sorbitol on the activation energy of larger alcohols is stronger than that on the smaller ones. Results shown in Table 6.3 are consistent with such expectation. Also shown in Table 6.3 is that adding CNC increased the activation energy significantly. This is simply because, as mentioned earlier, CNC likely reduces the chain mobility.

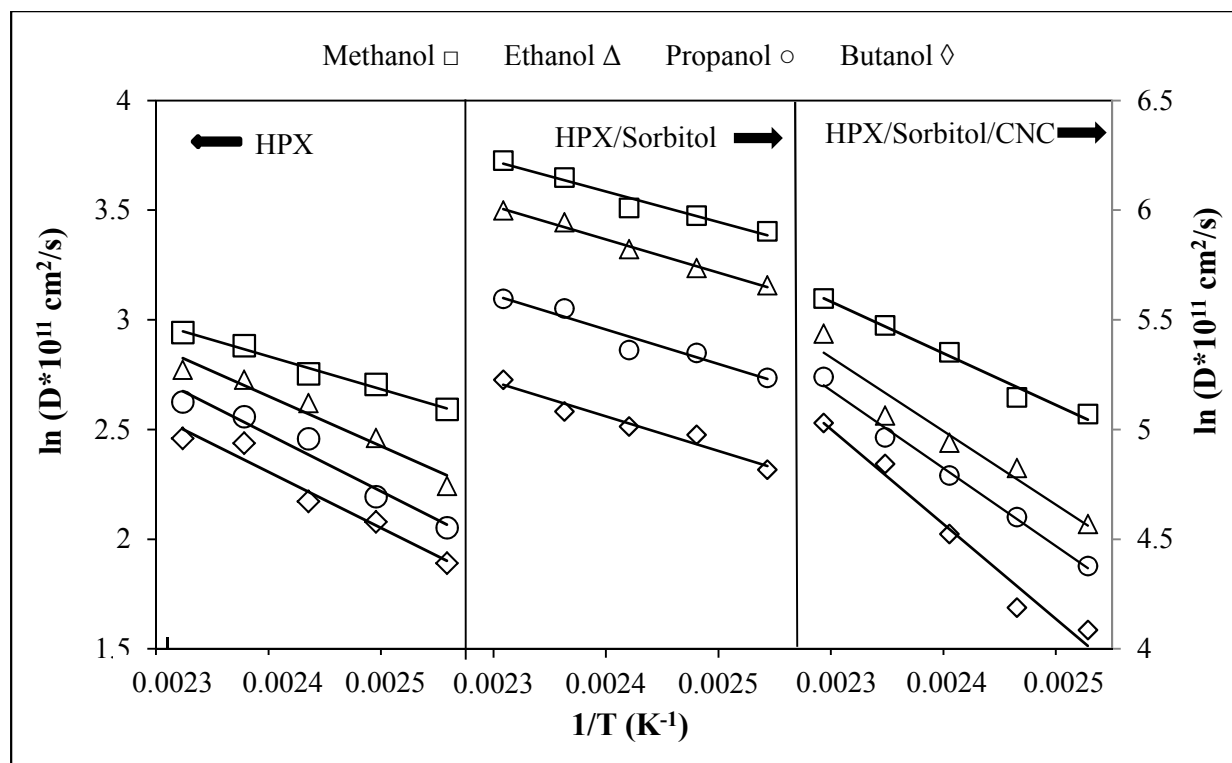


Figure 6.6. Temperature dependence of infinite dilution diffusion coefficient of alcohols (Methanol \square , Ethanol Δ , Propanol \circ , Butanol \diamond) in HPX films. (Data regarding HPX reads from left axis, HPX/Sorbitol and HPX/Sorbitol/CNC read from right axis)

Table 6.3. Activation energies of diffusion for solvents in HPX films

	E_a (kJ mol ⁻¹)			
	Methanol	Ethanol	Propanol	Butanol
HPX	12.4	18.9	21.5	21.2
HPX/sorbitol	11.6	12.6	13.0	13.1
HPX/sorbitol/CNC	19.5	27.9	29.5	35.9

6.4.3. Permeability coefficient

Permeability coefficients of the primary alcohols and water were calculated using Equation 6.1. It is worth noting that both solubility and diffusivity were measured at infinite dilution and that solubility depends mainly on solvent characteristics as well as the interactions between the components involved while diffusivity not only on the interactions but also on the size of the penetrants and the free volume characteristics of the polymer matrix [22].

Figure 6.7 indicates that permeability of neat HPX films show a minimum over the range of molecular weight of the alcohols used that is similar to that observed for the solubility coefficient data. On the other hand, permeability of the alcohol in the modified HPX films decreases with increasing size of alcohol. The trend is similar to that of the measured diffusion coefficients of the alcohols. Since solubility of the alcohols shows a minimum over their range of molecular weight, it suggests that diffusion dominates permeability at high molecular weights. However, this is not the case for water permeability (see Table 6.2) that high permeability coefficients of water are attributed to higher water solubility in the HPX films. The permeability coefficients were in the decreasing order of water >> methanol > ethanol > propanol > butanol. Comparing the permeability of the neat HPX film with the plasticized HPX (HPX/sorbitol) film shows a huge increase in permeability due to addition of sorbitol (up to 14 times for butanol, more than 50 times for methanol and up to 4 times for water). This is due to the fact that generally plasticizers increase diffusion coefficient [146] and consequently permeability increases.

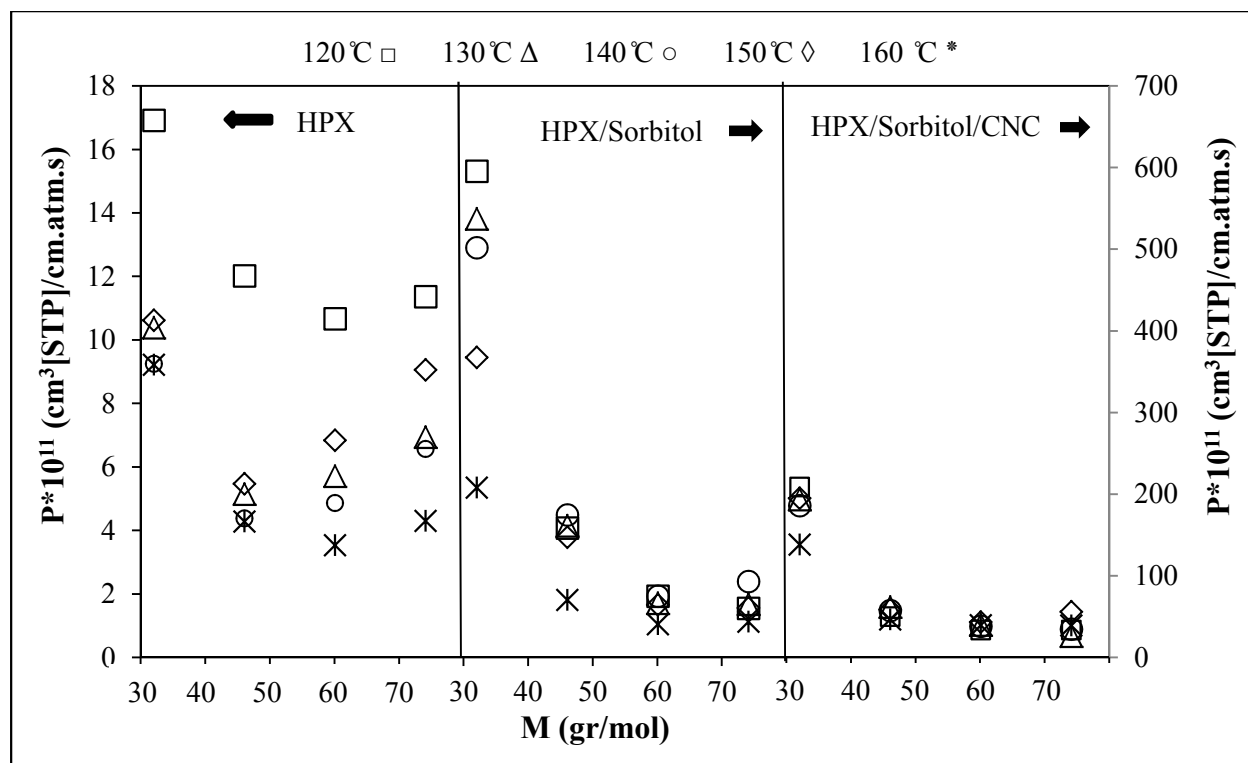


Figure 6.7. Dependence of infinite dilution permeability coefficient of alcohols in HPX films on molecular weight of alcohols at 120 °C □, 130 °C Δ, 140 °C ○, 150 °C ◇ and 160 °C * . (Data regarding HPX reads from left axis, HPX/Sorbitol and HPX/Sorbitol/CNC read from right axis)

Table 6.4 summarizes selected permeability coefficients of methanol, ethanol and water in polymers that are commonly used in food packaging as well as some natural polymers as reported by other researchers at different experimental conditions. Due to large solubility in water, HPX films are poor barriers to water compared to other polymers. However, permeability coefficients of methanol and ethanol in HPX and HPX/Sorbitol/CNC films are comparable with permeabilities in LDPE and polystyrene. Also, comparing permeability values of HPX films with poly (3-Hydroxybutyrate) (PHB), a biopolymer belonging to polyesters class suitable for food packaging [163], shows that permeability coefficients of alcohols in HPX films (above 120 °C) are 3 to 4 orders of magnitude lower than those in PHB (at 50-65 °C). HPX/sorbitol/CNC

polymer has the potential to be used in multi-layered packaging for reduction of permeability of alcohols along with a water barrier polymer. For better understanding of the transport mechanism at temperatures of intended application, collection of permeability data at low temperatures and higher concentrations of the solvents is needed. However, at low temperatures, especially below the T_g of HPX, a significant amount of surface adsorption will take place. This will prevent us from using Equations 6.6 and 6.10 to obtain the solubility and diffusivity, respectively. Further theoretical work is required to extend the technique to low temperatures for better comparison with commercial polymers.

Table 6.4. Permeability coefficients of methanol, ethanol and water in the studied polymers at 120 °C compared to polymers that are commonly used in food packaging.

		Methanol	Ethanol	Water
Permeability Coefficient	HPX			
	at 120 °C	16.9	12.0	1001*10 ⁴
	HPX/Sorbitol			
$\times 10^{-11} \text{ cm}^3 [\text{STP}] \text{ cm}^{-1} \text{ atm}^{-1} \text{ s}$	at 120 °C	595	158	3297*10 ⁴
	HPX/Sorbitol/CNC			
	at 120 °C	209	49.9	942*10 ⁴
Permeation rate	Polyethylene, LDPE	2.4-3.2	0.79-1.6	0.39-0.59
	at 24 °C	(222-296)	(160-323)	(154-232)
	Polystyrene	0.39-2.4	0.39	0.79-3.9
[164]	at 24 °C	(40-222)	(80)	(311-1538)
	EVOH			0.55-2.4
	at 40 °C	-	-	(90-380)
$\text{g.mm.m}^{-2}.\text{day}^{-1} *$	Cellulosic plastic	-	-	0.39

	at 40 °C			(150)
Permeability Coefficient [163]	PHB	1130-2090	890-1230	750-1900
Barrer**	at 50-65 °C	(85.8-159)	(67.6-93.5)	(57-144)
		*10 ⁴	*10 ⁴	*10 ⁴
	Hydroxypropylmethyl cellulose	-	-	19.68
Water vapor permeability [70]	At 80 °C			(19910)
×10⁻¹¹ g.m⁻¹.s⁻¹.Pa⁻¹	Arabinoxylan			12.7
	+15%glycerol	-	-	(12923)
	At 80 °C			

^aValues shown in parentheses are permeability coefficients in the units of $\times 10^{-11} \text{ cm}^3 [\text{STP}] \text{ cm}^{-1} \text{ atm}^{-1} \text{ s}^{-1}$ for comparison purpose. ^bThe permeability coefficients (in parentheses) have been calculated from permeation rates (VTR) as: permeability coefficient= $VTR/(\Delta p \cdot \rho)$, where ρ is the permeate density and Δp is $P_v - P_0$ (permeates vapor pressure and external pressure of the permeate which in the case of organic vapors, is assumed to be zero) [164].

^c1 Barrer = $76 \times 10^{-10} \text{ cm}^3 [\text{STP}] \text{ cm}^{-1} \text{ atm}^{-1} \text{ s}^{-1}$ [163], [165].

Depending on the combined effect of solubility and diffusivity, permeability can have a positive or negative temperature dependence [166]. Figure 6.8 and Figure 6.9 show the temperature

dependence of permeability of the alcohols and water in the three HPX films. Permeability of alcohols is insensitive to temperature in neat HPX and HPX/sorbitol/CNC film. This is because solubility and diffusivity have opposite temperature dependence, thereby offsetting the effect of each other. However, permeability of methanol and water in HPX/sorbitol film decreases significantly with increasing temperature. Even though diffusivity of water and methanol increases with increasing temperature, reduction in solubility coefficient reduces permeability as temperature increases showing that breaking of the polar bonds of water and methanol with HPX by temperature is the dominant factor in reduction of permeability rather than increase of free volume due to temperature.

Although adding sorbitol to HPX lowers the T_g of HPX, thereby facilitating the film formation process, it significantly decreases barrier properties of the film. Adding CNC helps improve barrier properties but the films still exhibit high permeability to water but promising barrier to alcohols. Using CNC with different physical properties (e.g., higher number of hydrogen bond forming moieties, higher aspect ratio, etc.) may help reduce diffusivity further, thereby permeability.

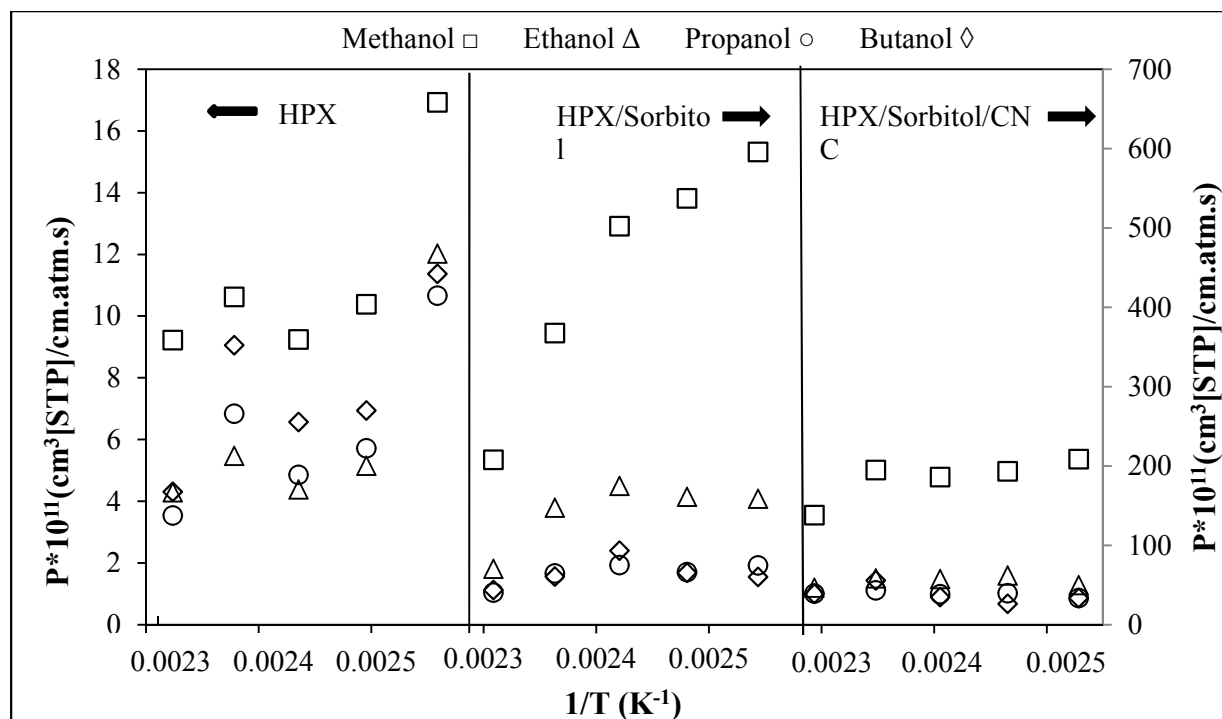


Figure 6.8. Effect of temperature on permeability coefficients of alcohols (Methanol \square , Ethanol Δ , Propanol \circ , Butanol \diamond) in HPX films.

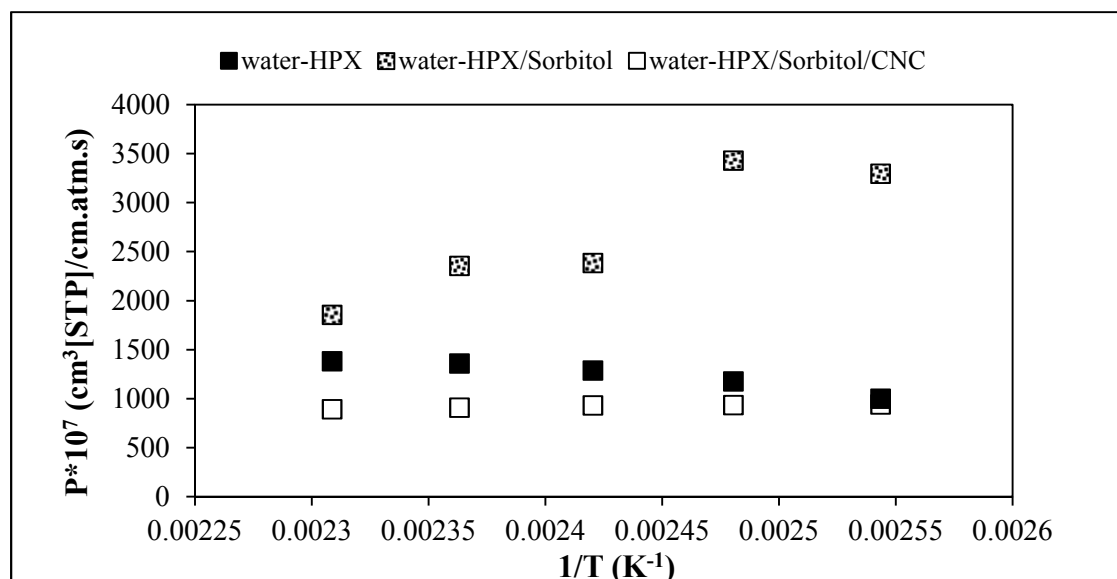


Figure 6.9. Effect of temperature on the permeability coefficient of water in HPX, HPX/Sorbitol and HPX/Sorbitol/CNC films.

6.5. Conclusion

The permeability of a series of primary alcohols including methanol, ethanol, propanol and butanol in hydroxylpropyl xylan (HPX) films with and without additives was investigated at temperatures (120 – 160 °C) higher than HPX's glass transition temperature. In particular, solubility and diffusion coefficients at infinite dilution were measured using the technique of inverse gas chromatography. Permeability was then calculated by multiplying the solubility and diffusion coefficients. It was observed that solubility of alcohols exhibited a minimum over the molecular weight range of the primary alcohols used while diffusivity decreased with increasing molecular weight. Similar behaviour was observed for HPX films containing additives. While sorbitol decreases solubility and increases diffusivity, CNC does not alter solubility much but significantly decreases diffusivity. Permeability in the neat HPX film showed a minimum over the range of molecular weight of the alcohols, indicating solubility controlled the permeation process especially at high alcohol's molecular weights. Addition of sorbitol increased permeability significantly for methanol and ethanol but less on propanol and butanol. Also, the temperature dependence of permeability is stronger for the low molecular weight alcohols than for the high molecular weight ones. Although adding sorbitol increased permeability coefficients, significantly, adding CNC would more or less keep barrier characteristics of HPX for larger molecules.

Chapter 7

7. Effect of Humidity on the Permeability of Alcohols in Hydroxypropyl Xylan Films

7.1. Introduction

Recently, we have demonstrated that hydroxypropyl xylan (HPX), a hydrophilic amorphous biopolymer, has the potential to be used as a food packaging material [62]. We also studied the possibility of lowering the water diffusivity of the material by adding nano-sized filler cellulose nanocrystalline (CNC) and found that CNC does not increase the material's water barrier property [74]. It is worth noting that the HPX films studied, also contained a food grade plasticizer namely sorbitol to lower its glass transition temperature for the targeted applications. Nonetheless, given the hydrophilic nature of HPX, it is expected that it a good barrier material for food aroma that is mostly made up of low molecular weight organic compounds such as alcohols and aldehydes. Therefore, more recently, we studied the permeation behavior of four low molecular weight alcohols (methanol, ethanol, propanol and butanol) in neat HPX film and films modified by sorbitol and/or CNC [75]. Films used in that study included neat HPX film, sorbitol modified HPX film (HPX/Sorbitol: 60/40 wt%) and sorbitol/CNC modified film (HPX/Sorbitol/CNC: 60/35/5 wt%). It was shown that the HPX/Sorbitol/CNC film is a good alcohols barrier material. However, a HPX/Sorbitol/CNC film cannot be used alone and should be used along with a water barrier film. The question here is: how would humidity affect the alcohols barrier properties of the HPX films?

A modified version of this chapter has been published as: "Effect of Humidity on the Permeability of Alcohols in Hydroxypropyl Xylan Films" Fatemeh Bayati, Yaman Boluk, and Phillip Choi, ACS Sustainable Chem. Eng., 4 (5), 2016, 2578-2583

In the context of food packaging, temperature and relative humidity are the two external factors that influence the barrier property of the packaging material and consequently the quality of the packaged food. The humidity effect is noticeable for commonly used hydrophobic food packaging materials such as polyolefins [19]. Therefore, it is expected that humidity would have more pronounced effect on hydrophilic polymers such as HPX. Much research has been done on studying the effect of humidity on sorption, diffusion and permeability of small molecules such as aroma molecules in polymer packaging films. Studies show different behaviors for the permeation of aroma molecules in different polymer films [13]. In particular, Delassus et al. [12] and Johansson and Leufvén [13] showed that in the presence of humidity, the permeability of aldehydes in ethylene vinyl alcohol (EVOH) is increased while a maximum was observed for permeability of alcohols in EVOH at a relative humidity (RH) of 50%. Furthermore, Johansson and Leufvén [13] reported a maximum in the permeability of aldehydes in high-density polyethylene (HDPE) and linear low-density polyethylene (LLDPE), also at 50% RH. However, decrease in the permeability of alcohols in HDPE and LLDPE was observed when humidity is increased (no maximum was observed). They explained the observed difference in the behaviors of aldehydes and alcohols in terms of their differences in polarities and abilities to form hydrogen bonds with the water absorbed in the films. They also showed that differences in sorption, diffusion and permeation under humid conditions are a combination of the plasticizing effect of water, aroma-water interaction and their competition for interaction with the polymer matrix. By increasing the RH, Lopez-Carballo et al. [167] observed a minimum in the permeability of α -pinene and ethyl butanoate in EVOH-32 over a RH range of 0 – 100% while Zhang et al. [168] reported increase in the permeability of limonene in EVOH and nylon 6,6 with increasing RH. Moreover, Aucejo et al. [14] showed that sorption of alcohols in EVOH was

increased at high levels of RH due to the water plasticizing effect and increased polarity of the medium as a result of increasing amount of water in the system. Generally, transport of aroma in hygroscopic materials such as nylon, poly(vinyl alcohol), poly(vinyl acetate), EVOH, polyamides and uncoated cellophane are mostly affected by humidity because they all contain a high number of hydroxyl moieties (OH) while hydrophobic polymers such as poly(ethylene terephthalate) (PET), low-density polyethylene (LDPE) and acrylonitrile copolymer are less- or un-affected by humidity [169], [170].

The above works suggest that effect of presence of water on transport of aroma compounds can be categorized by the hydrophobic or hydrophilic characteristics of the films [171]. For hydrophobic polymers, low or no effect of water on the aroma transfer in them is observed while for hydrophilic polymers, two phenomena may be responsible: 1) Plasticization of the polymer due to the sorption of water which results in an increase in diffusivity and permeability while the solubility could be increased, decreased or not altered; 2) Competitive sorption of water and the aroma compounds while no plasticization occurs. In a losing competition of non-polar compounds to highly polar water molecules for absorption sites of a polar polymer, solubility and permeability of the aroma compounds would decrease with increasing RH while diffusivity stays constant or even decreases. On the other hand, when studying the sorption of polar aroma compounds in hydrophilic polymer in the presence of water, two opposite effects are present: sorption in favor of water at low RH and of aroma at high RH due to increased polarity of the polymer matrix at high RH (for polymers such as EVOH) or decrease in sorption of aroma by increasing RH in polymers such as cellophane and methylcellulose due to filled free volume of the polymer by water.

Given the above discussion, it is clear that both diffusivity and solubility will affect permeability of a packaging polymer. Using the following equation, permeability coefficient (P) is obtained as the product of solubility coefficient (S) times diffusion coefficient (D):

$$P = S \times D \quad (7.1)$$

To this end, inverse gas chromatography (IGC) is the most ideal technique to study the permeation of aroma at infinite dilution in the presence of humidity as information about diffusivity and solubility can be obtained simultaneously. In the present work, IGC was used to study effect of humidity on the transport of alcohols in the HPX films (neat HPX, HPX/Sorbitol: 60/40 wt%, and HPX/Sorbitol/CNC: 60/35/5 wt%) that were previously studied in dry condition by Bayati et al. [75].

7.2. Materials and Method

7.2.1. Materials and Alcohols

Sorbitol (a food grade plasticizer), glass beads (with a diameter range of 150 – 212 μm which were used as the inert support onto which HPX films were coated), methanol, ethanol, and butanol were purchased from Sigma Aldrich (Oakville, ON, Canada). Propanol was purchased from Baxter Burdick and Jackson (B&J Brand). The alcohols were HPLC-grade with purity > 99.8% and were injected as vapor in the amount of less than 0.1 μl using a 0.5 μl Hamilton syringe. Cellulose nanocrystals (CNC) was provided by Alberta Innovates Technology Future (AITF) and was used as a natural filler.

HPX was prepared based upon the method used by Jain et al.[62]. Xylan was dissolved in sodium hydroxide solution (pH 10) under nitrogen at room temperature with constant stirring for

2 h. The solution was cooled using an ice bath following dropwise addition of propylene oxide under nitrogen. The reaction was continued by stirring for 12 h at ambient temperature. Using acetone and with brisk stirring, HPX was precipitated from the solution and further collected by filtration. The final product was dried in vacuum for 24 h [74]. The degree of substitution of the HPX obtained from the solution with pH 10 would be 0.1-0.2.[62] Using ¹H-NMR, our previous work [131] showed the presence of HP groups along the xylan backbone in the structure of HPX.

7.2.2. Column Preparation

Three separate IGC columns containing neat HPX, HPX/Sorbitol (60/40 wt%) and HPX/Sorbitol/CNC (60/35/5 wt%) were prepared by dissolving a total amount of 1 g of the dry compounds in distilled water ca. 30 – 35 ml. After stirring for one hour at 60 °C, the solution was filtered to remove undesirable insoluble materials. Ten milliliters of the solution were then mixed with 20 g of glass beads using an evaporating flask attached to a rotary evaporator. The flask connected to vacuum was partially immersed in a water bath that was set at 60 °C. Drying was carried out for about 10 hours leaving the glass beads coated with a thin layer of HPX or HPX with additives. The coated beads were sieved to obtain coated particles less than 200 µm. A measured amount of the sieved, coated glass beads was used to determine the percentage of loading of the polymer using thermal gravimetric analysis (TGA). One end of a 100 cm of stainless steel column with ¼ inch outer diameter was blocked with glass wool. The column was filled with a known amount of the coated glass beads by providing constant tapping. Tapping the column was to minimize voids in the column. The mass of stationary phase in the column was determined based upon the loading of the coated glass beads and their mass in the column. Before the column was installed in the GC chamber, the other end of the column was also blocked with glass wool.

7.2.3. Inverse Gas Chromatography (IGC)

An Agilent 7890A series GC equipped with a flame ionization detector (FID) was used for the experiments. Each column was installed in the oven and was conditioned at 140 °C overnight. The injector and detector temperatures were set at 250 and 300 °C, respectively, to prevent condensation of the injected vapors. Methane was used as the non-interacting probe to determine the dead volume of the column and the carrier gas was helium. The retention volume was determined based on the difference in the volumes of carrier gas swept through the column between methane and each alcohol used. In order to provide the desired humidity in the carrier gas, helium was humidified first before it was introduced into the column installed in the GC chamber. Figure 7.1 shows a schematic diagram of the humidifying setup attached to the GC. Dry gas enters the water tank at room temperature. Humid gas leaving the humidifier mixes with adjustable flow rate of dry gas to provide the desired humidity condition. Entering a digital hygrometer, humidity of the gas is monitored before entering the column. Three RH levels were used for this work and they were 30, 50 and 70% at room temperature (25 °C) each with $\pm 3\%$ errors.

For diffusivity and solubility measurements, column temperature was set at 120 °C while various flow rates of carrier gas (15 – 70 ml/min) was adjusted to determine the Van Deemter curves (see description below). In order to meet infinite dilution concentration of the injected solvents (alcohols), injections of the vapors was less than 0.1 μl . However, it was found that even at higher amounts of up to 0.2 μl , infinite dilution condition was achieved as the retention times were found not to be affected by the amount of the solvent injected. At least 5 injections were done to measure retention time and peak width. The collected data were reproducible with less than 5% variation. The solubility coefficients were obtained from the average of solubility

coefficients at each flow rate. The solubility coefficients obtained are reported with the standard deviation from the average of values from different flow rates. Diffusion data are presented with the standard deviation regarding the uncertainties from the slope of Van Deemter curves.

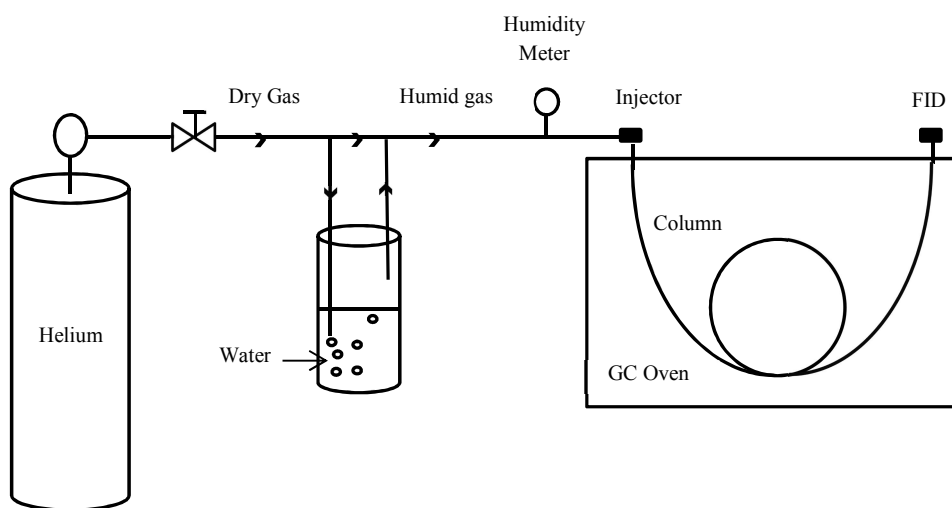


Figure 7.1. A Schematic diagram of the humidifier setup used for humidifying the carrier gas

7.2.3.1. Determination of Diffusion Coefficient

Van Demeter equation was used to obtain diffusion coefficients. The equation has been described in chapter 5, [74] as well as some other studies by Etxabarren et al.[132] and Kalaouzis and Demertzis [172]. Van Deemter curves were obtained by plotting height equivalent to theoretical plate, H , (from peak widths and retention times) versus linear velocity of carrier gas, V . From the slope, C , of linear part of the curves at higher flow rates, diffusion coefficient, D , can be obtained from:

$$D = \frac{8}{\pi^2} \frac{k}{(1+k)^2} \frac{d_f^2}{C} \quad (7.2)$$

where d_f is the thickness of polymer coating on the inert support (previously discussed by Bayati et al. [75]) and k is the partition ratio defined as:

$$k = \frac{t_r - t_m}{t_m} \quad (7.3)$$

where t_r is retention time of the injected solvent and t_m is retention time of the marker (methane).

7.2.3.2. Determination of Solubility Coefficient

At infinite dilution, solubility coefficients, S , can be calculated from the specific retention volume of each solvent under the given experimental conditions using the following equation:

[151]

$$S = V_g^0 \frac{\rho}{p_0} \exp \left[(2B_2 - V_1) j \frac{p_0}{RT} \right] \quad (7.4)$$

Where ρ is polymer density, B_2 is the second virial coefficient of the solvent characterizing the interaction between the solvent molecules, V_1 is the solvents molar volume, R is the gas constant and V_g^0 is the specific retention volume of the solvent defined as: [133], [173]

$$V_g^0 = \frac{V_N}{w_s} * \frac{27.315}{T} \quad (7.5)$$

where w_s is the weight of the polymeric stationary phase, T is the absolute temperature of the column and V_N is the net retention volume of the solvent defined as:

$$V_N = F_c(t_r - t_m) \quad (7.6)$$

$$F_c = F * j * \frac{T_c}{T_{fl}} * \frac{P_0 - P_w}{P_0} \quad (7.7)$$

$$j = \frac{\left(\frac{P_i}{P_0}\right)^2 - 1}{\left(\frac{P_i}{P_0}\right)^3 - 1} * \frac{3}{2} \quad (7.8)$$

where F_c is the corrected flow rate, T_{fl} is the flow meter temperature, P_w is water vapor pressure at flowmeter temperature, P_0 is the pressure at the outlet of the column, P_i is the inlet pressure of the column and j is the compressibility factor. As mentioned before permeability is calculated using Equation 7.1.

7.3. Results and Discussion

7.3.1. Diffusion Coefficient

Diffusion coefficients of the alcohols in HPX films at various levels of RH are shown in Figure 7.2 (values tabulated in Table 7.1). As can be seen in the figure, diffusion coefficient exhibits a maximum at around 50% RH over the RH range used in this study for all alcohols. Increase in the diffusivity of alcohols over the range of 0 – 50% of RH is likely due to the plasticizing and swelling effects. According to Aucejo et al.[14], absorbed water molecules are able to form hydrogen bonds with the polymer chains, such as HPX, that contain hydrogen bond forming moieties and break the inter-chain hydrogen bonds. This will in turn increase the chain flexibility and the corresponding free volume redistribution rate, thereby favouring the diffusion of the alcohol molecules [167]. In addition, the absorbed water swells the polymer and increases the amount of free volume, facilitating the diffusion [174].

Table 7-1. Measured infinite dilution solubility coefficients (cm^3 [STP]/ cm^3 .atm), infinite dilution diffusion coefficients ($\times 10^{-11}$ cm^2/s) and calculated infinite dilution permeability coefficients ($\times 10^{-11}$ cm^3 [STP]/ cm .atm.s) of alcohols in HPX films with and without additives at 120°C and under different levels of relative humidity.

	RH	Methanol			Ethanol			Propanol			Butanol		
	%	S	D	P	S	D	P	S	D	P	S	D	P
HPX	0	1.46±0.05	13.3±1.9	19.5	1.26±0.20	9.0±1.6	11.3	1.35±0.22	6.7±0.7	9.0	1.91±0.08	5.9±1.1	11.4
	30	1.08±0.23	18.6±1.1	20.0	0.78±0.09	19.0±3.3	14.5	0.94±0.15	12.6±1.4	11.8	2.41±0.15	16.5±1.0	39.9
	50	1.15±0.13	28.3±7.5	32.5	0.94±0.22	21.9±1.9	20.5	2.57±0.26	17.4±2.5	45.0	2.79±0.17	15.6±2.0	43.6
	70	0.99±0.13	22.9±1.4	22.7	0.62±0.11	20.0±3.3	12.5	1.23±0.21	16.2±2.8	19.8	2.89±0.29	12.6±2.2	36.5
HPX/Sorbitol	0	1.64±0.09	442±66	724	0.57±0.09	276±41	157	0.39±0.01	183±11.9	70.8	0.46±0.08	178±39	81.7
	30	1.25±0.22	1386±229	1732	0.41±0.01	810±77	330	0.33±0.06	772±213	256	0.40±0.03	589±38	233
	50	1.23±0.21	1649±95	2037	0.53±0.10	870±109	464	0.41±0.07	313±59	128	0.50±0.08	593±88	295
	70	0.48±0.10	511±123	244	0.21±0.04	338±23	72.1	0.24±0.01	246±23	60.1	0.38±0.07	357±34	136
HPX/Sorbitol/CNC	0	2.05±0.23	170±12	249	0.76±0.10	76.8±6.1	58.3	0.76±0.22	63.9±2.5	48.4	0.87±0.05	56.2±8.9	48.9
	30	2.69±0.27	116±11	311	1.25±0.11	65.1±13.7	81.6	1.07±0.16	91.6±9.7	98.0	1.29±0.16	57.1±0.9	73.8
	50	2.57±0.52	266±16	685	1.01±0.21	153±9	155	0.78±0.03	128±5	99.3	0.96±0.03	98.8±19.1	94.6
	70	2.50±0.33	111±7	277	0.96±0.16	86.9±16.3	83.2	0.74±0.17	73.4±10.9	54.6	1.04±0.14	50.4±7.7	52.2

At high water concentrations (i.e., 50 – 70% RH), researchers showed that water clustering is able to slow down the diffusion of the alcohols.[175], [176] Here, water clusters would fill up free volume holes offsetting the plasticizing effect.[141] To predict possibility of water clustering, Henry’s law was used to estimate the amount of water absorbed in the polymer films at different levels of RH. Using the specific retention volumes, V_g^0 , as defined in Equation (5), of water at infinite dilution in HPX films, the weight-fraction-based Henry’s constants were calculated as follows:[177]

$$H_{12}^0 = \left(\frac{27.315R}{V_g^0 M_1} \right) \quad (7.9)$$

where M_1 is the molecular weight of water and R is the universal gas constant. Using the above equation, water contents at different levels of RH for the three films were calculated and are summarized in Table 7.2.

Table 7-2. Estimated water contents in HPX films at 120 °C based on Henry’s law.

% RH	Weight fraction of water		
	HPX	HPX/Sorbitol	HPX/Sorbitol/CNC
30	0.007	0.004	0.003
50	0.012	0.006	0.004
70	0.017	0.009	0.006

Formation of water clusters in a variety of polymers has been studied extensively. Clustering data for water in cellulose derivatives such as cellulose triacetate (CTA), cellulose acetate (CA),

cellulose monoacetate (CMA), and ethyl cellulose (EC) obtained from their sorption isotherms at room temperature [178] show that contrary to hydrophobic polymers such as hydroxypropyl cellulose (HPC) in which water tends to have a high tendency to form clusters at very low levels of RH, polar polymers exhibit a strong antipathy to clustering and it only takes place at high levels of RH. Critical RH above which water clusters of absorbed water start to form in some cellulose derivatives estimated at 25 °C are reported as: EC and CMA at 30% RH with water contents at 0.017 and 0.046, respectively; CA at 40% RH with water content at 0.027; CTA at 50% RH with water content at 0.021; and cellulose at 70% RH with water content at more than 0.030 [178], [179]. In general, sorption capacity increases at low temperatures [180]; it is expected that water contents of our systems would be comparable or even higher than those of the aforementioned polymers. Nonetheless, given the water content of the neat HPX film at 70% RH, water clusters might form in the film, thereby lowering the corresponding alcohols' diffusion coefficients.

For the films containing sorbitol and/or CNC, the estimated water contents are lower than those of the neat HPX film and seem not to be sufficient for the formation of water cluster. Nevertheless, the substantial decreases in the diffusivity of the alcohols in both the HPX/Sorbitol and HPX/Sorbitol/CNC films from 50% to 70% RH suggests that the alcohols, methanol in particular, do not diffuse as a separate entity at high humidity. Rather, a few water molecules may surround each alcohol molecule (methanol and water are a highly miscible pair) and increase its apparent size, thereby lowering the diffusivity. Molecular dynamics simulation may provide us with some insights into this speculation. Such an effect is expected to diminish as the size of alcohol decreases. And our data seem to corroborate with this expectation.

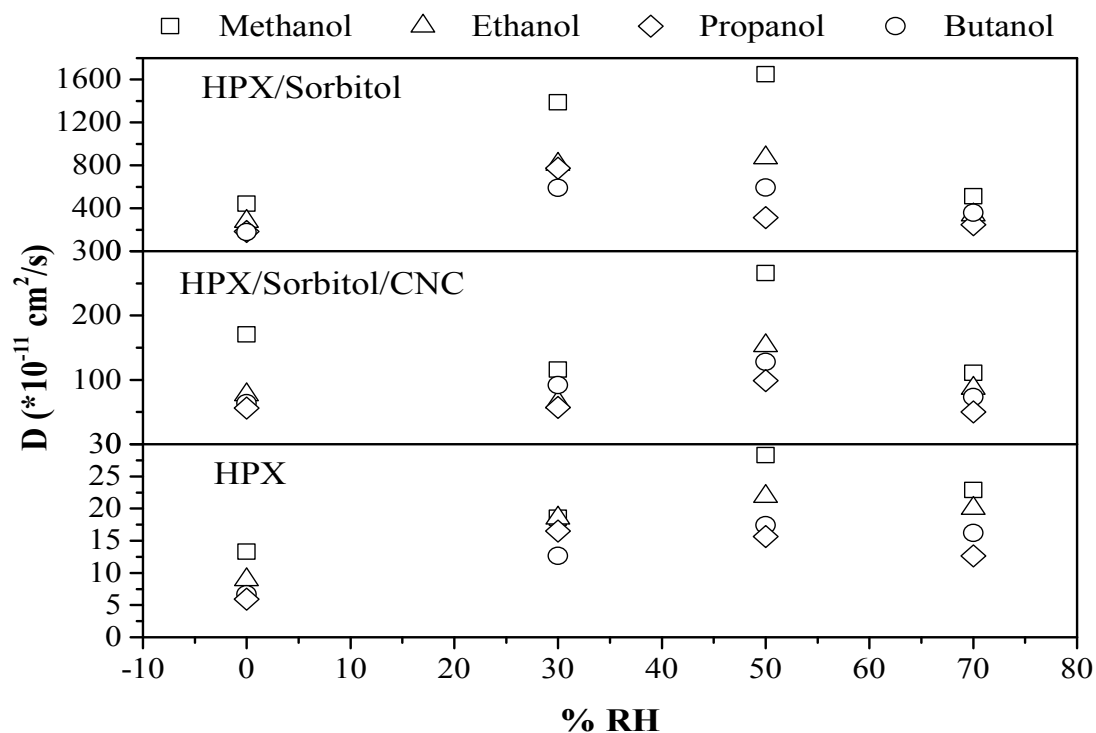


Figure 7.2. Infinite dilution diffusion coefficients of alcohols in HPX, HPX/Sorbitol and HPX/Sorbitol/CNC at 120 °C and under different levels of relative humidity.

7.3.2. Solubility Coefficient

Figure 7.3 shows the effect of RH (0 – 70%) on the solubility of the alcohols in the HPX films (values shown in Table 7.1). As can be seen in Figure 7.3, taking out the two outliers (methanol in the HPX/Sorbitol film at 70% RH and butanol in the HPX film at 50% RH), solubility of the alcohols in all HPX films is more or less insensitive to the RH. This simply suggests that solubility of the alcohols at infinite dilution in the films is not affected by the amount of absorbed water in the polymer. In fact, this is somewhat expected given the water content results shown in Table 7.2, as water content does not change significantly over the RH range used (0-70%).

Nevertheless, there is one noteworthy observation. For the neat HPX film, butanol exhibited higher solubility than the rest of the alcohols (except at 50% RH where solubility of butanol and propanol were relatively similar) while those alcohols showed comparable solubility. This is due to its higher condensability and higher hydrophobicity of HPX. However, addition of sorbitol and CNC increased the polarity of the films (both sorbitol and CNC contained a high number of hydroxyl moieties). Therefore, methanol, which is the most polar alcohol used in this study, exhibited the highest affinity for the films.

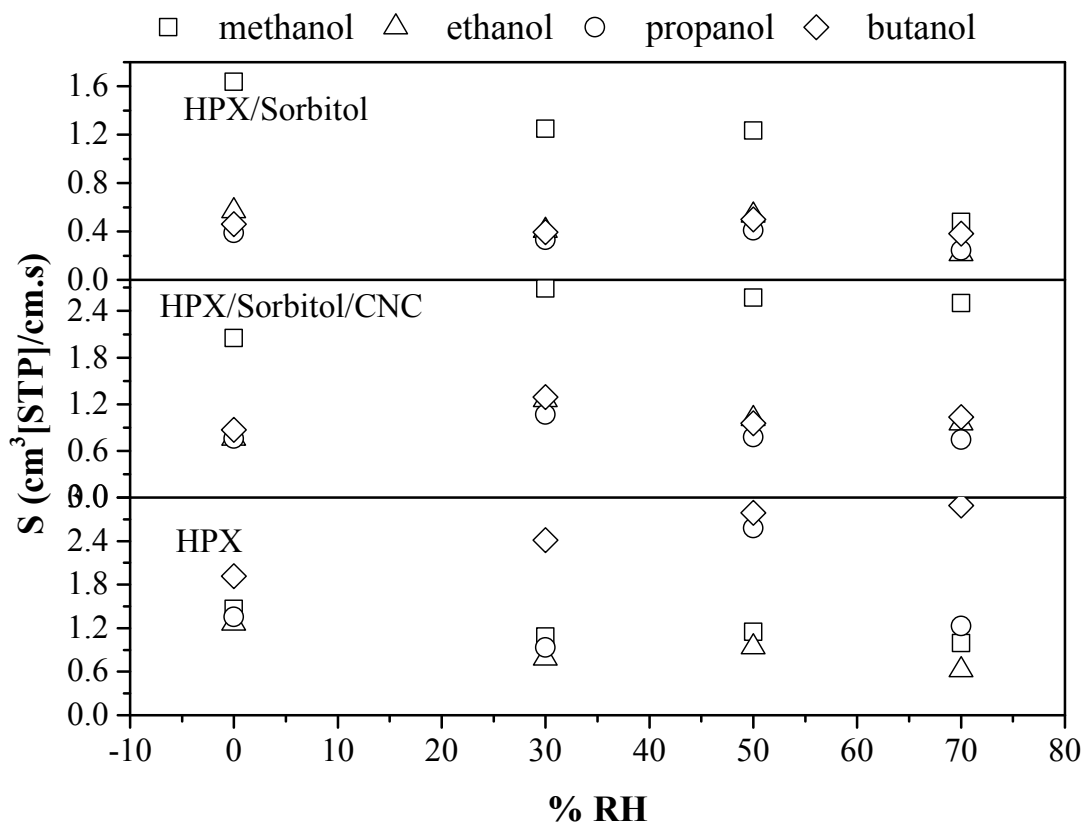


Figure 7.3. Infinite dilution solubility coefficients of alcohols in HPX, HPX/Sorbitol and HPX/Sorbitol/CNC at 120°C and under different levels of relative humidity.

7.3.3. Permeability Coefficient

Permeability coefficients of the alcohols through the HPX films over the RH range of 0 – 70% were calculated using Equation 7.1 along with their measured diffusion coefficients and solubility coefficients and the results are shown in Figure 7.4 (values tabulated in Table 7.1). The trend of the permeability data is similar to that of the diffusion coefficient; that is, it shows a maximum at around 50% RH for all alcohols in all films. This obviously attributed to the fact that solubility is relatively insensitive to the RH. In other words, diffusivity dominates the permeation process in these films (except for butanol in neat HPX). While humidity results in higher permeability of butanol in HPX compared to the other alcohols, the modified films remain the most permeable to methanol. Obviously, the films are not suitable for being used a barrier material to alcohols when there is moisture present in the environment. And such films should be used in a multi-film setup along with polymer films exhibiting high water barrier properties. Meeting this condition, HPX/Sorbitol/CNC films remain the best option for being used as barrier to the large molecule alcohols (ethanol, propanol and butanol) considering their flexibility [74] and comparable permeability coefficients with neat HPX.

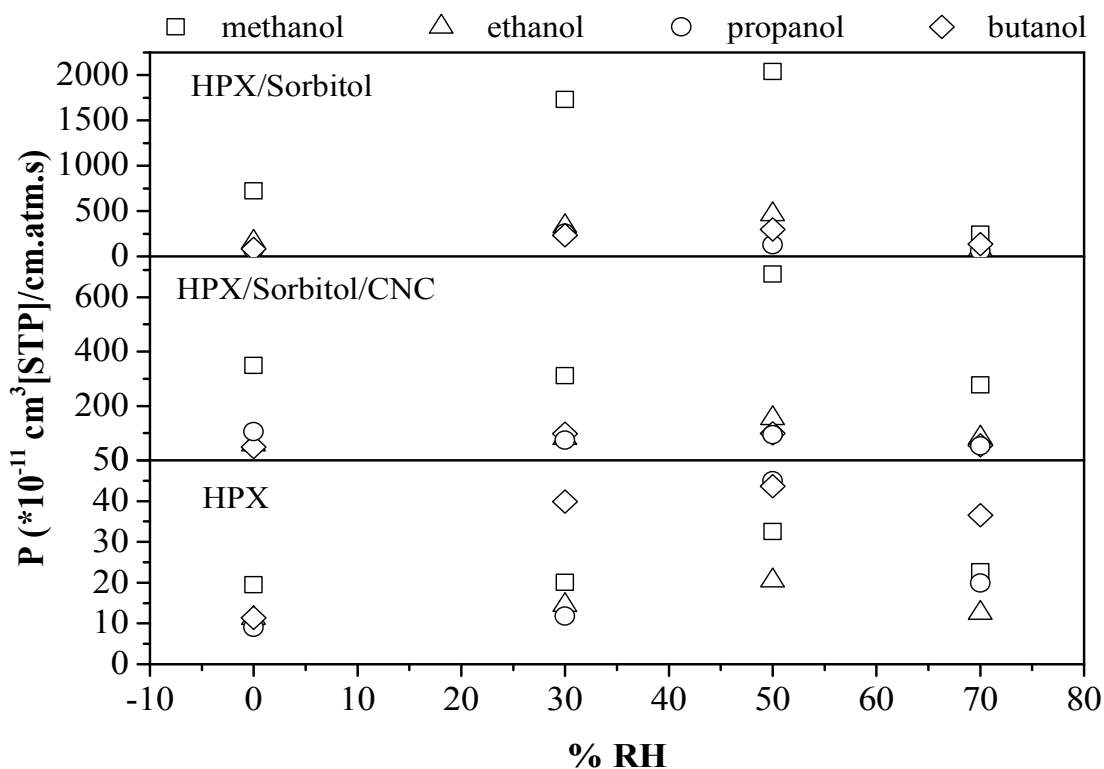


Figure 7.4. Infinite dilution permeability coefficients of alcohols in HPX, HPX/Sorbitol and HPX/Sorbitol/CNC films at 120 °C and under different levels of relative humidity.

7.4. Conclusion

The permeability of low molecular weight alcohols (methanol, ethanol, propanol and butanol) in HPX films was investigated based on diffusion and solubility coefficient measurements at different levels of relative humidity (0 – 70% RH). Diffusion coefficients showed a maximum at about 50% RH for all the alcohols while solubility coefficients were more or less insensitive to the RH. Plasticizing and swelling were the two factors that increased the diffusivity and consequently permeability of the alcohols at RH below 50%. Water content data estimated using the measured weight-fraction-based Henry's constants suggested that water clustering probably took place in the neat HPX film at 70% RH, thereby slowing the diffusion while for the

plasticized films, the data suggested that alcohols, methanol in particular, do not diffuse as individual molecules. Rather, they diffuse as alcohol-water clusters, thereby increasing their apparent size.

With diffusivity being the dominant factor in determining permeability behaviour, permeability coefficients followed the same pattern as diffusion coefficients at different RHs. This led to the barrier properties of the HPX films being reduced at RH up to 50%. In contrast, at higher RH, the barrier properties would be, more or less, similar to those of dry conditions. Consequently, HPX films are better barriers to alcohols in dry or highly humid conditions. However, it is important to investigate mechanical properties of the films at high humidity to consider their applicability under those conditions. In order to use the HPX films in humid environments, either diffusion characteristics of the films should be improved or they should be used along with water barrier polymer films.

Chapter 8

8. Conclusions and Future Works

8.1. Conclusions

Hydroxypropyl xylan (HPX) was introduced as a biopolymer with potential to be used in food packaging applications. In order for HPX to be applicable in food packaging as coating or transparent film, it should be able to provide sufficient mechanical and barrier properties. Inverse gas chromatography (IGC) was used to determine barrier properties of water and primary alcohols (C₁-C₄) (representing aroma in food) at infinite dilution in HPX films. Diffusion, solubility, and permeability coefficient were the parameters measured by IGC to determine barrier properties of HPX films. Neat HPX would provide rigid, brittle films from aqueous solution. In order to improve uniformity of the films and produce films with appropriate flexibility, different amounts of sorbitol a common plasticizer used in food industry was added to HPX solution which decreased T_g and increased diffusivity. Since, diffusivity is an important factor in determining barrier properties, cellulose nanocrystals, (CNC) a known natural polymer to improve the barrier properties was used to compensate the effect of added plasticizer. Accordingly, effect of the additives, solvent molecular weight, temperature, and humidity on the barrier properties of HPX was investigated and the concluding results are summarized as:

Additives:

- Sorbitol decreased T_g of the polymer by breaking the hydrogen bonding network of HPX. A direct impact of this would be on higher segmental mobility of the HPX which effectively enhances the small molecules mobility.
- Sorbitol decreased solubility of water and alcohols compared to the neat films. But collectively, addition of sorbitol increased permeability significantly for methanol and ethanol but in lesser extent in the case of propanol and butanol.
- Observed correlation between water diffusivity and concentration of additives indicates the applicability of free volume theory for diffusion of water.
- Generally, CNC hindered the diffusion coefficient but did not affect the solubility significantly. Based on our results it can be concluded that barrier characteristics of HPX for larger molecules would be intact.

Molecular weight of the Solvents:

- Solubility of alcohols exhibited a minimum over the molecular weight range of the primary alcohols used while diffusivity decreased with increasing molecular weight.
- Permeability in the neat HPX film showed a minimum over the range of molecular weight of the alcohols, indicating solubility-controlled permeation, especially at high alcohol's molecular weights.

Temperature:

- The stronger hydrogen bond between the solvent and HPX more obvious the decrease of solubility by temperature was.

- Increasing temperature increased diffusion coefficient, following Arrhenius law.
- The temperature dependence of permeability is stronger for the low molecular weight alcohols than for the high molecular weight ones.

Humidity:

- Diffusion coefficients showed a maxima over the range of humidity studied at about 50% RH. In less humid environment Plasticizing and swelling of the polymer by water increased diffusion coefficient while at higher humidity alcohol-water clusters were the possible reason for hindered diffusivity. Diffusion coefficient of methanol was the most affected among all.
- Solubility coefficients of the alcohols were more or less insensitive to relative humidity.
- Diffusivity was the dominant factor in determining permeability behaviour over the range of humidity studied, especially for smaller molecules.
- HPX films are better barriers to alcohols in dry while in humid conditions should be used with accompany of high water barrier materials.

8.2. Future Work

- We found that HPX with specific concentrations of additives can keep barrier properties close to neat HPX while forming non-brittle films. In order for the HPX to be applicable in packaging industry, a complete study on certain mechanical properties of HPX and additives is required.
- Knowing the barrier properties of HPX against the oxygen gas is a necessity. But due to some technical limitations this task could not be completed in this work. Based on the

end-use-application of the HPX, a comprehensive study on the barrier properties of gases, e.g. oxygen, CO₂, N₂, etc. is suggested using IGC or gravimetric methods.

- In addition to gases, barrier properties to other chemicals, such as fat, non-polar aromas (e.g. limonene) should be studied.
- Our choice of operating temperature for determination of diffusion coefficient using IGC was dictated by the limitations of the equipment. Using gravimetric methods, diffusion coefficient can be obtained at ambient temperature. However, it will be time consuming and not precise at infinite dilution. This method can be used to determine diffusion coefficients at finite concentrations of the solvents at glassy state of the polymer and extrapolate it to infinite dilution for comparison purposes.
- The measured diffusion coefficients provide the self-diffusion coefficient of the solutes in the infinite dilution. With the available experimental data, free volume theory can be used to analyse the correlation of the self-diffusion coefficient with different system parameters like polymer molecular weight and temperature. Also, using results from IGC and applying Darken equation we can calculate the mutual diffusion coefficients for manufacturing processes and compare the results with gravimetric/sorption results if available.
- The interaction of flavor compounds of the food with the packaging will affect the packaging and also alter the quality of the packed food. So, thermodynamic adsorption properties such as enthalpy of adsorption, Gibbs free energy of adsorption, partition coefficient and etc. need to be studied for the cases of direct contact between packaging and food. In an attempt to address this problem in this work, some of the adsorption data was measured for interaction of HPX films with C₁ to C₆ alcohols, two aldehydes

(hexanal and heptanal), and limonene. Part of these results has been provided in Appendix A. Further experiments are required for completing the results of this section.

- HPX was introduced as a hydrophilic polymer with certain barrier properties. Further modification of the polymer can result in a totally different polymer which is immiscible with water. Acetylation has been proposed as way of increasing hydrophobicity of the polymers. This method was applied on HPX and some of the preliminary data regarding substitution of hydroxyl group of HPX with acetyl groups is provided in appendix B. Due to inability to form a proper film, further analysis of the acetylated HPX was not pursued in this work. However, upon tuning of acetylation method it might be possible to improve the film forming properties while the resulted polymer is still insoluble in water.
- Lipid-based fillers can be investigated as a way of improving water barrier properties of the films.

Bibliography

- [1] S. Wetzel, L. C. Duchesne, and M. F. Laporte, *Bioproducts from Canada's Forests New partnerships in the Bioeconomy*. Netherland: Springer, 2006.
- [2] M. Gröndahl, L. Eriksson, and P. Gatenholm, "Material Properties of Plasticized Hardwood Xylans for Potential Application as Oxygen Barrier Films.," *Biomacromolecules*, vol. 5, no. 4, pp. 1528–35, 2004.
- [3] D. González, V. Santos, and J. C. Parajó, "Manufacture of Fibrous Reinforcements for Biocomposites and Hemicellulosic Oligomers from Bamboo," *Chem. Eng. J.*, vol. 167, no. 1, pp. 278–287, Feb. 2011.
- [4] A. Höije, M. Gröndahl, K. Tømmeraas, and P. Gatenholm, "Isolation and Characterization of Physicochemical and Material Properties of Arabinoxylans from Barley husks," *Carbohydr. Polym.*, vol. 61, no. 3, pp. 266–275, Aug. 2005.
- [5] A. Ebringerová, "Structural Diversity and Application Potential of Hemicelluloses," *Macromol. Symp.*, vol. 232, no. 1, pp. 1–12, Dec. 2006.
- [6] A. Saxena, T. J. Elder, J. Kenvin, and A. J. Ragauskas, "High Oxygen Nanocomposite Barrier Films Based on Xylan and Nanocrystalline Cellulose," *Nano-Micro Lett.*, vol. 2, no. 4, pp. 235–241, 2010.
- [7] A. Saxena and A. J. Ragauskas, "Water Transmission Barrier Properties of Biodegradable Films Based on Cellulosic Whiskers and Xylan," *Carbohydr. Polym.*, vol. 78, no. 2, pp. 357–360, 2009.

- [8] S. A. Paralikar, J. Simonsen, and J. Lombardi, "Poly(vinyl alcohol)/Cellulose Nanocrystal Barrier Membranes," *J. Memb. Sci.*, vol. 320, no. 1–2, pp. 248–258, Jul. 2008.
- [9] R. a. Khan, S. Beck, D. Dussault, S. Salmieri, J. Bouchard, and M. Lacroix, "Mechanical and Barrier Properties of Nanocrystalline Cellulose Reinforced Poly(caprolactone) Composites: Effect of Gamma Radiation," *J. Appl. Polym. Sci.*, vol. 129, no. 5, pp. 3038–3046, Sep. 2013.
- [10] M. Bulota, B. Maasdam, and S. Tiekstra, "Breakthrough Technologies More with Less," 2013.
- [11] S. Zhang, A. Tsuboi, H. Nakata, and T. Ishikawa, "Activity Coefficients and Diffusivities of Solvents in Polymers," *Fluid Phase Equilib.*, vol. 194–197, pp. 1179–1189, 2002.
- [12] P. T. DeLassus, J. C. Tou, M. A. Babinec, D. C. Rulf, B. K. Karp, and B. A. Howell, "Transport of Apple Aromas in Polymer Films," in *Food and Packaging Interactions*, J. H. Hotchkiss, Ed. Washington D.C.: American Chemical Society, 1988, pp. 11–27.
- [13] F. Johansson and A. Leufven, "Food Packaging Polymer Films as Aroma Vapor Barriers at Different Relative Humidities," *J. Food Sci.*, vol. 59, no. 6, pp. 1328–1331, 1994.
- [14] S. Aucejo, M. J. Pozo, and R. Gavara, "Effect of Water Presence on the Sorption of Organic Compounds in Ethylene-Vinyl Alcohol Copolymers," *J. Appl. Polym. Sci.*, vol. 70, no. 4, pp. 711–716, 1998.
- [15] E. B. Schaper, "High Barrier Plastics Packaging and Ethylene Vinyl Alcohol Resins (a Marriage)," in *Food Packaging Technology (ASTM STP 1113)*, D. K. Henyon, Ed. American Society for Testing and Material, 1991, pp. 31–36.

- [16] J. K. Cage, "1. Introduction to Food Packaging Page," in *Food Packaging Technology (STP1113)*, D. K. Henyon, Ed. ASTM International, 1991, pp. 3–12.
- [17] L. W. McKeen, "1. Introduction to Use of Plastics in Food Packaging," in *Plastic Films in Food Packaging*, First Edit., S. Ebnesajjad, Ed. Elsevier Inc., 2013, pp. 1–15.
- [18] C. Oswin, "The selection of plastics films for food packaging," *Food Chem.*, vol. 8, pp. 121–127, 1982.
- [19] V. Siracusa, "Food Packaging Permeability Behaviour: A Report," *Int. J. Polym. Sci.*, vol. 2012, pp. 1–11, 2012.
- [20] K. Marsh and B. Bugusu, "Food Packaging-Roles, Materials, and Environmental Issues," *J. Food Sci.*, vol. 72, no. 3, pp. R39–R55, 2007.
- [21] Industry Canada, "Industry Profile for the Canadian Plastic Products Industry," 2012.
- [22] G. Chooudalakis and A. D. Gotsis, "Recent Developments in the Permeability of Polymer Clay Nanocomposites," in *Handbook of Polymernanocomposites. Processing, Performance and Application Volume A: Layered Silicates*, J. K. Pandey, K. R. Reddy, A. K. Mohanty, and M. Misra, Eds. Springer, 2014, pp. 415–451.
- [23] M. Salame and S. Steingiser, "Barrier Polymers," *Polym. Plast. Technol. Eng.*, vol. 8, no. 2, pp. 155–175, 1977.
- [24] S. D. F. Mihindukulasuriya and L. T. Lim, "Nanotechnology Development in Food Packaging: A Review," *Trends Food Sci. Technol.*, vol. 40, no. 2, pp. 149–167, 2014.
- [25] V. Siracusa, P. Rocculi, S. Romani, and M. D. Rosa, "Biodegradable Polymers for Food

- Packaging: A Review,” *Trends Food Sci. Technol.*, vol. 19, no. 12, pp. 634–643, 2008.
- [26] C. Johansson, J. Bras, I. Mondragon, P. Nechita, D. Plackett, P. Simon, D. G. Svetec, S. Virtanen, M. G. Baschetti, C. Breen, F. Clegg, and S. Aucejo, “Renewable Fibers and Bio-Based Materials for Packaging Applications – A Review of Recent Developments,” *BioResources*, vol. 7, no. 2, pp. 2506–2552, 2012.
- [27] E. Rudnik, “Compostable Polymer Properties and Packaging Applications,” in *Plastic Films in Food Packaging*, First Edit., no. 2008, S. Ebnesajjad, Ed. Elsevier Inc., 2013, pp. 217–248.
- [28] F. Li, M. Erika, and L. Piergiovanni, “The Potential of NanoCellulose in the Packaging Field: A Review,” *Packag. Technol. Sci.*, vol. 28, pp. 475–508, 2015.
- [29] A. Elidrissi, S. El Barkany, H. Amhamdi, and A. Maaroufi, “Elaboration of the New Cellulose Derivative Films (HECA) Based on ‘Stipa Tenacissima’ Cellulose of Eastern Morocco,” *J. Mater. Environ. Sci.*, vol. 1, no. 3, pp. 197–204, 2010.
- [30] N. Cordeiro, C. Gouveia, A. G. O. Moraes, and S. C. Amico, “Natural Fibers Characterization by Inverse Gas Chromatography,” *Carbohydr. Polym.*, vol. 84, no. 1, pp. 110–117, 2011.
- [31] D. Allsopp, K. J. Seal, and C. C. Gaylarde, *Introduction to Biodeterioration*, 2nd ed. Cambridge, UK: Cambridge University Press, 2004.
- [32] S. Paunonen, “Strength and Barrier Enhancements of Cellophane and Cellulose Derivative Films: A Review,” *BioResources*, vol. 8, no. 2, pp. 3098–3121, 2013.
- [33] A. Aluigi, C. Vineis, A. Ceria, and C. Tonin, “Composite Biomaterials from Fibre Wastes:

- Characterization of Wool-Cellulose Acetate Blends,” *Compos. Part A Appl. Sci. Manuf.*, vol. 39, no. 1, pp. 126–132, 2008.
- [34] T. Yamashiki, T. Matsui, K. Kowsaka, M. Saitoh, K. Okajima, and K. Kamide, “New Class of Cellulose Fiber Spun from the Novel Solution of Cellulose by Wet Spinning Method,” *J. Appl. Polym. Sci.*, vol. 44, pp. 691–698, 1992.
- [35] M. Terbojevich, A. Cosani, G. Conio, A. Ciferri, and E. Bianchi, “Mesophase Formation and Chain Rigidity in Cellulose and Derivatives. 3. Aggregation of Cellulose in N,N-Dimethylacetamide-Lithium Chloride,” *Macromolecules*, vol. 18, no. 4, pp. 640–646, 1985.
- [36] M. Popa and N. Belc, “Packaging,” in *Food Safety: A Practical and Case Study Approach*, Richard J. Marshal, Ed. Springer Science & Business Media, 2006, pp. 68–87.
- [37] L. C. Tomé, C. M. B. Goncalves, M. Boaventura, L. Brandao, A. M. Mendes, A. J. D. Silvestre, C. P. Neto, A. Gandini, C. S. R. Freire, and I. M. Marrucho, “Preparation and Evaluation of the Barrier Properties of Cellophane Membranes Modified with Fatty Acids,” *Carbohydr. Polym.*, vol. 83, no. 2, pp. 836–842, 2011.
- [38] S. Mura, F. Corrias, G. Stara, M. Piccinini, N. Secchi, D. Marongiu, P. Innocenzi, J. Irudayaraj, and G. F. Greppi, “Innovative Composite Films of Chitosan, Methylcellulose, and Nanoparticles,” *J. Food Sci.*, vol. 76, no. 7, pp. 54–60, 2011.
- [39] Y. Li, C. F. Shoemaker, J. Ma, X. Shen, and F. Zhong, “Paste Viscosity of Rice Starches of Different Amylose Content and Carboxymethylcellulose Formed by Dry Heating and the Physical Properties of their Films,” *Food Chem.*, vol. 109, no. 3, pp. 616–623, 2008.

- [40] B. Ghanbarzadeh, H. Almasi, and A. A. Entezami, "Improving the Barrier and Mechanical Properties of Corn Starch-Based Edible Films: Effect of Citric Acid and Carboxymethyl Cellulose," *Ind. Crops Prod.*, vol. 33, no. 1, pp. 229–235, 2011.
- [41] C. Mu, J. Guo, X. Li, W. Lin, and D. Li, "Preparation and Properties of Dialdehyde Carboxymethyl Cellulose Crosslinked Gelatin Edible Films," *Food Hydrocoll.*, vol. 27, no. 1, pp. 22–29, 2012.
- [42] P. Rachtanapun and N. Rattanapanone, "Synthesis and Characterization of Carboxymethyl Cellulose Powder and Films from *Mimosa pigra*," *J. Appl. Polym. Sci.*, vol. 122, pp. 3218–3226, 2011.
- [43] C. Miao and W. Y. Hamad, "Cellulose Reinforced Polymer Composites and Nanocomposites: A Critical Review," *Cellulose*, vol. 20, no. 5, pp. 2221–2262, 2013.
- [44] Z. Akbari, T. Ghomashchi, and S. Moghadam, "Improvement in Food Packaging Industry with Biobased Nanocomposites," *Int. J. Food Eng.*, vol. 3, no. 4, pp. 1–26, 2007.
- [45] M. Ioelovich, "Cellulose As a Nanostructured Polymer: a Short Review," *BioResources*, vol. 3, no. 4, pp. 1403–1418, 2008.
- [46] M. M. De Souza Lima and R. Borsali, "Rodlike Cellulose Microcrystals: Structure, Properties, and Applications," *Macromol. Rapid Commun.*, vol. 25, no. 7, pp. 771–787, 2004.
- [47] M. D. Sánchez-García, L. Hilliou, and J. M. Lagarón, "Morphology and Water Barrier Properties of Nanobiocomposites of κ /I-Hybrid Carrageenan and Cellulose Nanowhiskers," *J. Agric. Food Chem.*, vol. 58, no. 24, pp. 12847–12857, 2010.

- [48] J. B. A. da Silva, F. V. Pereira, and J. I. Druzian, "Cassava Starch-Based Films Plasticized with Sucrose and Inverted Sugar and Reinforced with Cellulose Nanocrystals," *J. Food Sci.*, vol. 77, no. 6, pp. 14–19, 2012.
- [49] J. M. Lagaron, R. Catalá, and R. Gavara, "Structural Characteristics Defining High Barrier Properties in Polymeric Materials," *Mater. Sci. Technol.*, vol. 20, no. 1, pp. 1–7, 2004.
- [50] R. Sun, X. F. Sun, and J. Tomkinson, "Hemicelluloses and Their Derivatives," in *Hemicelluloses: Science and Technology*, P. Gatenholm and M. Tenkanen, Eds. 2004 American Chemical Society, 2003, pp. 2–22.
- [51] M. Ibrahim, "Clean Fractionation of Biomass - Steam Explosion and Extraction," Virginia Polytechnic Institute and State University, 1998.
- [52] R. H. Marchessault, "Isolation and Properties of Xylan: Rediscovery and Renewable Resource," in *Hemicelluloses: Science and Technology*, P. Gatenholm and M. Tenkanen, Eds. American Chemical Society, 2003, pp. 158–166.
- [53] J. Hartman, A. C. Albertsson, M. S. Lindblad, and J. Sjöberg, "Oxygen Barrier Materials from Renewable Sources: Material Properties of Softwood Hemicellulose-Based Films," *J. Appl. Polym. Sci.*, vol. 100, pp. 2985–2991, 2006.
- [54] J. Hartman, A.-C. Albertsson, and J. Sjöberg, "Surface- and Bulk-Modified Galactoglucomannan Hemicellulose Films and Film Laminates for Versatile Oxygen Barriers," *Biomacromolecules*, vol. 7, no. 6, pp. 1983–1389, 2006.
- [55] S. Tejinder, "Preparation and Characterization of Films Using Barley and Oat β -Glucan Extracts," *Cereal Chem.*, vol. 80, no. 6, pp. 728–731, 2003.

- [56] B. Ş. Kayserilioğlu, U. Bakir, L. Yilmaz, and N. Akkaş, “Use of Xylan, an Agricultural by-Product, in Wheat Gluten Based Biodegradable Films: Mechanical, Solubility and Water Vapor Transfer Rate Properties,” *Bioresour. Technol.*, vol. 87, no. 3, pp. 239–246, 2003.
- [57] R. L. Whistler and J. R. Daniel, “Starch,” in *Kirk-Othmer Encyclopedia of Chemical Technology*, 3rd ed., H. F. Mark, D. F. Othmer, C. G. Overberger, and G. T. Seaborgand, Eds. John Wiley & Sons, Inc., 1983, pp. 492–507.
- [58] T. G. Majewicz and T. J. Podlas, “Cellulose Ethers,” in *Kirk-Othmer Encyclopedia of Chemical Technology*, 4th ed., vol. 5, M. Howe- Grant, Ed. Wiley, 1993, pp. 541–563.
- [59] A. Ebringerova and T. Heinze, “Xylan and xylan derivatives – biopolymers with valuable properties , 1 Naturally occurring xylans structures , isolation procedures and properties,” *Macromol. Rapid Commun.*, vol. 21, pp. 542–556, 2000.
- [60] M. L. T. M. Polizeli, A. C. S. Rizzatti, R. Monti, H. F. Terenzi, J. A. Jorge, and D. S. Amorim, “Xylanases from Fungi: Properties and Industrial Applications,” *Appl. Microbiol. Biotechnol.*, vol. 67, no. 5, pp. 577–591, 2005.
- [61] W. G. Glasser, R. K. Jain, and M. A. Sjostedt, “Thermoplastic Pentosan-Rich Polysaccharides from Biomass,” 5430142, 1995.
- [62] R. K. Jain, M. Sjostedt, and W. G. Glasser, “Thermoplastic Xylan Derivatives with Propylene Oxide,” *Cellulose*, vol. 7, no. 4, pp. 319–336, 2001.
- [63] N. G. V Fundador, Y. Enomoto-Rogers, A. Takemura, and T. Iwata, “Syntheses and Characterization of Xylan Esters,” *Polym. (United Kingdom)*, vol. 53, no. 18, pp. 3885–

3893, 2012.

- [64] I. Šimkovic, O. Gedeon, I. Uhliariková, R. Mendichi, and S. Kirschnerová, “Xylan Sulphate Films,” *Carbohydr. Polym.*, vol. 86, no. 1, pp. 214–218, 2011.
- [65] E. I. Goksu, M. Karamanlioglu, U. Bakir, L. Yilmaz, and U. Yilmazer, “Production and Characterization of Films from Cotton Stalk Xylan,” *J. Agric. Food Chem.*, vol. 55, no. 26, pp. 10685–91, Dec. 2007.
- [66] C. Péroval, F. Debeaufort, D. Despré, and A. Voilley, “Edible Arabinoxylan-Based Films. 1. Effects of Lipid Type on Water Vapor Permeability, Film Structure, and other Physical Characteristics,” *J. Agric. Food Chem.*, vol. 50, no. 14, pp. 3977–3983, 2002.
- [67] A. Escalante, A. Gonçalves, A. Bodin, A. Stepan, C. Sandström, G. Toriz, and P. Gatenholm, “Flexible Oxygen Barrier Films from Spruce Xylan,” *Carbohydr. Polym.*, vol. 87, no. 4, pp. 2381–2387, 2012.
- [68] T. Koshijima, T. E. Timell, and M. Zinbo, “The Number-Average Molecular Weight of Native Hardwood Xylans,” *J. Polym. Sci. PART C*, vol. 11, pp. 265–279, 1965.
- [69] P. Zhang and R. L. Whistler, “Mechanical properties and water vapor permeability of thin film from corn hull arabinoxylan,” *J. Appl. Polym. Sci.*, vol. 93, no. 6, pp. 2896–2902, 2004.
- [70] D. Phan The, F. Debeaufort, C. Péroval, D. Despré, J. L. Courthaudon, and A. Voilley, “Arabinoxylan-Lipid-Based Edible Films and Coatings. 3. Influence of Drying Temperature on Film Structure and Functional Properties,” *J. Agric. Food Chem.*, vol. 50, no. 8, pp. 2423–2428, 2002.

- [71] D. Phan The, C. Péroval, F. Debeaufort, D. Despré, J. L. Courthaudon, and A. Voilley, “Arabinoxylan-Lipids-Based Edible Films and Coatings. 2. Influence of Sucroester Nature on the Emulsion Structure and Film Properties.,” *J. Agric. Food Chem.*, vol. 50, no. 2, pp. 266–272, 2002.
- [72] C. Péroval, F. Debeaufort, a. M. Seuvre, B. Chevet, D. Despré, and a. Voilley, “Modified arabinoxylan-based films. Part B. Grafting of omega-3 fatty acids by oxygen plasma and electron beam irradiation,” *J. Agric. Food Chem.*, vol. 51, pp. 3120–3126, 2003.
- [73] C. Peroval, F. Debeaufort, A.-M. Seuvre, P. Cayot, B. Chevet, D. Despré, and A. Voilley, “Modified Arabinoxylan-Based Films Grafting of Functional Acrylates by Oxygen Plasma and Electron Beam Irradiation,” *J. Memb. Sci.*, vol. 233, no. 1–2, pp. 129–139, 2004.
- [74] F. Bayati, Y. Boluk, and P. Choi, “Diffusion Behavior of Water at Infinite Dilution in Hydroxypropyl Xylan Films with Sorbitol and Cellulose Nanocrystals,” *ACS Sustain. Chem. Eng.*, vol. 2, no. 5, pp. 1305–1311, 2014.
- [75] F. Bayati, Y. Boluk, and P. Choi, “Inverse Gas Chromatography Study of the Permeability of Aroma through Hydroxypropyl Xylan Films,” *ACS Sustain. Chem. Eng.*, vol. 3, no. 12, pp. 3114–3122, 2015.
- [76] S. C. George and S. Thomas, “Tansport Phenomena through Polymeric Systems,” *Prog. Polym. Sci.*, vol. 26, no. 6, pp. 985–1017, 2001.
- [77] H. F. Mark, *Encyclopedia of Polymer Science and Technology, Concise*, 3rd Editio. Wiley, 2013.

- [78] R. M. Felder and G. S. Huvard, "Permeation, Diffusion, and Sorption of Gases and Vapors," in *Methods of Experimental Physics Polymers Physical Properties*, R. A. Fava, Ed. Academic Press, 1980, pp. 315–378.
- [79] A. Javaid, "Membranes for Solubility-Based Gas Separation Applications," *Chem. Eng. J.*, vol. 112, no. 1–3, pp. 219–226, 2005.
- [80] C. Wang, P.-C. Lai, S. H. Syu, and J. Leu, "Effects of CF₄ Plasma Treatment on the Moisture Uptake, Diffusion, and WVTR of Poly(ethylene terephthalate) Flexible Films," *Surf. Coatings Technol.*, vol. 206, no. 2–3, pp. 318–324, 2011.
- [81] G. Choudalakis, A. D. Gotsis, H. Schut, and S. J. Picken, "The free volume in acrylic resin/laponite nanocomposite coatings," *Eur. Polym. J.*, vol. 47, no. 3, pp. 264–272, 2011.
- [82] J. Crank, "Methods of Measurement," in *Diffusion in Polymers*, J. Crank and G. S. Park, Eds. New York: Academic Press, 1968, pp. 1–39.
- [83] N. Lützow, A. Tihminlioglu, R. P. Danner, J. L. Duda, A. De Haan, G. Warnier, and J. M. Zielinski, "Diffusion of toluene and n-heptane in polyethylenes of different crystallinity," *Polymer (Guildf.)*, vol. 40, pp. 2797–2803, 1999.
- [84] S. Stern, "Polymers for Gas Separations: the Next Decade," *J. Memb. Sci.*, vol. 94, pp. 1–65, 1994.
- [85] J. S. Vrentas, J. L. Duda, and H.-C. Ling, "Free-Volume Equations for Polymer-Penetrant Diffusion," *J. Memb. Sci.*, vol. 40, pp. 101–107, 1989.
- [86] M. H. Cohen and D. Turnbull, "Molecular Transport in Liquids and Glasses," *J. Chem. Phys.*, vol. 31, pp. 1164–1169, 1959.

- [87] D. Arnould and L. Robert, "Solute Diffusion in Polymers by Capillary Column Inverse Gas Chromatography," in *Inverse Gas Chromatography Characterization of Polymers and Other Materials*, vol. 391, D. R. Lloyd, T. C. Ward, H. P. Schreiber, and C. C. Pizana, Eds. American Chemical Society, 1989, pp. 87–106.
- [88] S. Mohammadi-Jam and K. E. Waters, "Inverse Gas Chromatography Applications: A Review.," *Adv. Colloid Interface Sci.*, vol. 212, pp. 21–44, Oct. 2014.
- [89] A. V. Kiselev and Y. I. Yashin, *Gas Adsorption Chromatography*, 1st ed. New York and London: Plenum Press, 1969.
- [90] O. Smidsrød and J. E. Guillet, "Study of Polymer-Solute Interactions by Gas Chromatography," *Macromolecules*, vol. 2, no. 3, pp. 272–277, 1969.
- [91] A. Voelkel, B. Strzemieska, K. Adamska, and K. Milczewska, "Inverse gas chromatography as a source of physiochemical data.," *J. Chromatogr. A*, vol. 1216, no. 10, pp. 1551–66, Mar. 2009.
- [92] R. P. Danner, F. Tihminlioglu, R. K. Surana, and J. L. Duda, "Inverse Gas Chromatography Applications in Polymer – Solvent Systems," *Fluid Phase Equilib.*, vol. 148, pp. 171–188, 1998.
- [93] H. M. McNair and J. M. Miller, *Basic Gas Chromatography*, 2nd ed. John Wiley & Sons, 2009.
- [94] P. J. Kalaouzis and P. G. Demertzis, "Influence of a monomeric plasticizer on the water-sorption behaviour of food-grade plastics packaging materials," *Polym. Int.*, vol. 32, pp. 125–130, 1993.

- [95] D. G. Gray and J. E. Guillet, "Gas Chromatographic Method for the Study of Sorption on Polymers," *Macromolecules*, vol. 5, no. 3, pp. 316–321, 1972.
- [96] N. A. Belov, A. P. Safronov, and Y. P. Yampolskii, "Inverse-Gas Chromatography and the Thermodynamics of Sorption in Polymers," *Polym. Sci. Ser. A*, vol. 54, no. 11, pp. 859–873, 2012.
- [97] C. a. Pawlisch, a. Macris, and R. L. Laurence, "Solute diffusion in polymers. 1. The use of capillary column inverse gas chromatography," *Macromolecules*, vol. 20, pp. 1564–1578, 1987.
- [98] D. G. Gray and J. E. Guillet, "Studies of Diffusion in Polymers by Gas Chromatography," *Macromolecules*, vol. 6, no. 2, pp. 223–227, 1973.
- [99] J. J. van Deemter, F. J. Zuiderweg, and A. Klinkenberg, "Longitudinal Diffusion and Resistance to Mass Transfer as Causes of Nonideality in Chromatography," *Chem. Eng. Sci.*, vol. 5, pp. 271–289, 1956.
- [100] I. Hadj Romdhane and R. P. Danner, "Polymer-Solvent Diffusion and Equilibrium by Inverse Gas-Liquid Chromatography," *AICHE*, vol. 39, no. 4, pp. 625–635, 1993.
- [101] R. P. Danner, "Measuring and Correlating Diffusivity in Polymer–Solvent Systems Using Free-Volume Theory," *Fluid Phase Equilib.*, vol. 362, pp. 19–27, 2014.
- [102] A. E. Bolvari, T. C. Ward, P. A. Koning, and D. P. Sheehy, "Experimental Techniques for Inverse Gas Chromatography," in *Inverse Gas Chromatography Characterization of Polymers and Other Materials*, D. R. Lloyd, T. C. Ward, H. P. Schreiber, and C. C. Pizaña, Eds. American Chemical Society, 1989, pp. 12–19.

- [103] T. J. Bruno, "a Review of Capillary and Packed Column Gas Chromatographs," *Sep. Purif. Rev.*, vol. 29, pp. 27–61, 2000.
- [104] J. Cazes and R. P. W. Scott, "The Mechanism of Retention Molecular Interactions, the Thermodynamics of Distribution, the Plate Theory, and Extensions of the Plate Theory," in *Chromatography Theory*, Marcel Dekker, INC., 2002, p. 496.
- [105] A. J. P. Martin and R. L. M. Synge, "A New Form of Chromatogram Employing two Liquid Phases 1. A Theory of Chromatography 2. Application to the Micro-Determination of the Higher Monoamino-Acids in Proteins," *Biochem. J.*, vol. 35, no. 12, pp. 1358–1368, 1941.
- [106] S. W. Mayer and E. R. Tompkins, "Ion Exchange as a Separations Method. IV. A Theoretical Analysis of the Column Separations Process," *J. Am. Chem. Soc.*, vol. 69, no. 11, pp. 2866–2874, 1947.
- [107] E. Glueckauf, "Theory of Chromatography: Part 9. The 'Theoretical Plate' Concept in Column Separations," *Trans. Faraday Soc.*, vol. 51, pp. 34–44, 1955.
- [108] A. S. Said, "Theoretical-Plate Concept in Chromatography," *Am. Inst. Chem. Eng. J.*, vol. 2, no. 4, pp. 477–481, 1956.
- [109] L. Lapidus and N. R. Amundson, "Mathematics of Adsorption in Beds. VI. The Effect of Longitudinal Diffusion in Ion Exchange and Chromatographic Columns," *J. Phys. Chem.*, vol. 56, no. 8, pp. 984–988, 1952.
- [110] J. C. Giddings, "Role of Column Pressure Drop in Gas Chromatographic Resolution," *Anal. Chem.*, vol. 36, no. 4, pp. 741–744, 1964.

- [111] K. Ogan and R. P. W. Scott, "Optimization of Capillary Parameters for Gas Chromatography," *HRC CC. J. High Resolut. Chromatogr. Chromatogr. Commun.*, vol. 7, no. 7, pp. 382–388, 1984.
- [112] E. A. Walker and J. F. Palframan, "Techniques in Gas Chromatography Part II*. Developments in the van Deemter Rate Theory of Column Performance A Review," *Analyst*, vol. 94, no. 1121, pp. 609–615, 1969.
- [113] J. V Hinshaw, "Practical Gas Chromatography," in *LCGC Europe*, no. November, W. Engewald and K. Dettmer-Wilde, Eds. 2014, pp. 624–629.
- [114] A. Etxeberria, J. Alfageme, C. Uriarte, and J. J. Iruin, "Inverse Gas Chromatography in the Characterization of Polymeric Materials," *J. Chromatogr.*, vol. 607, pp. 227–237, 1992.
- [115] O. F. von Meien, E. C. Biscaia Jr., and R. Nobrega, "Polymer-Solute Diffusion and Equilibrium Parameters by Inverse Gas Chromatography," *AICHE J.*, vol. 43, no. 11, pp. 2932–2943, 1997.
- [116] A. A. Korolev, V. E. Shiryaeva, T. P. Popova, and A. A. Kurganov, "Effect of the Pressure of the Carrier Gas on the Parameters of the Van Deemter Equation for Monolithic Silica Gel Gas Chromatography Columns," *Russ. J. Phys. Chem.*, vol. 80, no. 5, pp. 781–785, 2006.
- [117] J. M. Braun and J. E. Guillet, "A Model of the Gas Chromatographic Behavior of Polymer Stationary Phases through their Glass Transitions," *Macromolecules*, vol. 9, no. 4, pp. 617–621, 1976.

- [118] M. Kawakami and S. Kagawa, "Measurements of the Solubility Coefficients of Gases and Vapors in Natural Rubber by Gas Chromatographic Technique," *Bull. Chem. Soc. Jpn.*, vol. 51, no. 1, pp. 75–78, 1978.
- [119] D. H. Everett and C. T. H. Stoddart, "The Thermodynamics of Hydrocarbon Solutions from G.L.C Measurements Part 1.- Solutions in Dinonyl Phthalate," *Trans. Faraday Soc.*, vol. 57, pp. 746–754, 1961.
- [120] A. J. B. Cruickshank, M. L. Windsor, and C. L. Young, "The Use of Gas-Liquid Chromatography to Determine Activity Coefficients and Second Virial Coefficients of Mixtures. I. Theory and Verification of Method of Data Analysis," *Proc. R. Soc. London A*, vol. 295, pp. 259–270, 1966.
- [121] A. Saxena, T. J. Elder, and A. J. Ragauskas, "Moisture barrier properties of xylan composite films," *Carbohydr. Polym.*, vol. 84, no. 4, pp. 1371–1377, Apr. 2011.
- [122] O. Akpınar, O. Ak, A. Kavas, U. Bakir, and L. Yılmaz, "Enzymatic production of xylooligosaccharides from cotton stalks," *J. Agric. Food Chem.*, vol. 55, no. 14, pp. 5544–51, Jul. 2007.
- [123] T. Jeoh and F. a. Agblevor, "Characterization and fermentation of steam exploded cotton gin waste," *Biomass and Bioenergy*, vol. 21, no. 2, pp. 109–120, Aug. 2001.
- [124] A. M. Stepan, A. Höije, H. A. Schols, P. D. Waard, and P. Gatenholm, "Arabinose Content of Arabinoxylans Contributes to Flexibility of Acetylated Arabinoxylan Films," *J. Appl. Polym. Sci.*, vol. 125, pp. 2348–2355, 2012.
- [125] N. G. V. Fundador, Y. Enomoto-Rogers, A. Takemura, and T. Iwata, "Acetylation and

- characterization of xylan from hardwood kraft pulp,” *Carbohydr. Polym.*, vol. 87, no. 1, pp. 170–176, Jan. 2012.
- [126] M. Gröndahl, A. Gustafsson, and P. Gatenholm, “Gas-Phase Surface Fluorination of Arabinoxylan Films,” *Macromolecules*, vol. 39, pp. 2718–2721, 2006.
- [127] V. P. Martino, R. a. Ruseckaite, A. Jiménez, and L. Averous, “Correlation between Composition, Structure and Properties of Poly(lactic acid)/Polyadipate-Based Nano-Biocomposites,” *Macromol. Mater. Eng.*, vol. 295, no. 6, pp. 551–558, May 2010.
- [128] N. M. L. Hansen and D. Plackett, “Sustainable Films and Coatings from Hemicelluloses: a Review.,” *Biomacromolecules*, vol. 9, no. 6, pp. 1493–505, Jun. 2008.
- [129] E. Fortunati, M. Peltzer, I. Armentano, L. Torre, a Jiménez, and J. M. Kenny, “Effects of Modified Cellulose Nanocrystals on the Barrier and Migration Properties of PLA Nano-Biocomposites.,” *Carbohydr. Polym.*, vol. 90, no. 2, pp. 948–56, Oct. 2012.
- [130] T. Huq, S. Salmieri, A. Khan, R. a Khan, C. Le Tien, B. Riedl, C. Fraschini, J. Bouchard, J. Uribe-Calderon, M. R. Kamal, and M. Lacroix, “Nanocrystalline cellulose (NCC) reinforced alginate based biodegradable nanocomposite film.,” *Carbohydr. Polym.*, vol. 90, no. 4, pp. 1757–63, Nov. 2012.
- [131] D. Zhou, F. Bayati, and P. Choi, “On the weak dependence of water diffusivity on the degree of hydrophobicity of acetylated hydroxypropyl xylan.,” *Carbohydr. Polym.*, vol. 98, no. 1, pp. 644–9, Oct. 2013.
- [132] C. Etxabarren, M. Iriarte, A. Etxeberria, C. Uriarte, and J. J. Iruin, “Determination of the Diffusion Coefficients of Organic Solvents in Polyepichlorohydrin : A Comparative Study

- of Inverse Gas Chromatography and Sorption Methods,” *J. Appl. Polym. Sci.*, vol. 89, pp. 2216–2223, 2003.
- [133] P. J. Kalaouzis and P. G. Demertzis, “Water Sorption and Water Vapour Diffusion in Food-Grade Plastics Packaging Materials: Effect of a Polymeric Plasticizer,” *Packag. Technol. Sci.*, vol. 5, no. February, pp. 133–144, 1992.
- [134] M. G. A. Vieira, M. A. da Silva, L. O. dos Santos, and M. M. Beppu, “Natural-based plasticizers and biopolymer films: A review,” *Eur. Polym. J.*, vol. 47, no. 3, pp. 254–263, Mar. 2011.
- [135] V. Y. Senichev and V. V. Tereshatov, “Effect of Plasticizers on Properties of Plasticized Materials,” in *Handbook of Plasticizers*, 2nd editio., G. Wypych, Ed. ChemTec Publishing, 2012, pp. 237–247.
- [136] J. R. Fried, S. Y. Lai, L. W. Kleiner, and M. E. Wheeler, “Experimental Assessment of the Thermodynamic Theory of the Compositional Variation of Tg: PVC Systems,” *J. Appl. Polym. Sci.*, vol. 27, no. 8, pp. 2869–2883, 1982.
- [137] A. Dufresne, *Nanocellulose: from Nature to High Performance Tailored Materials*. de Gruyter, 2012.
- [138] Y. Li, H. Ren, and A. J. Ragauskas, “Rigid polyurethane foam reinforced with cellulose whiskers: Synthesis and characterization,” *Nano-Micro Lett.*, vol. 2, no. 2, pp. 89–94, Jul. 2010.
- [139] G. Czeremuskin, P. Mukhopadhyay, and S. Sapiuha, “Elution Behavior of Chemically Different Probes on the Evaluation of Surface Properties of Cellulose by Inverse Gas

- Chromatography,” *J. Colloid Interface Sci.*, vol. 194, no. 1, pp. 127–37, Oct. 1997.
- [140] A. Dufresne, D. Pupeyre, and M. R. Vignon, “Cellulose Microfibrils from Potato Tuber Cells : Processing and Characterization of Starch – Cellulose Microfibril Composites,” *Polymer (Guildf.)*, vol. 76, no. 14, pp. 2080–2092, 1999.
- [141] D. Cava, J. M. Lagarón, F. Martínez-Giménez, and R. Gavara, “Inverse Gas Chromatography Study on the Effect of Humidity on the Mass Transport of Alcohols in an Ethylene-Vinyl Alcohol Copolymer Near the Glass Transition Temperature.,” *J. Chromatogr. A*, vol. 1175, no. 2, pp. 267–74, Dec. 2007.
- [142] M. E. Vallejos, M. S. Peresin, and O. J. Rojas, “All-Cellulose Composite Fibers Obtained by Electrospinning Dispersions of Cellulose Acetate and Cellulose Nanocrystals,” *J. Polym. Environ.*, vol. 20, no. 4, pp. 1075–1083, 2012.
- [143] C. Sammon, J. Yarwood, and N. Everall, “A FTIR – ATR study of liquid diffusion processes in PET films : comparison of water with simple alcohols,” *Polymer (Guildf.)*, vol. 41, pp. 2521–2534, 2000.
- [144] T. Varzakas and C. Tzia, Eds., *Food Engineering Handbook: Food Engineering Fundamentals*. CRC Press, 2014.
- [145] F. Johansson and A. Leufven, “Concentration and Interactive Effects on the Sorption of Aroma Liquids and Vapors into Polypropylene,” *J. Food Science*, vol. 62, no. 2, pp. 355–358, 1997.
- [146] P. T. DeLassus and G. Strandburg, “Flavor and Aroma Permeability in Plastics,” in *Food Packaging Technology, ASTM STP 1113*, 1991, pp. 64–73.

- [147] J. P. Dumont and J. Adda, "Occurrence of Sesquiterpenes in Mountain Cheese Volatiles," *J. Agric. Food Chem.*, vol. 26, no. 2, pp. 364–367, Mar. 1978.
- [148] I. Yajima, T. Yanai, M. Nakamura, H. Sakakibara, and T. Habu, "Flavor Components of Cooked Rice," *Agric. Biol. Chem.*, vol. 42, no. 6, pp. 1229–1233, 1978.
- [149] G. S. Fisher, M. G. Legendre, N. V. Lovgren, W. H. Schuller, and J. a. Wells, "Volatile Constituents of Southernpea Seed [*Vigna Unguiculata* (L.) Walp.]," *J. Agric. Food Chem.*, vol. 27, no. 1, pp. 7–11, Jan. 1979.
- [150] N. V. Lovgren, C. H. Vinnett, and A. J. S. Angelo, "Gas Chromatographic Profile of Good Quality Raw Peanuts," *Peanut Sci.*, vol. 9, pp. 93–96, 1980.
- [151] Q. G. Zhang, Q. L. Liu, J. Lin, J. H. Chen, and A. M. Zhu, "Analyzing Solubility and Diffusion of Solvents in Novel Hybrid Materials of Poly(Vinyl Alcohol)/ γ -Aminopropyltriethoxysilane by Inverse Gas Chromatography," *J. Mater. Chem.*, vol. 17, no. 46, pp. 4889–4895, 2007.
- [152] Q. Zhou and K. R. Cadwallader, "Inverse Gas Chromatographic Method for Measurement of Interactions Between Soy Protein Isolate and Selected Flavor Compounds Under Controlled Relative Humidity.," *J. Agric. Food Chem.*, vol. 52, no. 20, pp. 6271–7, Oct. 2004.
- [153] A. Voelkel, "Physicochemical Measurements," in *Gas Chromatography*, C. F. Poole, Ed. Elsevier, 2012, pp. 477–494.
- [154] R. P. W. Scott, "Peak Dispersion," in *Techniques and Practice of Chromatography*, New York: Marcel Dekker, INC., 1995, pp. 69–100.

- [155] R. Gavara, R. Catala, S. Aucejo, D. Cabedo, and R. Hernandez, "Solubility of Alcohols in Ethylene-vinyl Alcohol Copolymers by Inverse Gas Chromatography," *J. Polym. Sci. Part B Polym. Phys.*, vol. 34, pp. 1907–1915, 1996.
- [156] R. A. Talja, H. Helén, Y. H. Roos, and K. Jouppila, "Effect of Various Polyols and Polyol Contents on Physical and Mechanical Properties of Potato Starch-Based Films," *Carbohydr. Polym.*, vol. 67, pp. 288–295, 2007.
- [157] S. Gaudin, D. Lourdin, D. Le Botlan, J. L. Ilari, and P. Colonna, "Plasticisation and Mobility in Starch-Sorbitol Films," *J. Cereal Sci.*, vol. 29, pp. 273–284, 1999.
- [158] P. Myllärinen, R. Partanen, J. Seppälä, and P. Forssell, "Effect of Glycerol on Behaviour of Amylose and Amylopectin Films," *Carbohydr. Polym.*, vol. 50, pp. 355–361, 2002.
- [159] A. P. Mathew and A. Dufresne, "Plasticized Waxy Maize Starch: Effect of Polyols and Relative Humidity on Material Properties," *Biomacromolecules*, vol. 3, pp. 1101–1108, 2002.
- [160] S. Matteucci, Y. Yampolskii, B. D. Freeman, and I. Pinnau, "Transport of Gases and Vapors in Glassy and Rubbery Polymers," in *Materials Science of Membranes for Gas and Vapor Separations*, B. Freeman, Y. Yampolskii, and I. Pinnau, Eds. John Wiley & Sons, 2006, pp. 30–40.
- [161] L. Friedman and P. G. Carpenter, "Diffusion Velocity and Molecular Weight. I. The Limits of Validity of the Stokes-Einstein Diffusion Equation," *J. Am. Chem. Soc.*, vol. 61, no. 7, pp. 1745–1747, 1939.
- [162] I. M. Balashova, R. P. Danner, P. S. Puri, and J. L. Duda, "Solubility and Diffusivity of

- Solvents and Nonsolvents in,” *Ind. Eng. Chem. Res.*, vol. 40, pp. 3058–3064, 2001.
- [163] L. H. Poley, M. G. Da Silva, H. Vargas, M. O. Siqueira, and R. Sánchez, “Water and Vapor Permeability at Different Temperatures of Poly (3-Hydroxybutyrate) Dense Membranes,” *Polímeros*, vol. 15, no. 1, pp. 22–26, 2005.
- [164] L. K. Massey, *Permeation Properties of Plastics and Elastomers (2) A Guide to Packaging and Barrier Materials*, 2nd ed. Elsevier Inc., 2003.
- [165] S. A. Stern, “The ‘Barrer’ Permeability Unit,” *J. Polym. Sci. Part A-2*, vol. 6, pp. 1933–1934, 1968.
- [166] Q. Zhou, B. Guthrie, and K. R. Cadwallader, “Development of a System for Measurement of Permeability of Aroma Compounds Through Multilayer Polymer Films by Coupling Dynamic Vapour Sorption with Purge-and-Trap/Fast Gas Chromatography,” *Packag. Technol. Sci.*, vol. 17, no. 4, pp. 175–185, Jul. 2004.
- [167] G. López-Carballo, D. Cava, J. M. Lagarón, R. Catalá, and R. Gavara, “Characterization of the Interaction Between two Food Aroma Components, α -pinene and Ethyl Butyrate, and Ethylene-Vinyl Alcohol Copolymer (EVOH) Packaging films as a function of environmental humidity,” *J. Agric. Food Chem.*, vol. 53, no. 18, pp. 7212–7216, 2005.
- [168] Z. Zhang, L. Lim, and M. Tung, “Limonene Transport and Mechanical Properties of EVOH and Nylon 6, 6 Films as Influenced by RH,” *J. Appl. Polym. Sci.*, vol. 79, no. 2001, pp. 1949–1957, 2001.
- [169] C. Caner, “Sorptions Phenomena in Packaged Foods: Factors Affecting Sorptions Processes in Package-Product Systems,” *Packag. Technol. Sci.*, vol. 24, pp. 259–270, 2011.

- [170] K. Cooksey, "Important Factors for Selecting Food Packaging Materials Based on Permeability," in *Flexible Packaging Conference*, 2004, pp. 1–12.
- [171] C. Dury-Brun, P. Chalier, S. Desobry, and A. Voilley, "Multiple Mass Transfers of Small Volatile Molecules Through Flexible Food Packaging," *Food Rev. Int.*, vol. 23, no. 3, pp. 199–255, 2007.
- [172] P. J. Kalaouzis and P. G. Demertzis, "Water sorption and water vapour diffusion in food-grade plastics packaging materials: Effect of a polymeric plasticizer," *Packag. Technol. Sci.*, vol. 5, no. February, pp. 133–144, 1992.
- [173] G. Guiochon and C. L. Guillemin, *Quantitative Gas Chromatography for Laboratory Analyses and On-Line Process Control*. Elsevier Science Publishers B.V., 1988.
- [174] M. Kurek, A. Guinault, A. Voilley, K. Galić, and F. Debeaufort, "Effect of Relative Humidity on Carvacrol Release and Permeation Properties of Chitosan Based Films and Coatings.," *Food Chem.*, vol. 144, pp. 9–17, 2014.
- [175] S. Despond, E. Espuche, and A. Domard, "Water Sorption and Permeation in Chitosan Films : Relation between Gas Permeability and Relative Humidity," *J. Polym. Sci. Part B Polym. Phys.*, vol. 39, pp. 3114–3127, 2001.
- [176] A. Misra, D. J. David, J. A. Snelgrove, and G. Matis, "Clustering of Absorbed Water in Amorphous Polymer Systems," *J. Appl. Polym. Sci.*, vol. 31, pp. 2387–2398, 1986.
- [177] L. Zhao and P. Choi, "Differences between Ziegler–Natta and Single-Site Linear Low-Density Polyethylenes as Characterized by Inverse Gas Chromatography," *Macromol. Rapid Commun.*, vol. 25, no. 4, pp. 535–541, Feb. 2004.

- [178] J. S. Aspler and D. G. Gray, "An Inverse Gas-Chromatographic Study of the Interaction of Water with some Cellulose Derivatives," *J. Polym. Sci. Polym. Phys. Ed.*, vol. 21, pp. 1675–1689, 1983.
- [179] H. W. Starkweather Jr., "Clustering of Water in Polymers," *Polym. Lett.*, vol. 1, pp. 133–138, 1963.
- [180] H. Levine and L. Slade, "Water as a Plasticizer: Physico-Chemical Aspects of Low Moisture Polymeric Systems," in *Water Science Reviews 3: Volume 3: Water Dynamics*, F. Franks, Ed. Cambridge University Press, 1988, pp. 79–120.
- [181] A. W. Adamson and A. P. Gast, *Physical Chemistry of Surfaces Sixth Edition*, 6th ed. New York: Wiley, 1976.
- [182] S. L. McMullin, R. a. Bernhard, and T. a. Nickerson, "Heats of Adsorption of Small Molecules on Lactose," *J. Agric. Food Chem.*, vol. 23, no. 3, pp. 452–458, May 1975.
- [183] W. P. Shen, V.K., Siderius, D.W., and Krekelberg, Ed., "NIST Standard Reference Simulation Website, NIST Standard Reference Database Number 173, National Institute of Standards and Technology," in *Gaithersburg, MD, 20899*, 2014.
- [184] A. Boutboul, F. Lenfant, P. Giampaoli, A. Feigenbaum, and V. Ducruet, "Use of Inverse Gas Chromatography to Determine Thermodynamic Parameters of Aroma–Starch Interactions," *J. Chromatogr. A*, vol. 969, no. 1–2, pp. 9–16, Sep. 2002.
- [185] T. G. Aspelund and L. a. Wilson, "Adsorption of Off-flavor Compounds onto Soy Protein : A Thermodynamic Study," *J. Agric. Food Chem.*, vol. 31, no. 3, pp. 539–545, May 1983.

- [186] H. Eser and F. Tihminlioglu, "Determination of Thermodynamic and Transport Properties of Solvents and Non Solvents in Poly(L-lactide-co-glycolide)," *J. Appl. Polym. Sci.*, vol. 102, no. 3, pp. 2426–2432, Nov. 2006.
- [187] K. J. Edgar, C. M. Buchanan, J. S. Debenham, P. a. Rundquist, B. D. Seiler, M. C. Shelton, and D. Tindall, "Advances in cellulose ester performance and application," *Prog. Polym. Sci.*, vol. 26, no. 9, pp. 1605–1688, 2001.

Appendix A: Study of thermodynamic parameters of adsorption of small molecules on HPX films

A.1. Abstract

Five alcohols (C₁-C₆), two aldehydes (hexanal, heptanal) and limonene representing aroma in food were selected to study adsorption enthalpies through the films formed by a biopolymer namely hydroxypropyl xylan (HPX) with and without additives by inverse gas chromatography. Thermodynamic parameters of enthalpy of adsorption, Gibb's free energy of adsorption, and other thermodynamic data was used to determine the strength of adsorption of the solvents on HPX and to determine modes of adsorption using heat of adsorption data.

Enthalpy of adsorption and Gibbs free energy of adsorption were measured at temperatures (30 – 45 °C) significantly below the glass transition temperatures (T_g) of HPX films to ensure that the main retention mechanism was adsorption. On the other hand, the weight fraction activity coefficients at infinite dilution were measured over a range of temperatures that were above the T_gs of HPX films.

The adsorption results showed that the selected alcohols and aldehydes exhibited affinity for the HPX film surfaces and that the affinity of alcohols for HPX increased with increase of the carbon chain length. Comparison of ΔG_s values for hexanol and hexanal confirms a more favorable interaction between HPX and hexanol promoted by dominating effect of polarity to condensability. Despite the affinity for the HPX surface, the infinite dilution weight fraction activity coefficients at elevated temperatures (120 – 160 °C) showed that alcohols are immiscible with HPX films. The immiscibility became more pronounced when sorbitol and cellulose nanocrystals (CNC) were added as the additives were hydrophilic.

A.2. Theory

The free energy of adsorption of the probe on the polymer can be estimated by:

$$\Delta G_a = -RT_c \ln K_p \quad (\text{A. 1})$$

where K_p is the partition coefficient and is obtained by:

$$K_p = \frac{V_g^0 \rho T_c}{27 \cdot 315} \quad (\text{A. 2})$$

where ρ is the density of the polymer.

The enthalpy of adsorption ΔH_a is obtained from the slope of linear graph of $\ln V_g^0$ vs. $1/T$ from using the method of Kiselev and Yashin:

$$\frac{-\Delta H_a}{R} = \frac{d \ln V_g^0}{d 1/T} \quad (\text{A. 3})$$

The sorption isotherms were calculated depending on the solvent partial vapor pressure p (pa) and the corresponding solvent uptake, a (gr gr⁻¹).

The adsorption constant, S (gr gr⁻¹ pa⁻¹), which is a Henry's type constant can be determined from the slope of the linear isotherms:

$$a = S * p \quad (\text{A. 4})$$

The equilibrium partial pressure, p , of the solvent vapor entering the detector can be related to the experimental chromatogram by: [95]

$$p = \frac{n_s R T_c h}{F_c S_{cal}} \quad (\text{A. 5})$$

Where n is the moles of the solvent injected, h is the calibration peak height, S_{cal} is the peak area.

The solvent uptake which is the amount of the solvent adsorbed corresponding to this partial pressure p is given by:

$$a = \frac{m_s S_{ads}}{m_p S_{cal}} \quad (\text{A. 6})$$

Where m_s (gr) is the weight of the solvent injected, S_{ads} is the peak are between the retention time of the non-retained peak, the peak height and the diffused side of the peak, m_p is the stationary phase (polymer) weight (gr).

A.3. Experimental conditions

For the thermodynamic properties studies, the experiments were run at temperatures well below the glass transition temperature, at 30, 35, 40, 45 °C. The carrier gas flow rate was 20 ml/min and various amounts of samples from 0.05 to 0.5 μl were injected at each temperature for each solvent.

A.4. Results and Discussion

At the very low concentration of the solvents injected, the peak retention volumes were almost constant while the peaks were sharp with only slight tailing. In this region the adsorption isotherms were linear indicating that the thermodynamic information could be properly derived from the retention data on HPX films. It is possible to obtain the enthalpies of adsorption and thermodynamic properties by gas chromatography if bulk sorption into the polymer is not the factor contributing to retention of the solvents. This will be the case when the solvents have low tendency to dissolve in or swell the polymer. This effect will be negligible in polymers if the

working condition is well below the glass transition temperature of the polymer where bulk sorption is very slow [95]. In addition, at infinite dilution concentration of the solvent, only the solvent-polymer interaction is important while the solvent-solvent interaction is negligible. Consequently, the enthalpy of adsorption, ΔH_a , determines the strength of interaction between the solvent and the polymer [152]. HPX is a polymer with glass transition temperature of 137.4°C [74].

The experiments for obtaining thermodynamic properties were run at temperatures well below the glass transition temperature of the polymer, 30-45 °C, to reduce the effect of bulk sorption on solvent retention.

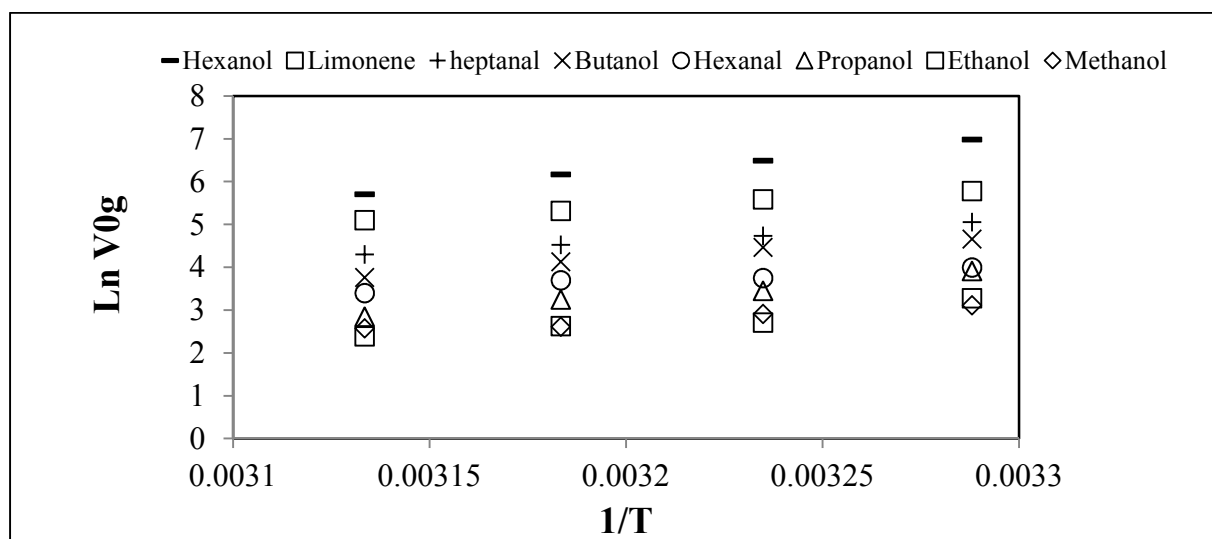
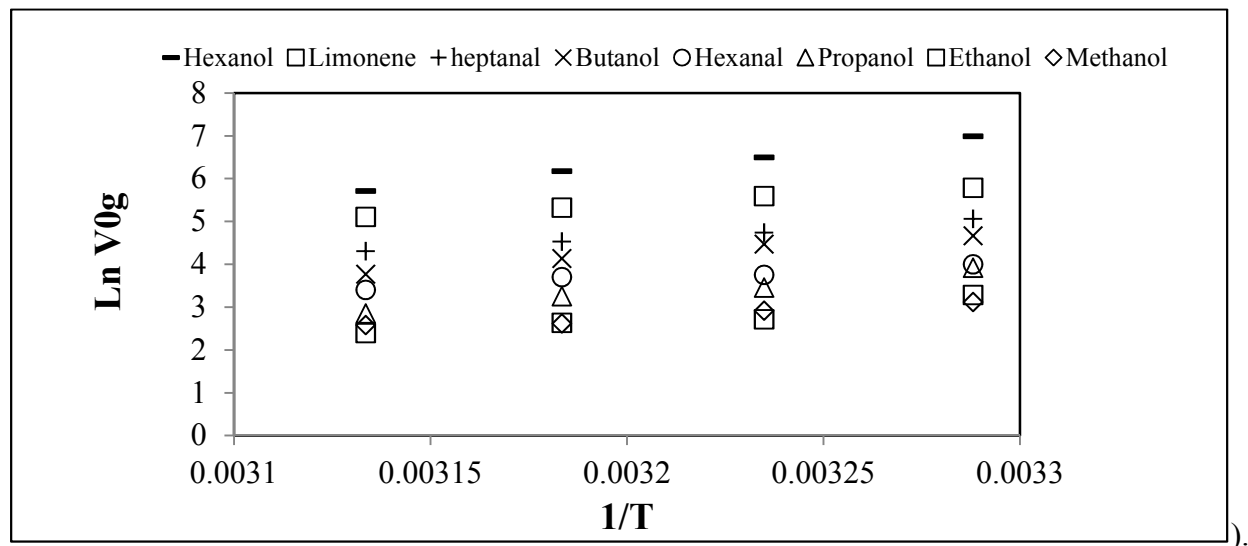


Figure A. 1. Specific retention volume as a function of temperature for solvents-HPX

A.4.1. Enthalpy of adsorption

The enthalpy of adsorption, ΔH_a , gives information about endothermic or exothermic character of the interaction of the solvent and the polymer. The enthalpy of solvent-polymer interaction at very low concentrations of the solvent is obtainable when the adsorption isotherm is linear.

Enthalpies of adsorption ΔH_a for each aroma compound were determined from the graphs of $\ln V_g^0$ vs. $1/T$ for temperatures of 30-45 °C with increments of 5 °C. The linearity of the graph can be ascribed as reaching the equilibrium state between the solvent and the polymer (



The slope of the straight lines obtained is equal to $\Delta H_a/R$ according to equation:

$$\Delta H_a = -R \frac{\partial(\ln V_g)}{\partial(\frac{1}{T})} \quad (\text{A. 7})$$

The correlation coefficient describing the fit to the lines were more than 98% except for the solvents with lower boiling points, methanol and ethanol, which was 94% and 90%, respectively.

ΔH_a values for the studied solvents are presented in Table A.1. The negative values for ΔH_a indicates that the adsorption is an exothermic process. The values are lower than typical average chemical sorption values (84-168 kJ/mol) [181]. The decrease in value of ΔH_a by increasing the chain length in alcohols indicates stronger preferential adsorption of the larger alcohols. However comparison of the solvent molecules with similar chain length but different functional groups, hexanol and hexanal, suggests that adsorption of hexanol (ΔH_a : -67.23 kJ mol⁻¹) is stronger than adsorption of hexanal (ΔH_a : -23.77 kJ mol⁻¹). Similar values were previously

obtained for polar materials such as starch (-68.4 and -43.0 kJ mol⁻¹ for hexanol and hexanal, respectively) and lactose (-73.4 and -48.6 kJ mol⁻¹ for hexanol and hexanal, respectively)[152]. Hexanal shows being the less favorable to adsorb compared to all the other solvents due to its highest ΔH_a value while methanol the least favorable to adsorb among the alcohols. .

Comparing the values for heat of adsorption for the solvents with similar functional groups (alcohols), shows increase in enthalpies of adsorption as molecular weight increases. Similar behaviour has already been reported [89] [182]. Values for enthalpies of vaporization, ΔH_v , of each aroma was obtained from literature [183]. $|\Delta H_a|$ values of alcohols show higher values than their heat of vaporization $|\Delta H_v|$ indicating that enthalpies of adsorption are not only due to heat of condensation, but also due to some physico-chemical interactions between the solvents molecules and the HPX. For Methanol and ethanol, the more polar compounds, $|\Delta H_a| - |\Delta H_v|$ values are 10.4 and 9.8 KJ/mol indicating more possibility of interacting via hydrogen bond (Hydrogen bonds have energies of formation in the range of 10-40 KJ/mol, but generally about 20 KJ/mol [182], [184]. Hydrogen bonds can be formed between hydroxyl groups of HPX and methanol and ethanol. However for the other alcohols (C₃, C₄, C₆) hydrogen bond is less likely to be involved as they showed weak energies (5.2, 6.3 and 5.6 KJ/mol). In this case probably van der Waals dipole-dipole interaction (2.1-8.4 KJ/mol) [184] is involved. However, Aspelund and Wilson suggest that alcohols form two hydrogen bonds with soy protein [185].

Comparing ΔH_a values for the solvent shows highest value for hexanol (-77 KJ/mol) and the lowest for Hexanal (-23.77 KJ/mol). For hexanal possibly only weak forces (van der Waals forces) were involved which result in low affinity, while much higher value of ΔH_a for hexanol suggests presence of hydrogen bonding. Negative values of $|\Delta H_a| - |\Delta H_v|$ for hexanal,

heptanal and limonene, is described as the greater enthalpy required for vaporization of the solvents compared to desorption from the surface.

A.4.2. Gibbs free energy of adsorption

Gibbs free energy of adsorption of the solvents on HPX is given in Table A.1. The negative values for ΔG_a are indicating the natural interaction of the solvents with HPX. The slight increase in the values of ΔG_a by increasing temperature indicates that adsorption is more favorable at lower temperatures. This is indicative of physical adsorption whereas chemical adsorption shows opposite behaviour [182]. Also, hexanol shows highest interaction with HPX owing to its largest absolute values of ΔG_a compared to other solvents. The explanation is similar to that of ΔH_a . The ΔG_a values increased with an average of 1.96 kJ per methyl group added to the solvent chain length. Aspelund and Wilson obtained a value of 2.4 kJ/CH₂ for alcohols-soy system [185]. The results support the hypothesis that the larger molecules of alcohols have the highest tendency to interact with HPX at lower temperatures thus reducing its potential to migrate through the polymer.

A.4.3. Adsorption constant

The adsorption coefficient, S , reflects both strength of adsorption, reflected by ΔH_a , and the number of binding sites. Like ΔH_a , increasing chain length of the solvent increase S due to increase of vander Waals interaction. However the ΔG_a values for hexanol and Limonene were close, the adsorption constants for limonene were higher than that of hexanol.

Table A. 1. Heats of adsorption, adsorption constant and Gibbs free energy of adsorption of the solvents-HPX at infinite dilution

Temperature °C	ΔG_a (kJ mol ⁻¹)				S				ΔH_a (kJ mol ⁻¹)	* ΔH_v (kJ mol ⁻¹)
	30	35	40	45	30	35	40	45		
Methanol	-8.35	-7.59	-7.41	-6.97	1.7	1.3	1.2	1.7	-30.88	-37
Ethanol	-8.75	-7.49	-7.43	-6.97	3.07	1.5	1.3	1.1	-51.87	-42
Propanol	- 10.36	-9.38	-9.06	-8.18	3.7	2.4	2.0	1.7	-52.69	-47.5
Butanol	- 12.24	- 11.99	- 11.35	- 10.62	7.4	6.0	4.8	3.9	-57.29	-51
Hexanol	- 18.11	- 17.06	- 16.06	- 15.74	64.9	42.3	26.3	20.8	-67.23	-61.6
Hexanal	- 10.56	- 10.16	- 10.13	-9.99	10.3	9.3	8.3	7.21	-23.77	-44.5
Heptanal	- 13.24	- 12.68	- 12.39	- 11.95	24.9	20.3	18.4	16.8	-41.88	-48
Limonene	- 15.07	- 14.86	- 14.44	- 13.85	72.1	63.4	49.7	38.2	-36.97	-44

*Values for ΔH_v obtained from [183]

A.4.4. Weight fraction activity coefficient

The weight fraction activity coefficient of the solvents at infinite dilution Ω_1^∞ was obtained at various temperatures above the glass transition temperature to give an idea about polymer solvent compatibility. $\Omega_1^\infty < 5$ is indication of good solvents, $5 < \Omega_1^\infty < 10$ moderate solvents and $\Omega_1^\infty > 10$ bad solvent [186].

The weight fraction activity coefficient of the solvents in each polymer can be obtained from chromatographic data using the equation:

$$\Omega_1^\infty = \frac{RT}{P_1^s V_g^0 M_1} \exp\left(\frac{\{-P_1^s(B_{11}-V_1)\}}{RT}\right) \quad (\text{A. 8})$$

Where P_1^s is the saturation pressure of the solvent, M_1 is the molecular weight of the solvent and B_{11} is the second virial coefficient of the solvent and V_1 is the solvents molar volume. Values of infinite dilution weight fraction activity coefficient are indicated in Table A.2.

Table A. 2. Infinite dilution weight fraction activity coefficients for solvents in HPX films

	T (°C)	120	130	140	150	160
HPX	Methanol	260.3	256.5	197.3	135.1	149.7
	Ethanol	268.7	213.5	240.1	179.8	220.5
	Propanol	326.9	364.1	305.7	289.7	255.0
	Butanol	357.3	326.5	325.4	267.3	325.2
HPX/sorbitol	Methanol	136.4	126.5	108.7	108.2	200.8
	Ethanol	385.3	299.2	258.4	233.4	424.1
	Propanol	449.3	395.3	294.9	285.1	423.5
	Butanol	936.5	719.4	524.3	419.5	511.4
HPX/sorbitol/CNC	Methanol	147.8	144.9	140.4	123.7	167.4
	Ethanol	378.1	311.8	274.2	239.0	321.4
	Propanol	411.8	339.4	359.0	271.7	348.9
	Butanol	723.4	615.6	642.9	457.9	619.0

Figures A.2-A.4 summarize the measured infinite dilution activity coefficient of 4 alcohols in neat HPX and HPX with sorbitol and with sorbitol and CNC. The values of Ω_1^∞ for the studied solvents suggest incompatibility of the aforementioned alcohols with HPX polymers. For pure HPX and HPX with CNC and sorbitol, Ω_1^∞ is insensitive to the temperature. However, for the case of HPX with sorbitol, the change of Ω_1^∞ with temperature is more obvious especially for larger molecules indicating that sorbitol facilitates effect of temperature in increasing mobility of the chains and dissociating hydroxyl groups in the polymer chain. In general, the additives do not affect the Ω_1^∞ much for methanol and ethanol. But it does for propanol and butanol. This may be due to the fact that both sorbitol and CNC contains many hydroxyl moieties that make alcohols with longer alkyl chains not compatible with the additives. Nonetheless, with such large magnitude of the activity coefficients, it is expected that it will increase the rate of diffusion of the alcohols.

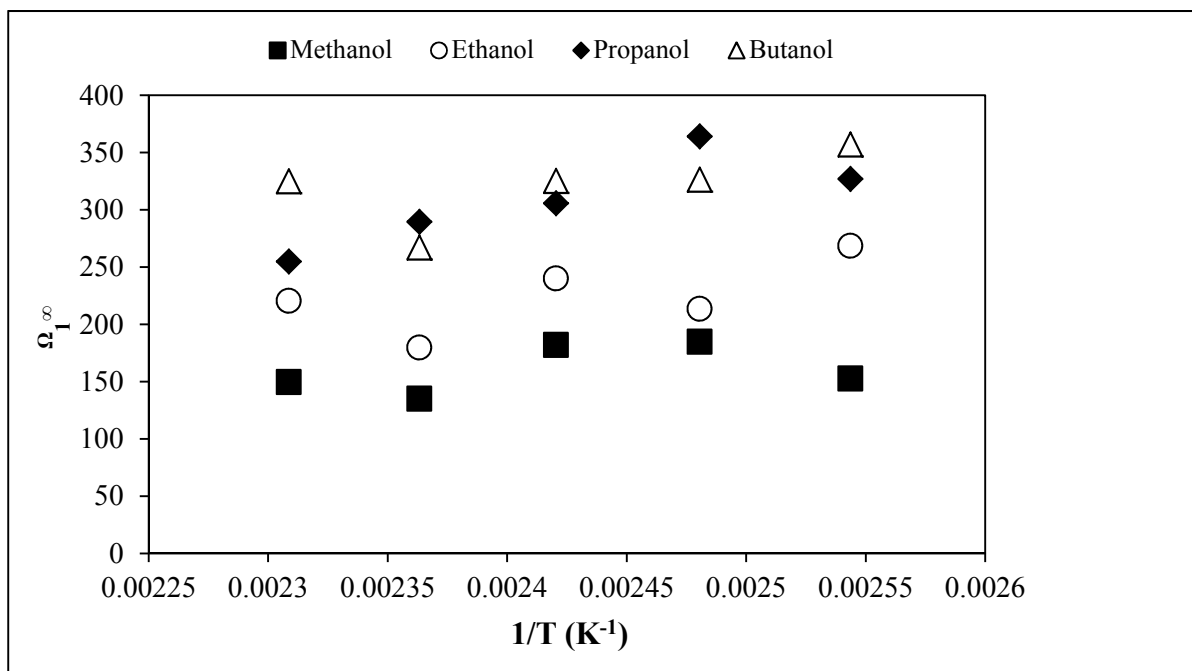


Figure A. 2. Temperature dependence of the weight fraction activity coefficient of alcohols in HPX in its rubbery state.

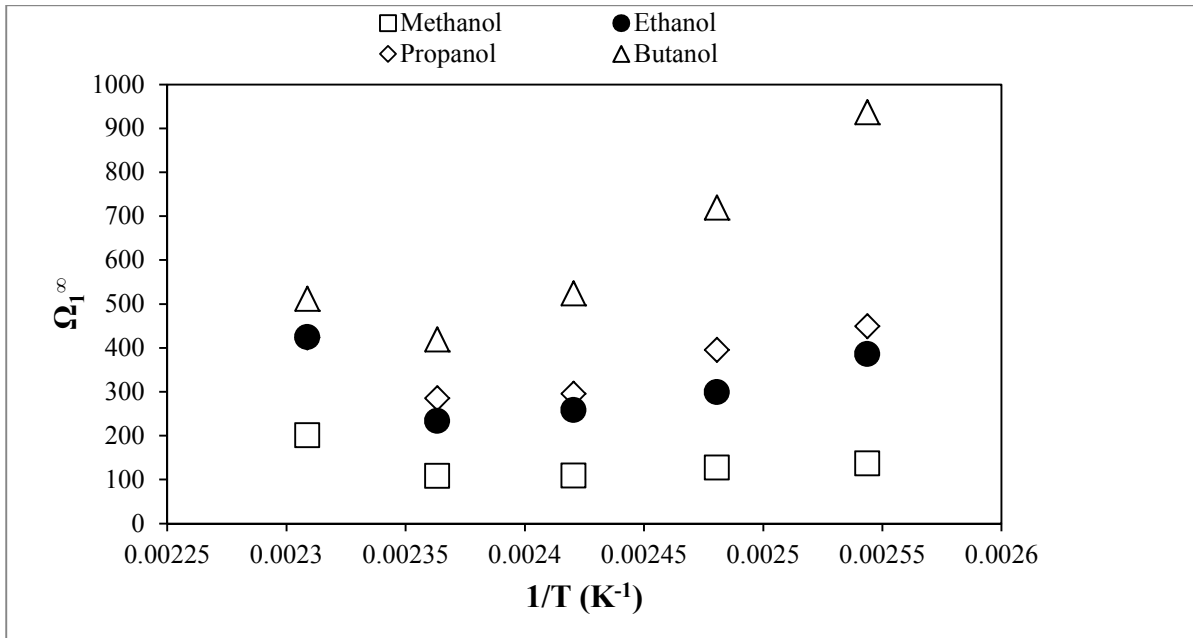


Figure A. 3. Temperature dependence of the weight fraction activity coefficient of alcohols in HPX/sorbitol in its rubbery state.

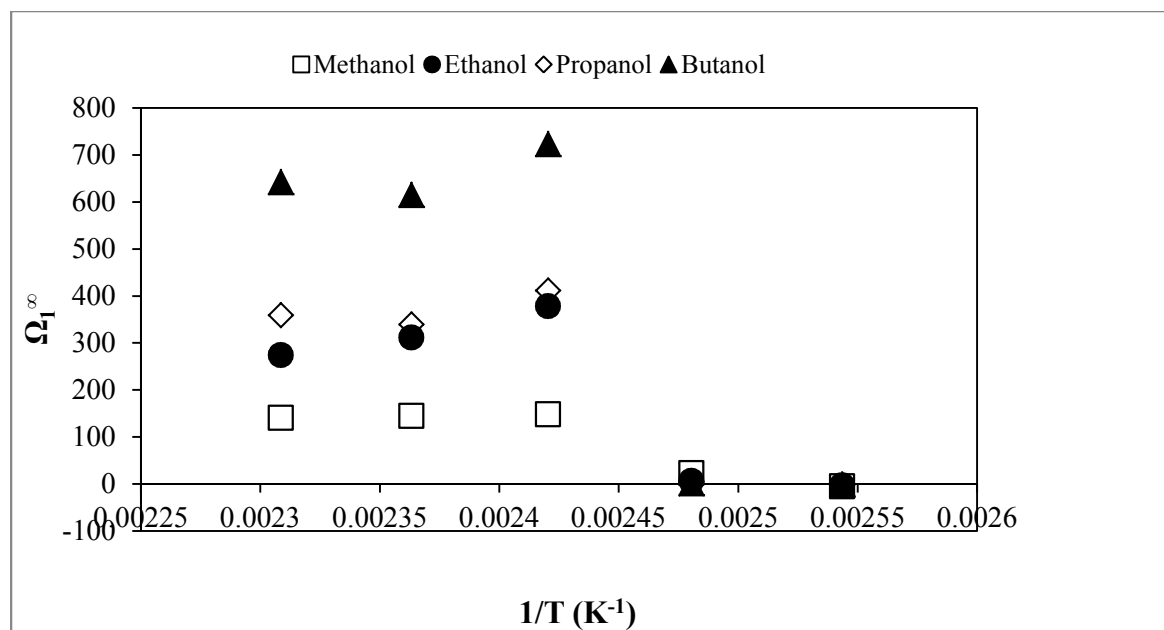


Figure A. 4. Temperature dependence of the weight fraction activity coefficient of alcohols in HPX/sorbitol/CNC in its rubbery state.

Appendix B: Acetylation of HPX

B.1. Acetylation of HPX

Acetylation of HPX can be used as part of modification of the polymer to a water-insoluble polymer for certain packaging applications. Acetoxypropyl xylan (APX) obtained from acetylation of hydroxypropyl xylan (HPX) is a hydrophobic biodegradable polymer useful for packaging applications due to its film forming properties depending on the degree of substitution of hydroxyl moieties on HPX with acetyl moieties. If the degree of substitution is too high, the resulting material forms erratic films soluble in most organic solvents such as tetrahydrofuran, chloroform, dimethyl sulfoxide, dimethylformamide and dimethylacetamide. Because of thermoplasticity and water insolubility, APX can also be used as structural polymer blends as rheology modifier and plasticizer.

Transparent and tough HPX films were acetylated and contact angle was measured to compare effect of acetylation on hydrophobicity of material Figure B.1. Degree of substitution is in relation with pH during propoxylation of Xylan. The most hydrophobic APX is obtained from HPX with more degree of substitution.

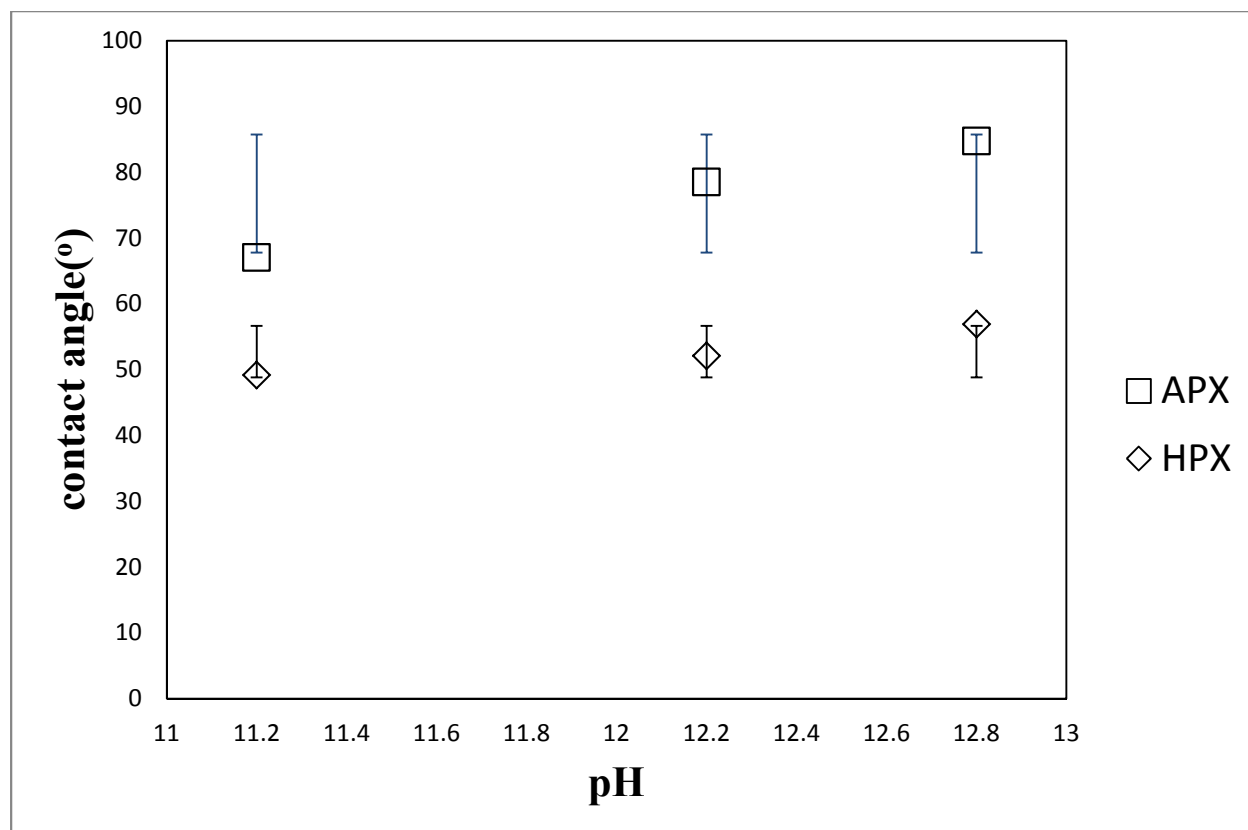


Figure B. 1. Effect of Acetylation on contact angle. (APX: acetylated HPX)

B.2. FTIR analysis of HPX and APX

Structural analysis of both HPX and APX was conducted by FTIR. The hydroxypropyl groups can be determined by FTIR as a CH-stretching at approximately 2950 cm^{-1} (Figure B.2). Acetylation is revealed by an elimination of the hydroxyl band at approximately 3400 cm^{-1} , and the appearance of an ester band at around 1745 cm^{-1} .

When the acetylating reaction takes place between acetic anhydride and HPX, the modification may be proved by the carbonyl ester band appearing at around 1745 cm^{-1} and the decrease of OH broad band intensity assigned to alcohol group at 3513 cm^{-1} .

The peaks located at $\sim 2971\text{ cm}^{-1}$ and $\sim 2931\text{ cm}^{-1}$ are attributed to $\nu(\text{C-H})$ and $\nu(\text{C-H}_2)$ groups respectively. The band located at 1656 cm^{-1} corresponds to the bending mode of the naturally absorbed water. The absorbance at 1377 cm^{-1} arises from the C-CH_3 vibration, moreover the peak at 1246 cm^{-1} is originated from $\nu(\text{C-O})$ ester vibration [29], [187]. The effect of acetic anhydride equivalent number added to the HPX is illustrated in Figure 9 by comparing the FTIR spectra of (1), (2) and (3). It shows that by increasing the fraction of acetic anhydride to the solution, the absorption band surface change and the ratio of $\nu(\text{C=O})$ to $\nu(\text{O-H})$ surfaces increases. The experiments based on FTIR spectra qualitatively show that the degree of substitution increases with increasing acetic anhydride amounts added [187].

The effect of acetic anhydride equivalent number added to the HPX is illustrated in Figure B.3 by comparing the FTIR spectra of (1), (2) and (3). It shows that by increasing the fraction of acetic anhydride to the solution, the absorption band surface change and the ratio of $\nu(\text{C=O})$ to $\nu(\text{O-H})$ surfaces increases. The experiments based on FTIR spectra qualitatively show that the degree of substitution increases with increasing acetic anhydride amounts added. (Edgar et al., 2001)

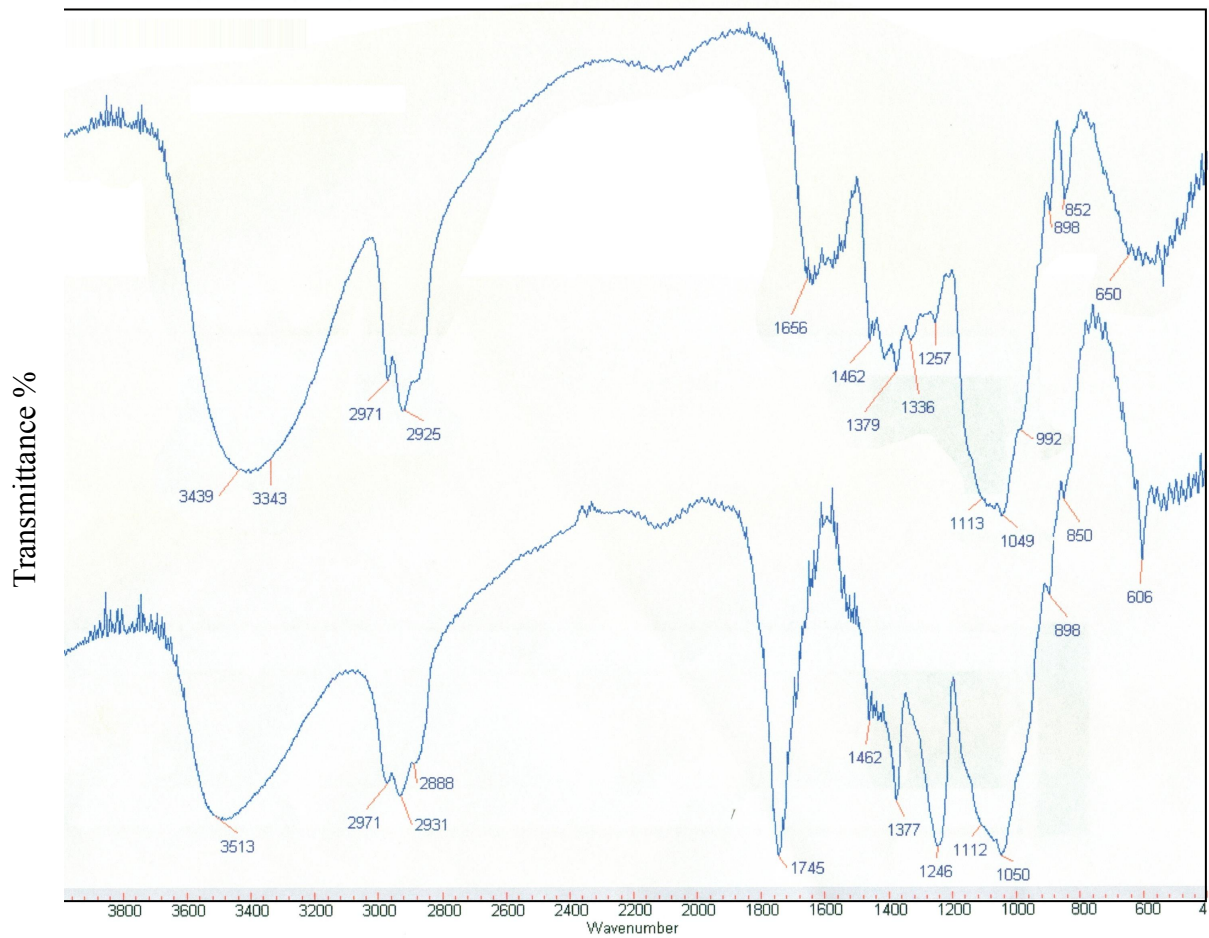


Figure B. 2. FT-IR spectra of HPX and APX

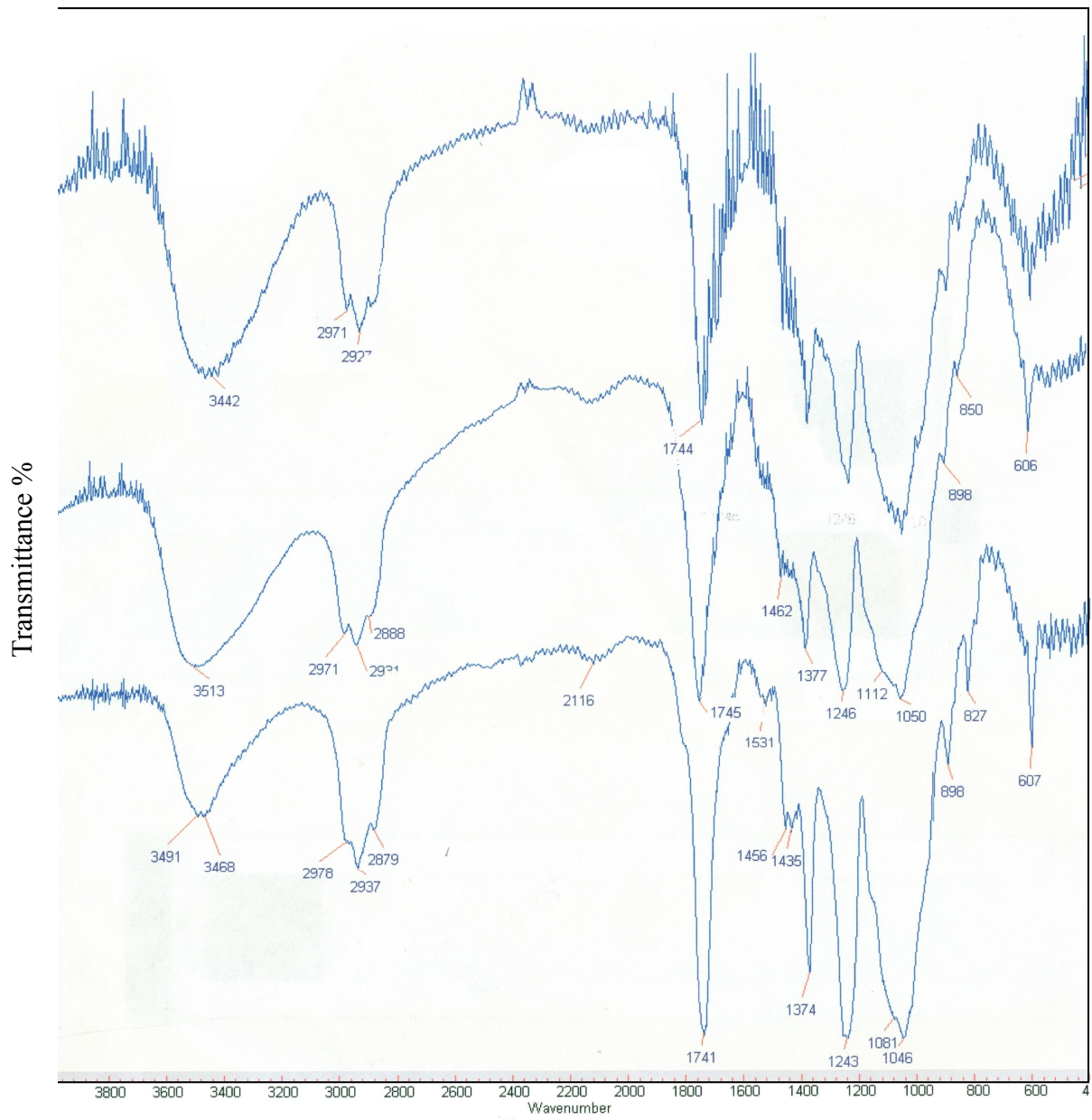


Figure B. 3. Comparison of FT-IR spectra of reaction with different amounts of acetic anhydride;

Acetic Anhydride to HPX ratio for : (1)>(2)>(3)